

Design and Synthesis of Near-Infrared Absorbing Aza-dipyrromethenes and Aza-BODIPYs

Ph.D. Thesis

By
PINJARI DILIP ANANDA



**DISCIPLINE OF CHEMISTRY
INDIAN INSTITUTE OF TECHNOLOGY INDORE
JANUARY 2024**

Design and Synthesis of Near-Infrared Absorbing Aza-dipyrromethenes and Aza-BODIPYs

A THESIS

*Submitted in partial fulfillment of the
requirements for the award of the degree
of*
DOCTOR OF PHILOSOPHY

by
PINJARI DILIP ANANDA



**DISCIPLINE OF CHEMISTRY
INDIAN INSTITUTE OF TECHNOLOGY INDORE**

January 2024

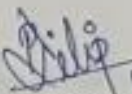


INDIAN INSTITUTE OF TECHNOLOGY INDORE

CANDIDATE'S DECLARATION

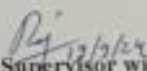
I hereby certify that the work which is being presented in the thesis entitled "**Design and Synthesis of Near-Infrared Absorbing Aza-dipyrromethenes and Aza-BODIPYs**" in the partial fulfillment of the requirements for the award of the degree of **DOCTOR OF PHILOSOPHY** and submitted in the **Department of Chemistry, Indian Institute of Technology Indore**, is an authentic record of my own work carried out during the time period from **December 2018** to **January 2024** under the supervision of **Dr. Rajneesh Misra, Professor, Discipline of Chemistry, IIT Indore**.

The matter presented in this thesis has not been submitted by me for the award of any other degree of this or any other institute.

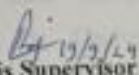
 19/09/2024.

Signature of the Student with date
(Pinjari Dilip Ananda)

This is to certify that the above statement made by the candidate is correct to the best of my/our knowledge.

 19/09/24
Signature of Thesis Supervisor with date
(Prof. Rajneesh Misra)

Pinjari Dilip Ananda has successfully given his/her Ph.D. Oral Examination held on **19/09/2024**

 19/09/24
Signature of Thesis Supervisor with date
(Prof. Rajneesh Misra)

ACKNOWLEDGEMENT

I would like to express my gratitude to several individuals who were supporting me to complete this long journey of Ph.D.

First of all I would like to offer my sincere gratitude to my supervisor Prof. Rajneesh Misra for shaping my career. His exemplary guidance, constant encouragement and careful monitoring throughout the journey are so great that, even my most profound gratitude is not enough. I truly dedicate this thesis to him as it would not have been possible without his persistent help, support and kindness.

I extend my profound thanks to my PSPC members Dr. Chelvam Venkatesh and Dr. Surya Prakash for their valuable suggestions and guidance.

I would like to express my special thanks of gratitude to Prof. Suhas S. Joshi [Director, Indian Institute of Technology Indore] for providing and accessing all the facilities at Indian Institute of Technology Indore.

I would like to express my thanks to IIT Indore and Ministry of Human Resource Development (MHRD) for infrastructure and to CSIR New Delhi, for financial help through fellowship.

I am grateful to Prof. Tushar Kanti Mukherjee (Head, Discipline of Chemistry, Indian Institute of Technology Indore) for his guidance and support. Also, I would like to extend my thanks to Prof. Suman Mukhopadhyay, Prof. Biswarup Pathak, Prof. Shaikh M. Mobin, Dr. Tridib Kumar Sarma, Prof. Anjan Chakraborty, Prof. Sampak Samanta, Prof. Sanjay Singh, Dr. Satya Bulusu, Dr. Chelvam Venkatesh, Dr. Amrendra Kumar Singh, Dr. Debayan Sarkar, Dr. Abhinav Raghuvanshi, Dr. Dipak Kumar Roy, Dr. Selvakumar Sermadurai, Dr. Pravarthana Dhanapal and Dr. Umesh A. Kshirsagar for their guidance and help during various activities.

I am thankful to Mr. Kinney Pandey, Mr. Ghansyam Bhavsar, Mr. Parthiban P K, Mr. Manish Kushwaha, Mr. Rameshwar and Ms. Vinita Kothari for their technical help and support.

I take this opportunity to express a deep sense of gratitude to my group members, Dr. Yuvraj Patil, Dr. Ramana Reddy, Dr. Gangala Sivakumar, Dr. Shubhra Bikash Maity, Dr. Ramireddy Eda, Dr. Madhurima Poddar, Dr. Yogajivan, Dr. Anupama, Dr. Faizal, Dr. Manju, Indresh, Charu, Wazid, Pankaj, Nikhil Ji, Deeksha, Ramakant, Amiy, Nitin, Kusum, Vivak, Shivangi, Akansha and Sandeep for their kind cooperation and cheerful support.

My heart-felt thanks to my splendid juniors and seniors at IIT Indore for their generous co-operation and help.

My Ph.D. journey at IIT Indore was exciting, fulfilling, and rewarding. I am taking a bagful of experiences and memories from here and would like to acknowledge each one who was a part of this beautiful journey.

Thank You...

PINJARI DILIP ANANDA

**DEDICATED TO
MY TEACHERS, FAMILY AND
FRIENDS**

- PINJARI DILIP ANANDA

SYNOPSIS

Near-infrared (NIR) absorbing chromophores have been extensively used in organic photovoltaics, light emitting devices, photothermal therapy, and bioimaging. Aza-boron-difluoride dipyrromethenes (Aza-BODIPYs) are a class of NIR absorbing dyes derived from BODIPY dyes by the replacement of *meso*-carbon with a nitrogen atom (Figure 1). In aza-BODIPY, the presence of a nitrogen atom at the *meso*-position with a lone pair of electrons perturbs the frontier energy levels, which leads to the lowering of the HOMO-LUMO gap as compared to the parent BODIPY. The aza-BODIPY dye possesses unique properties such as absorption covering the visible-NIR region, excellent photochemical and thermal stability. It has a fully conjugated framework, making it easy to modify its structure to improve absorption and emission properties. As compared to BODIPY, aza-BODIPY dyes show red shifted absorption and emission bands. The majority of literature reports describe aza-BODIPYs with tetraaryl substitutions on positions 1, 3, 5, and 7 of the pyrrole rings. The substitution of various aryl moieties at α and β -positions of the aza-BODIPY perturbs its photophysical and electrochemical properties significantly. Several studies on the photophysical and electrochemical investigations of aza-BODIPY dyes, along with their applications have been carried out over the past couple of decades.

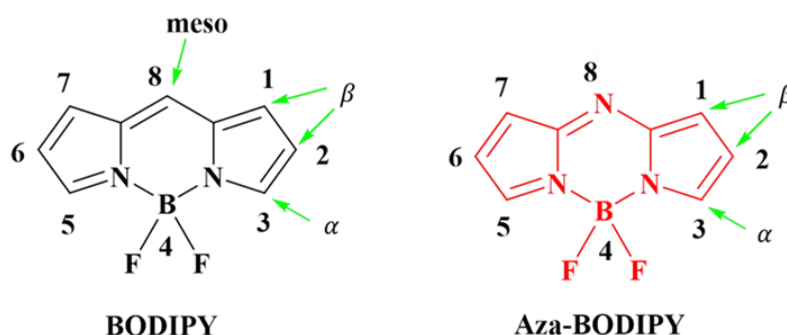


Figure 1. Chemical structure of BODIPY and aza-BODIPY dyes.

In this work, we explore different donor (triphenylamine, phenothiazine, *N,N* dimethylaniline, anisole etc.) and acceptor (TCBD) functionalized aza-BODIPY dyes. The optical and electrochemical properties of these donor-acceptor (D–A) chromophores along with computational calculations were studied. The aza-BODIPY derivatives presented in this work have been classified as the symmetrical aza-dipyrromethene and aza-BODIPY dyes based on the functionalization at the 1, 3, 5 and 7 positions (Figure 2). The functionalization of same donor or acceptor units on 1, 3, 5 and 7 positions or functionalization of same substituent at 1, 7 position and 3, 5 position results in symmetrical aza-BODIPY dyes. On the other hand, the substitution of various donor/acceptor units at one side on 1, 3, 5, and 7 positions results in unsymmetrical aza-BODIPY dyes (Figure 2).

The main objectives of the present study are:

1. To design and synthesis of donor-/acceptor functionalized aza-dipyrromethenes and aza-BODIPYs.
2. Investigate the optical and electrochemical properties of the donor-/acceptor functionalized aza-dipyrromethenes and aza-BODIPYs.
3. To study the effect of different donor functionalization on the optical and electrochemical properties of aza-BODIPY dye.
4. To understand the effect of incorporation of tetra-cyano acceptors (TCBD and DCNQ) on ethyne bridged donor functionalized aza-BODIPYs.
5. To tune the HOMO–LUMO energy gap by functionalizing donor/acceptor substituents to the aza-BODIPYs.
6. To understand the HOMOs and LUMOs of aza-BODIPY dyes and their energy levels energy with the help of DFT and the TD-DFT calculations.

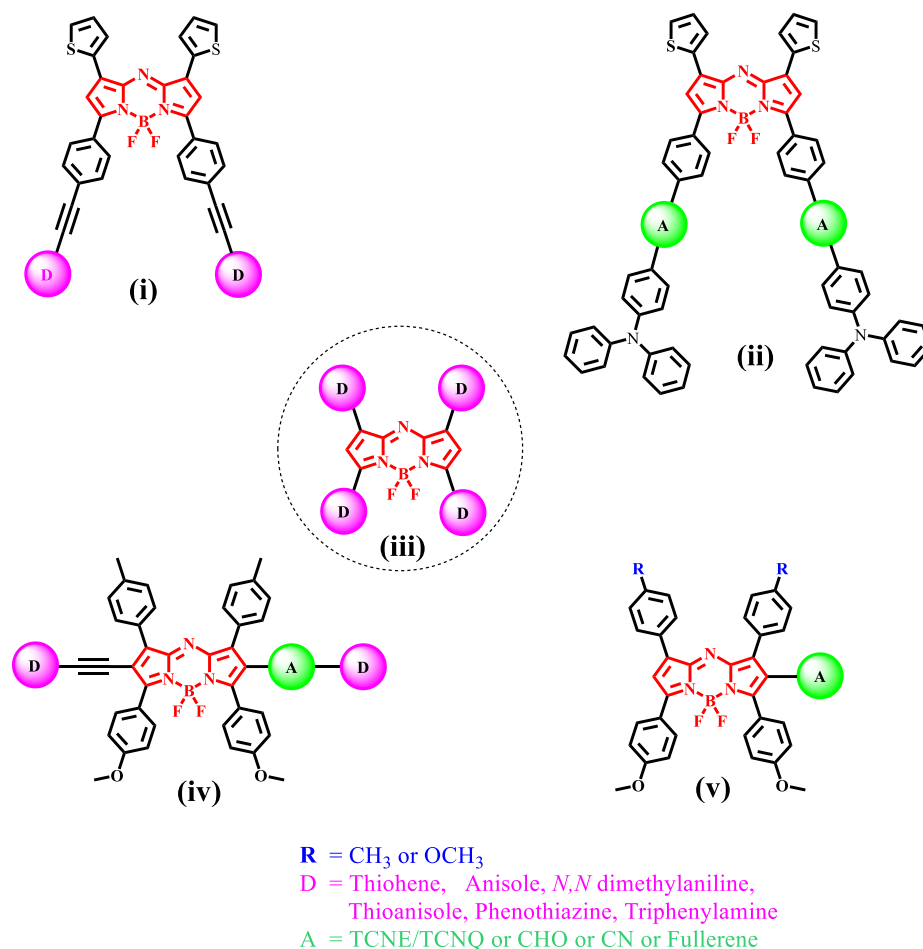


Figure 2. General classification of aza-BODIPYs in this work.

Chapter 1: Introduction

This chapter describes the synthesis and functionalization approaches of aryl substituted aza-BODIPY derivatives along with their applications in biomedicine and material science.

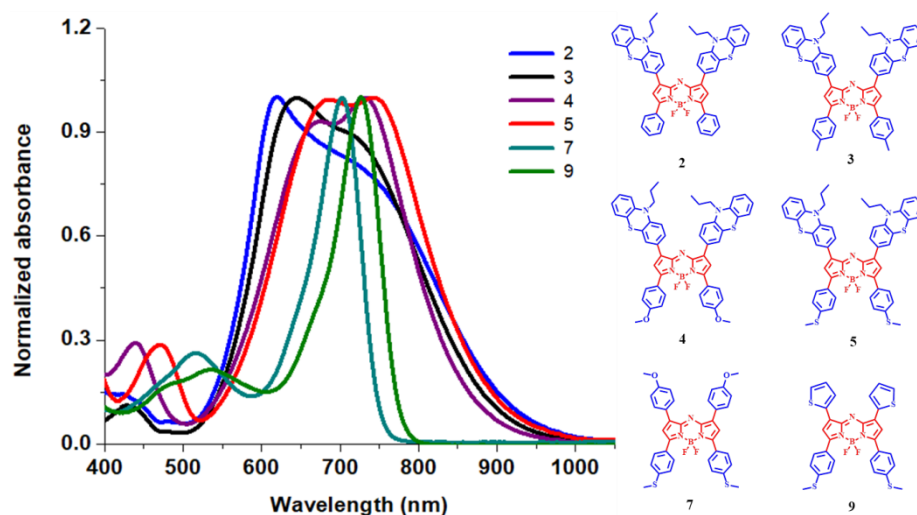
Chapter 2: Materials and experimental techniques

In this chapter we provided an overview of the general experimental methods, characterization techniques and details of instruments used in the characterization.

Chapter 3: NIR absorbing donor-acceptor functionalized aza-BODIPYs: synthesis, photophysical and electrochemical properties

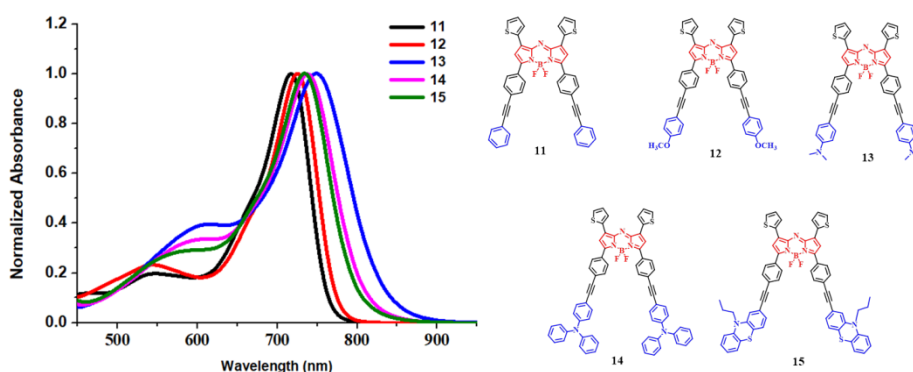
In Chapter 3, a series of tetra-aryl functionalized aza-boron-dipyrromethenes (aza-BODIPYs) **2–5**, **7**, and **9** were designed and synthesized by the condensation reaction followed by complexation

with boron trifluoride diethyl etherate ($\text{BF}_3 \cdot \text{OEt}_2$). Their photophysical and electrochemical properties were investigated and compared with previously reported tetraphenyl, tetraanisole, tetrathioanisole and tetrathienyl substituted aza-BODIPY dyes **1**, **6**, **8**, and **10**, with respect to variation in the number and strength of aryl donors respectively. The electronic absorption spectra of the aza-BODIPYs **1–10** exhibited a broad absorption covering the UV-visible to near-infrared region. The substitution of electron donating moieties on aza-BODIPY leads to exhibit good electronic communication with acceptor aza-BODIPY, resulting in broad and red shifted absorption towards near-infrared region. The aza-BODIPY **5** showed a red shifted absorption compared to other aza-BODIPY dyes (**2–4**, **7** and **9**) due to the strong electron donating nature of phenothiazine and thioanisole. The electrochemical studies on aza-BODIPY derivatives (**2–5**, **7** and **9**) show multiple oxidation and reduction potentials corresponding to donor and acceptor (aza-BODIPY) moieties. The computational calculations reveal strong donor-acceptor interaction between different donors and aza-BODIPY core, exhibiting low HOMO-LUMO gap values ranging from 1.81 to 2.19 eV.



Chapter 4: NIR absorbing different donor functionalized ethyne bridged α -aza BODIPYs

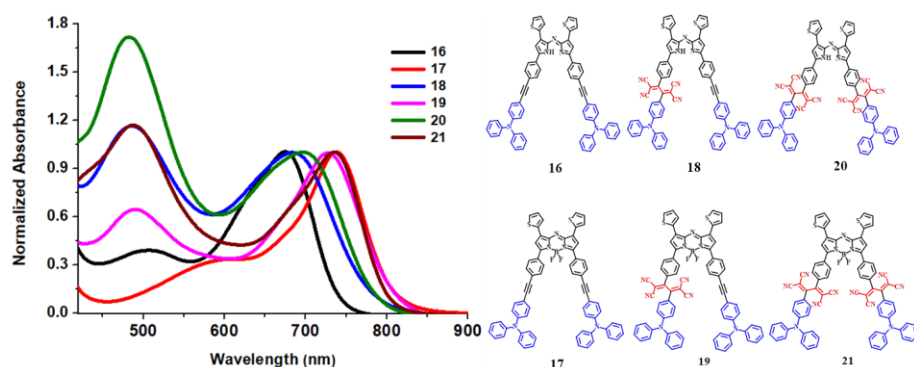
In Chapter 4, a set of donor-functionalized aza-BODIPYs **11–15** were designed and synthesized by using the Pd-catalyzed Sonogashira cross-coupling reaction followed by complexation with boron trifluoride diethyl etherate ($\text{BF}_3 \cdot \text{Et}_2\text{O}$), and studied their photophysical and redox properties. The absorption spectra of *N,N*-dimethylaniline substituted aza-BODIPY **13** show a red-shifted absorption compared to other donor substituted aza-BODIPYs **11**, **12**, **14**, and **15**. The electrochemical studies demonstrate that aza-BODIPYs **11–15** display two oxidation waves and two reduction waves due to aza-BODIPY core. The computational calculation reveal that the HOMOs of the aza-BODIPYs **11–15** are located on the donor (phenyl, anisole, *N,N*-dimethylamine, triphenylamine, phenothiazine) moiety, whereas the LUMOs are predominantly located on the acceptor (aza-BODIPY) moiety.



Chapter 5: Triphenylamine functionalized NIR absorbing α -aza-dipyrromethenes and α -aza-BODIPYs

In Chapter 5, a set of triphenylamine functionalized aza-dipyrromethenes and aza-BODIPYs **16–21** were designed and synthesized by the Pd-catalyzed Sonogashira cross-coupling reaction and [2 + 2] cycloaddition-retroelectrocyclization reaction. The effect of substitution of triphenylamine (TPA) donor and tetracyanoethylene (TCNE) acceptor on the photophysical and electrochemical properties were explored. The effect of BF_2 complexation was studied which

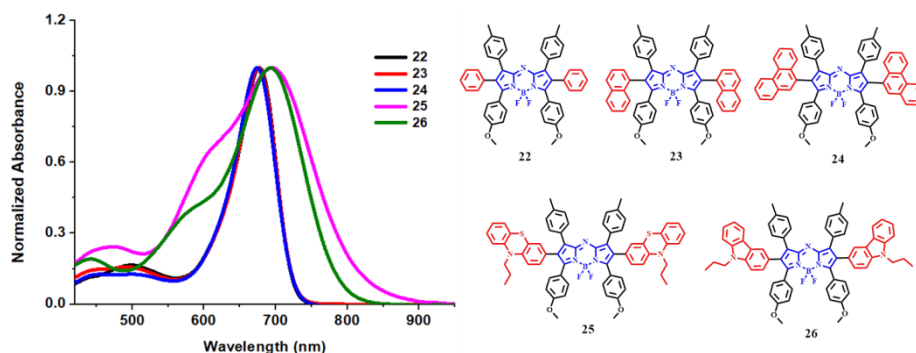
showed the incorporation of BF₂ leads to the red shift in absorption with decrease in HOMO-LUMO gap. The electrochemical analysis exhibited multiple oxidation and reduction waves. The results of photophysical and electrochemical studies show substantial donor-acceptor interaction of TPA donor with aza-BODIPY and tetracyanobutadiene (TCBD) core. The computational calculations for aza-dipyrromethenes and aza-BODIPYs **16–21** reveals that the electron density transfers from TPA (donor) to aza-BODIPY and tetracyanobutadiene (acceptor) core.



Chapter 6: Near-infrared Absorbing Different Donor Functionalized β -aza-BODIPYs

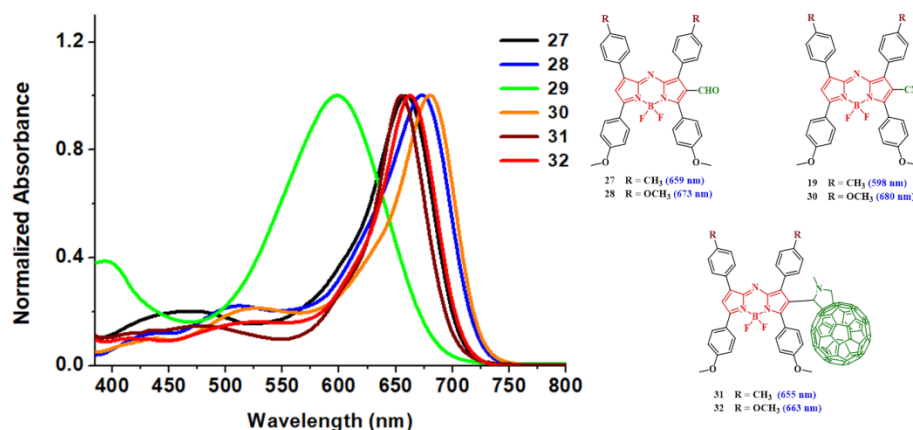
In chapter 6, we report the NIR absorbing 2,6-diarylated aza-BODIPYs **25** and **26** with phenothiazine and carbazole substituents were designed and synthesized by the Pd-catalyzed Suzuki cross-coupling reaction. Their photophysical and electrochemical properties were investigated and compared with 2,6-diarylated phenyl, naphthalene, and phenanthrene-substituted aza-BODIPYs **22**, **23**, and **24**, with respect to the variation in the strength of aryl donors respectively. The photophysical, electrochemical, and computational studies of these dyes were investigated, revealing donor-acceptor interactions and the tuning of the HOMO-LUMO gap. The electronic absorption spectra of phenothiazine and carbazole substituted aza-BODIPY dyes **25** and **26** showed a red-shifted absorption compared to those of aza-BODIPY dyes **22–24**, which are substituted with phenyl, naphthalene, and phenanthrene. The electrochemical properties of aza-BODIPY dyes

22–26 show multiple oxidation and reduction potentials due to donor and acceptor moieties. The computational calculations demonstrated a lower HOMO-LUMO gap for phenothiazine and carbazole functionalized aza-BODIPYs (**25** and **26**), compared to other aza-BODIPY derivatives (**22**, **23** and **24**).



Chapter 7: Exploring the effect of electron withdrawing functionalities (formyl, nitrile, and fullerene) on di and tetra-methoxy substituted β -aza-BODIPYs

In chapter 7, a series of formyl, nitrile, and fullerene substituted di- and tetra-methoxy based aza-BODIPYs (**27–32**) were designed and synthesized. Their photophysical properties revealed tunable absorption spanning from the ultraviolet to visible region. Significant red shift was observed in case of absorption of tetra-methoxy based aza-BODIPYs (**28**, **30**, and **32**) compared to their di-methoxy aza-BODIPY counterparts (**27**, **29**, and **31**), related to the strong electron donating ability of the methoxy substituent over the methyl substituent. The electrochemical study demonstrated that the substitution of electron-withdrawing groups (formyl, nitrile, and fullerene) resulted in additional low voltage reduction potential. The computational calculation for aza-BODIPYs **27–32** showed low HOMO–LUMO gap values and calculated absorption wavelengths are in good agreement with the experimental absorption values.



Chapter 8: Conclusions and future scope

This chapter summarizes the salient features of the work and prospects to design and synthesize new materials for the optoelectronic applications.

List of Publications

Including Thesis Papers:

1. Pinjari, D.,[‡] Alsaleh, A. Z.,[‡] Patil, Y., Misra, R., and D'Souza, F., (2020), Interfacing High-Energy Charge-Transfer States to a Near-IR Sensitizer for Efficient Electron Transfer upon Near-IR Irradiation. *Angew. Chem. Int. Ed.*, 59, 23697–23705. (DOI: 10.1002/anie.202013036). (Impact Factor = 16.823)
2. Pinjari D.,[‡] Imran M.,[‡] Dad P., Misra R., Zhao J., Near-IR-Absorbing Bis-Donor Functionalized Aza-BODIPY Derivatives: Synthesis and Photophysical Study by Using Transient Optical Spectroscopy. *Chem. Eur. J.*, 2024. (DOI: 10.1002/chem.202303799). (Impact Factor = 5.02)
3. Alsaleh, A. Z., Pinjari, D., Misra, R., and D'Souza, F., (2023), Far-Red Excitation Induced Electron Transfer in Bis Donor-AzaBODIPY Push-Pull Systems; Role of Nitrogenous Donors in Promoting Charge Separation. *Chem. Eur. J.*, 29 (53), e2023016. (DOI: 10.1002/chem.202301659). (Impact Factor = 5.02)
4. Alsaleh A. Z.,[‡] Pinjari D.,[‡] Das S.,[‡] Misra R. and D'Souza F., (2024), Broad-Band Capturing Tetracyanobutadiene Incorporated

Phenothiazine-azaBODIPY Push-Pull Systems: Excited State Charge Separation and Relaxation Dynamics, *J. Phys. Chem. C.*, 128, 17, 7188–7201 (DOI: 10.1021/acs.jpcc.4c00583). (Impact Factor = 3.7)

5. Pinjari D., Y. Patil, and Misra R., (2024), Near-Infrared Absorbing Aza-BODIPY Dyes for Optoelectronic Applications, *Chem. Asian J.*, e202400167. (DOI: 10.1002/asia.202400167. (Impact Factor = 4.84)

Additional Paper:

1. Guragain, M.,[‡] Pinjari, D.,[‡] Misra, R., and D'Souza, F., (2023), Zinc Tetrapyrrole Coordinated to Imidazole Functionalized Tetracyanobutadiene or cyclohexa-2,5-diene-1,4-diylidene-expanded-tetracyanobutadiene Conjugates: Dark vs. Light-Induced Electron Transfer. *Chem. Eur. J.*, 29 (68), e202302665. (DOI: 10.1002/chem.202302665). (Impact Factor = 5.02)

[‡] Authors having equal contribution

TABLE OF CONTENTS

1. List of Figures	xiii
2. List of Schemes	xvi
3. List of Tables	xviii
4. List of Charts	xix
5. Acronyms	xx
6. Nomenclature	xxi

Chapter 1: Introduction

1.1. Introduction	1
1.2. Donor-Acceptor system	1
1.3. Aza-BODIPY	3
1.4. General synthetic strategies	5
1.4.1. O'Shea's method for the synthesis of aza-BODIPY (6)	6
1.4.2. Carreira's method for the synthesis of aza-BODIPY (10)	6
1.4.3. Lukyanet's method for the synthesis of aza-BODIPY (14)	6
1.4.4. Jiang's synthesis of the morpholino-containing aza-BODIPY (18)	7
1.5. Photophysical properties	8
1.6. Applications of aza-BODIPY dyes	9
1.6.1. Organic Photovoltaics	9
1.6.2. Boron Neutron Capture Therapy	13
1.6.3. Photodynamic therapy (for cancer treatment)	16
1.6.4. Fluorescence sensors	20
1.6.5. Photo-redox catalysis	23
1.6.6. Photoacoustic probes	24
1.6.7. Energy-transferring chromophores in optoelectronics	27
1.7. References	31

Chapter 2: Materials and experimental techniques

2.1. Introduction	
2.2. Chemicals for synthesis	
2.3. Spectroscopic measurements	

- 2.3.1. Mass spectrometry
- 2.3.2. NMR spectroscopy
- 2.3.3. UV–vis spectroscopy
- 2.4. Electrochemical studies
- 2.5. Computational calculations
- 2.6. References

Chapter 3: NIR absorbing donor-acceptor functionalized aza-BODIPYs: synthesis, photophysical and electrochemical properties

3.1.	Introduction	52
3.2.	Results and Discussion	53
3.3.	Photophysical Properties	55
3.4.	Electrochemical Properties	57
3.5.	Computational studies	61
3.6.	Experimental Section	64
3.7.	Conclusion	67
3.8.	References	68

Chapter 4: NIR absorbing different donor functionalized ethyne bridged α -aza BODIPYs

4.1.	Introduction	76
4.2.	Results and Discussion	77
4.3.	Photophysical Properties	78
4.4.	Electrochemical Properties	81
4.5.	Theoretical Calculations	83
4.6.	Experimental Section	86
4.7.	Conclusion	90
4.8.	References	90

Chapter 5: Triphenylamine functionalized NIR absorbing α -aza-dipyrromethenes and α -aza-BODIPYs

5.1.	Introduction	94
5.2.	Results and Discussion	95

5.3.	Photophysical Properties	97
5.4.	Electrochemical Properties	99
5.5.	Theoretical Calculations	101
5.6.	Experimental Section	103
5.7.	Conclusion	107
5.8.	References	107
Chapter 6: Near-infrared Absorbing Different Donor Functionalized β-aza-BODIPYs		
6.1.	Introduction	114
6.2.	Results and Discussion	115
6.3.	Photophysical Properties	116
6.4.	Electrochemical Properties	118
6.5.	Theoretical Calculations	120
6.6.	Experimental Section	122
6.7.	Conclusion	125
6.8.	References	125
Chapter 7: Exploring the effect of electron withdrawing functionalities (formyl, nitrile, and fullerene) on di and tetra-methoxy substituted β-aza-BODIPYs		
7.1.	Introduction	131
7.2.	Results and Discussion	132
7.3.	Photophysical Properties	133
7.4.	Electrochemical Properties	135
7.5.	DFT Calculations	139
7.6.	Experimental Section	143
7.7.	Conclusion	146
7.8.	References	147
Chapter 8: Conclusions and future scope		
8.1.	Conclusions	156
8.2.	Future Scope	159
8.3.	References	159

LIST OF FIGURES

Chapter 1. Introduction

- Figure 1.1.** Schematic representation of HOMO and LUMO energy levels in D–A system. 3
- Figure 1.2.** The structure and numbering of BODIPY and aza-BODIPY molecules 4
- Figure 1.3.** Absorption spectra of donor/acceptor based aza-BODIPY dye (**19**). 8
- Figure 1.4.** UV-visible absorption of **31** and **32** in dichloromethane solution (S) and thin film (F). 11
- Figure 1.5.** Laser-induced breakdown spectroscopy (LIBS) elemental imaging of boron from tumor sections collected at day 16 showing the presence of remaining boron in tumors treated with aza-SWIR-BSH-01 (**37**). 15
- Figure 1.6.** Tumor growth curves in evaluation of tumor growth inhibition in HeLa-tumor bearing xenograft model mediated by PDT. 18
- Figure 1.7.** The pH dependence of absorption (solid lines) and emission spectra (dashed lines) of indicator **64** (a) and the state-of-the-art hydroxy-aza-BODIPY pH indicator (c) in hydrogel D4; (b) and (d) show the pH equilibria for the respective dyes. 22
- Figure 1.8.** a) Chemical structures of aza-BODIPY derivatives **77** (rHyP-1) and **78** (red-rHyP-1) used in photoacoustic imaging; (b) Normalized absorption spectra of **77** and **78** in chloroform. (c) PA spectra of **77** and **78** in chloroform. 27
- Figure 1.9.** Thin film UV–Vis spectra for (a) **79** and (b) **80** spin-coated from CHCl₃ solution. Fluorescence spectral changes of (c) **79** (5 mM) and (d) **80** (5 mM) upon

incremental addition of Co^{2+} (0 to 20 equiv.) in THF solution. 29

Figure 1.10. IPCE (%) curves of (i) **83** (C_{60}py_2 : $(\text{ZnP})_2$ -azaBODIPY tetrad), (ii) **82** ($(\text{ZnP})_2$ -azaBODIPY triad), and (iii) C_{60}py_2 : $(\text{ZnP})_2$ donor–acceptor systems electrophoretically deposited on the surface in acetonitrile solution containing (0.25 M LiI, 0.25 M butyl methyl imidazolium iodide (BMII), 0.05 M I₂) for I[–]/I₃[–] redox mediator. 31

Chapter 3: NIR absorbing donor-acceptor functionalized aza-BODIPYs: synthesis, photophysical and electrochemical properties

Figure 3.1. Chemical structures of tetra-aryl functionalized aza-BODIPYs **1–10**. 53

Figure 3.2. Normalized electronic absorption spectra of aza-BODIPYs **2–5**, **7** and **9** in DCM (1×10^{-5} M). 55

Figure 3.3. Cyclic voltammograms (CVs) of aza-BODIPYs **2–5**, **7** and **9** in dichloromethane containing 0.1 M solution of TBAPF₆ with a scan rate of 0.100 V/s. 58

Figure 3.4. Cyclic voltammograms (CVs) of aza-BODIPYs **2–5**, **7** and **9** in dichloromethane containing 0.1 M solution of TBAPF₆ with a scan rate of 0.100 V/s. 59

Figure 3.5. HOMO–LUMO energy level diagram of tetra-aryl substituted aza-BODIPYs **1** and **10**. 61

Figure 3.6. HOMO–LUMO energy level diagram of tetra-aryl substituted aza-BODIPYs **2–5**. 62

Figure 3.7. HOMO–LUMO energy level diagram of tetra-aryl substituted aza-BODIPYs **6–9**. 63

Chapter 4: NIR absorbing different donor functionalized ethyne bridged α -aza BODIPYs

Figure 4.1. Chemical structures of donor functionalized aza-BODIPY dyes **2–6**. 77

Figure 4.2. Normalized electronic absorption spectra of aza-BODIPYs **2–6** in DCM (1×10^{-5} M). 79

Figure 4.3. Cyclic voltammograms (CVs) and DPV plot of aza-BODIPYs **2–6**. 81

Figure 4.4. Cyclic voltammograms (CVs) and DPV plot of aza-BODIPYs **2–6**. 82

Figure 4.5. FMOs of aza-BODIPY dyes **2–6** at B3LYP/6-31G (d, p) level. 84

Figure 4.6. Energy level diagram for FMOs of aza-BODIPY dyes **2–6** estimated by DFT calculations. 85

Chapter 5: Triphenylamine functionalized NIR absorbing α -aza-dipyrromethenes and α -aza-BODIPYs

Figure 5.1. Chemical structures of aza-dipyrromethene and aza-BODIPY dyes **2–7**. 95

Figure 5.2. Normalized electronic absorption spectra of aza-BODIPYs **2–7** in DCM (1×10^{-5} M). 97

Figure 5.3. Cyclic voltammograms (CV) of plots of aza-dipyrromethenes and aza-BODIPYs **2–7**. 99

Figure 5.4. FMOs of aza-dipyrromethenes and aza-BODIPYs **2–7** at the B3LYP/6-31G(d, p) level. 101

Chapter 6: Near-infrared Absorbing Different Donor Functionalized β -aza-BODIPYs

Figure 6.1. Chemical structure of aza-BODIPYs **3–7**. 115

Figure 6.2. Normalized electronic absorption spectra of aza-BODIPYs **3–7** in DCM (1×10^{-5} M). 117

Figure 6.3.	Cyclic voltammograms (CVs) plots of aza-BODIPY dyes a) 3 , b) 4 , c) 5 , d) 6 and e) 7 .	119
Figure 6.5.	FMOs of aza-BODIPYs 3–7 at B3LYP/6-31G (d, p) level.	121
Figure 6.6.	Energy level diagram of the FMOs of the aza-BODIPYs 3–7 calculated by DFT calculations.	121
Chapter 7:	Exploring the effect of electron withdrawing functionalities (formyl, nitrile, and fullerene) on di and tetra-methoxy substituted β-aza-BODIPYs	
Figure 7.1.	Chemical structures of functionalized di- and tetra-methoxy substituted aza-BODIPYs 1–6 .	132
Figure 7.2.	Normalized electronic absorption spectra of aza-BODIPYs 1–6 in dichloromethane solvent (1×10^{-5} M).	134
Figure 7.3.	Cyclic voltammograms (CVs) plots of functionalized di- and tetra-methoxy based aza-BODIPYs 1–6 .	136
Figure 7.4.	Cyclic voltammograms (CVs) plots of functionalized di- and tetra-methoxy based aza-BODIPYs 1–6 .	137
Figure 7.5.	FMOs of functionalized di- and tetra-methoxy aza-BODIPYs 1–4 .	139
Figure 7.6.	FMOs of functionalized di- and tetra-methoxy aza-BODIPYs 5 and 6 .	140
Figure 7.7.	The HOMO–LUMO energy level diagram of di- and tetra-methoxy substituted aza-BODIPYs 1–6 .	141

LIST OF SCHEMES

Chapter 1: Introduction

Scheme 1.1.	O'Shea's method for synthesis of aza-BODIPY (6)
--------------------	--

Scheme 1.2.	Carreira's method for the synthesis of aza-BODIPY (10).	6
Scheme 1.3.	Lukyanet's method for the synthesis of aza-BODIPY (14).	6
Scheme 1.4.	Jiang's synthesis of the morpholino-containing aza-BODIPY (18).	7
Scheme 1.5.	Photooxygenation of 1-naphthol by using aza-BODIPY 72.	24
Chapter 3:	NIR absorbing donor-acceptor functionalized aza-BODIPYs: synthesis, photophysical and electrochemical properties	
Scheme 3.1.	Synthetic route for aryl functionalized aza-BODIPY dyes 2–5, 7 and 9.	54
Chapter 4:	NIR absorbing different donor functionalized ethyne bridged α-aza BODIPYs	
Scheme 4.1.	Synthetic route for donor functionalized aza-BODIPY dyes 2–6.	78
Chapter 5:	Triphenylamine functionalized NIR absorbing α-aza-dipyrromethenes and α-aza-BODIPYs	
Scheme 5.1.	Synthesis of TPA substituted aza-dipyrromethene 2 and aza-BODIPY 3.	96
Scheme 5.2.	Synthetic route for TCBD bridged aza-dipyrromethenes and aza-BODIPYs 4–7.	96
Chapter 6:	Near-infrared Absorbing Different Donor Functionalized β-aza-BODIPYs	
Scheme 6.1.	Synthetic route for donor functionalized aza-BODIPY dyes 3–7.	116
Chapter 7:	Exploring the effect of electron withdrawing functionalities (formyl, nitrile, and fullerene) on di and tetra-methoxy substituted β-aza-BODIPYs	

Scheme 7.1.	Synthesis of functionalized di- and tetra-methoxy substituted aza-BODIPYs 1–6 .	133
--------------------	--	-----

LIST OF TABLES

Chapter 1:	Introduction	
Table 1.1.	Solar cell power conversion efficiencies of aza-BODIPY dyes 20–34 .	13
Table 1.2.	Singlet oxygen quantum yields for aza-BODIPY derivatives 38–55 .	19
Chapter 3:	NIR absorbing donor-acceptor functionalized aza-BODIPYs: synthesis, photophysical and electrochemical properties	
Table 3.1.	Photophysical properties of tetra-aryl functionalized aza-BODIPY dyes 1–10 .	57
Table 3.2.	Electrochemical properties of tetra-aryl functionalized aza-BODIPYs 2–5, 7 and 9 .	60
Chapter 4:	NIR absorbing different donor functionalized ethyne bridged α-aza BODIPYs	
Table 4.1.	Photophysical and computational properties of aza-BODIPY dyes 2–6 .	80
Table 4.2	Electrochemical properties of aza-BODIPY dyes 2–6 .	83
Table 4.2.	Calculated major electronic transitions for 2–6 in the gas phase.	86
Chapter 5:	Triphenylamine functionalized NIR absorbing α-aza-dipyrromethenes and α-aza-BODIPYs	
Table 5.1.	Photophysical properties of TPA functionalized aza-dipyrromethenes and aza-BODIPYs 2–7 .	98

Table 5.2.	Electrochemical properties of aza-dipyrromethenes and aza-BODIPYs 2–7 .	100
Table 5.3.	Calculated major electronic transitions for aza-dipyrromethenes and aza-BODIPYs 2–7 in the gas phase.	102
Chapter 6:	Near-infrared Absorbing Different Donor Functionalized β-aza-BODIPYs	
Table 6.1.	The photophysical properties of aza-BODIPYs 3–7 .	118
Table 6.2.	Electrochemical properties of aza-BODIPYs 3–7 .	120
Chapter 7:	Exploring the effect of electron withdrawing functionalities (formyl, nitrile, and fullerene) on di and tetra-methoxy substituted β-aza-BODIPYs	
Table 7.1.	The photophysical and computational properties of aza-BODIPYs 1–6 .	135
Table 7.2.	Electrochemical properties of functionalized di- and tetra-methoxy based aza-BODIPYs 1–6 .	138
Table 7.3.	Calculated major electronic transition for aza-BODIPYs 1–6 in the gas phase.	142

LIST OF CHARTS

Chapter 1:	Introduction	
Chart 1.1.	Chemical structures of electron donor units.	2
Chart 1.2.	Chemical structures of electron acceptor units.	2
Chart 1.3.	Aza-BODIPYs based chromophore 20–34 .	10
Chart 1.4.	Aza-BODIPYs based chromophore 35–37 .	14
Chart 1.5.	Aza-BODIPYs based chromophore 38–55 .	17
Chart 1.6.	Aza-BODIPYs based chromophore 56–59 .	20
Chart 1.7.	Aza-BODIPYs based chromophore 60 and 66 .	21
Chart 1.8.	Aza-BODIPYs based chromophore 67–73 .	23
Chart 1.9.	Aza-BODIPYs based chromophore 74–76 .	25
Chart 1.10.	Aza-BODIPYs based chromophore 79–80 .	28

ACRONYMS

D–A	Donor–acceptor
NMR	Nuclear Magnetic Resonance
PPh ₃	Triphenylphosphine
DMF	Dimethylformamide
DCM	Dichloromethane
Ph	phenyl
IR	Infrared
UV-Vis	UV-Visible Spectroscopy
Calcd.	Calculated
CDCl ₃	Chloroform-d
ESI-MS	Electrospray Ionization- Mass Spectrometry
EtOH	Ethanol
MeOH	Methanol
THF	Tetrahydrofuran
TLC	Thin Layer Chromatography
TEA	Triethylamine

NOMENCLATURE

λ	Wavelength
ε	Extinction coefficient
α	Alfa
β	Beta
γ	Gamma
π	Pi
ϕ	Fluorescence quantum yield
σ	Sigma
\AA	Angstrom
nm	Nanometer
cm	Centimeter
$^{\circ}$	Degree
$^{\circ}\text{C}$	Degree Centigrade
mmol	Millimol
mL	Milliliter
μL	Microliter
a. u.	Arbitrary Unit

Chapter 1

1.1. General Introduction

The growing requirement of energy has captured the attention of scientific community towards generation of clean and renewable energy sources at low cost. The generation of energy from sunlight using solar cell devices is one of the most significant long-term solution. The π -conjugated polymers and small molecules are of significant interest due to their number of applications such as organic light-emitting diodes (OLEDs), organic solar cells (OSCs), two photon absorption and organic field-effect transistors (OFETs).^[1,2] The thermal stability, broad absorption in the visible region and low HOMO-LUMO gap values in small organic molecules make them potential candidate for optoelectronics.^[3] Donor-acceptor (D-A) approach is one of the useful ways to design the materials with absorption in Vis-NIR region with low band gap.

1.2. Donor-Acceptor Systems

The donor-acceptor (D-A) system consists of combination of electron rich donor with electron deficient acceptor through appropriate spacer (Figure 1.1).

Donor

The molecule which possesses the ability to donate the electron to another molecule is known as donor, for example, the groups containing heteroatoms with lone pair of electrons, amines, alcohols, sulphides etc. The other examples of metallocene derivatives such as ferrocene, ruthenocene and aromatic carbocycles are well known donors (Chart 1.2.). Triphenylamine (TPA), *N,N* dimethylaniline, phenothiazine, and carbazole are widely used donors for designing molecular systems with low HOMO-LUMO gap.^[4-6]

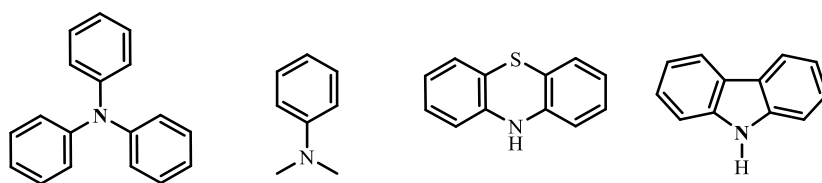


Chart 1.1. Chemical structures of electron donor units.

Acceptor

The molecule which possesses the ability to withdraw electrons from another molecule is known as acceptor. The acceptor strength of molecule to withdraw the electron depends on the lowest energy unoccupied molecular orbital (LUMO). Low lying the LUMO, stronger will be the accepting capacity of acceptor and *vice versa*. The examples of acceptors include amides, nitriles and esters, nitrogen rich heterocycles, boron complexes, ketones, tetracyano acceptors etc. (Chart 1.2.).

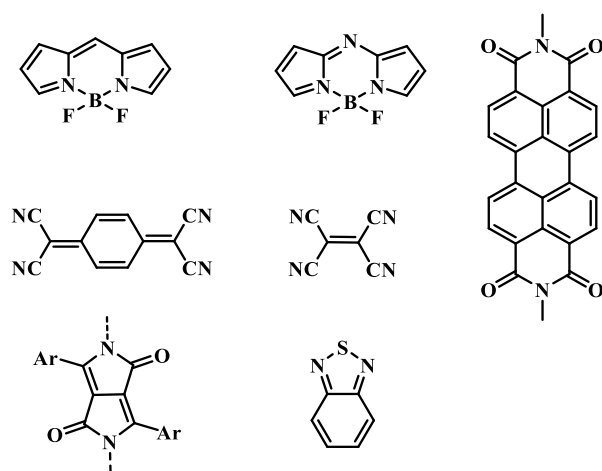


Chart 1.2. Chemical structures of electron acceptor units.

The LUMO of D-A system is stabilized as compared to individual donor and acceptor units, whereas the HOMO is destabilized as compared to that of individual donor and acceptor units (Figure 1.1.). The combination of donor and acceptor with appropriate π -linker (such as double or triple bond, aromatic ring) results in red shift of the absorption spectra with lowering of HOMO-LUMO gap.

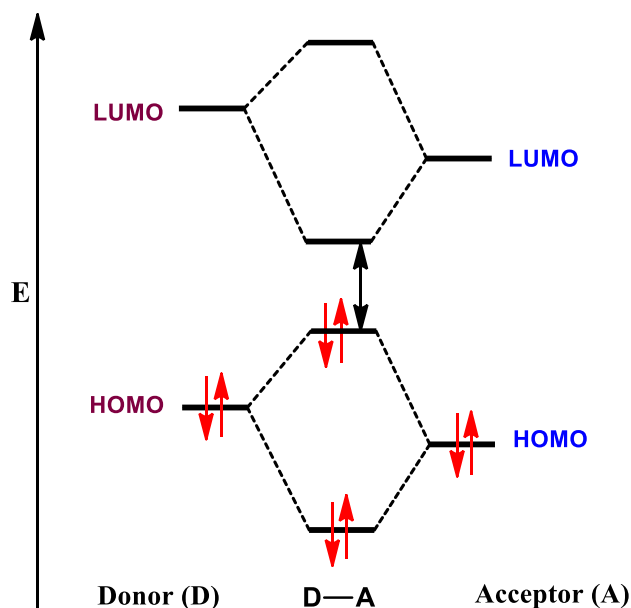


Figure 1.1. Schematic representation of HOMO and LUMO energy levels in D–A system.

The strength of D-A interaction depends on the strength of donor as well as strength of acceptor and the nature of π -linker also plays key role in determining the strength of D-A system.

The D-A systems exhibit various applications in diverse fields ^[7–9] such as;

- ❖ Organic Solar Cells (OSCs)
- ❖ Organic Light Emitting Diodes (OLEDs)
- ❖ Non-Linear Optics (NLO)
- ❖ Mechanochromism
- ❖ Organic Field Effect Transistors (OFETs)
- ❖ Photodynamic Therapy

1.3. Aza-boron-difluoride dipyrromethene (Aza-BODIPY)

Near-infrared (NIR) absorbing chromophores have been extensively used in variety of applications in organic photovoltaics, light emitting devices, photothermal therapy, and bioimaging.^[10–16] Aza-boron-difluoride dipyrromethene (Aza-BODIPY) are a class of NIR absorbing dyes derived from BODIPY by the replacement of *meso*-

carbon with a nitrogen atom (Figure 1.2.).^[17–21] In aza-BODIPY, the presence of a nitrogen atom in the *meso*-position with a lone pair of electrons perturbs the frontier energy levels, which leads to the lowering of the FMO energy gap as compared to the parent BODIPY.^[20,22–24]

The synthesis of BF₂-chelated BODIPY complex was reported in 1966 for the first time.^[25] In 1993, BF₂-chelated aza-BODIPY was reported.^[26] The majority of previously available reports describe aza-BODIPYs with tetraaryl substitutions on positions 1, 3, 5, and 7 of the pyrrole ring (Figure 1.2.).^[27–29]

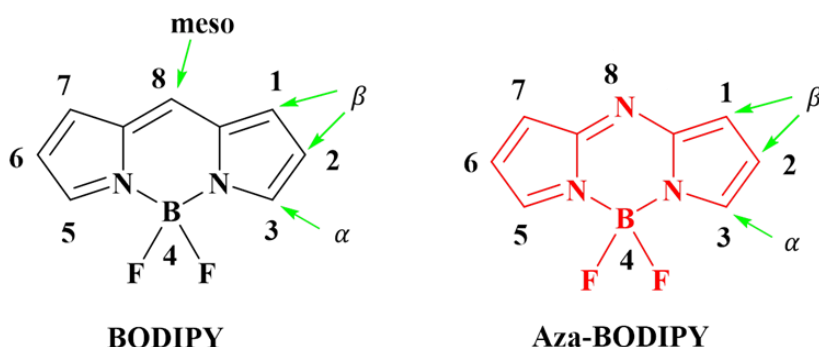


Figure 1.2. Chemical structure of BODIPY and aza-BODIPY dyes.

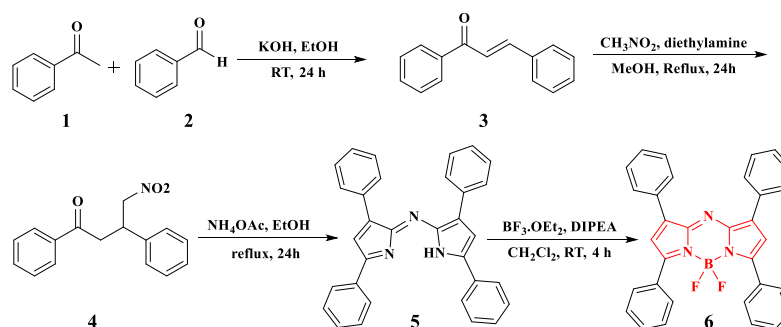
The aza-BODIPY dye possesses unique properties such as absorption covering the visible-NIR region, excellent photochemical and thermal stability.^[30–34] It has a fully conjugated framework, making it easy to modify its structure to improve spectral and fluorescence properties.^[35–37] The aza-BODIPYs exhibits red shifted absorption and emission bands as compared to BODIPY.^[38–40] The substitution of various aryl moieties at α , β -positions of the aza-BODIPY perturb its photophysical and electrochemical properties significantly.^[41–43] Several studies on the photophysical and electrochemical investigations of aza-BODIPY dyes, along with their applications have been carried out over the past couple of decades.^[44–46]

In this review, we have explained various synthetic strategies to synthesize aza-BODIPY dye, along with exploration of photophysical

properties of different aryl substituted aza-BODIPY derivatives. An overview of different aryl-substituted aza-BODIPY derivatives used in different applications such as organic photovoltaics, photodynamic therapy, boron neutron capture therapy, fluorescent probes, fluorescence sensing, photo-redox catalysis, and photoacoustic probes are provided. Furthermore, we have highlighted the change in optical properties and device performance associated with substituting various aryl moieties at different positions of the aza-BODIPY core.

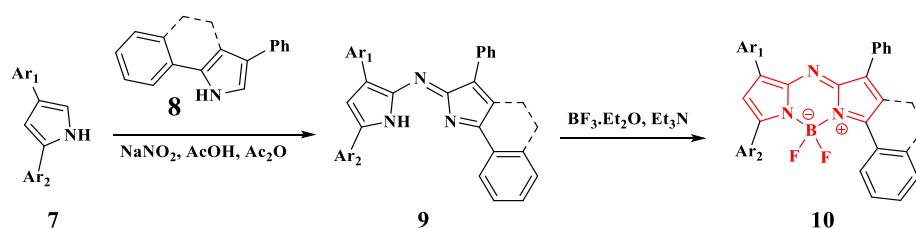
1.4. General synthetic strategies

Several routes have been reported till date for the synthesis of aza-BODIPY derivatives. Herein we describe few most commonly followed synthetic routes for the preparation of aza-BODIPY derivatives. In 2002, O'Shea and co-workers proposed the synthetic route for aza-BODIPY^[47], which has four steps, in which chalcone was synthesized in the first step by the aldol condensation of ketone (acetophenone) and benzaldehyde (aldehyde). The second step involves conversion of chalcone to its nitro derivative *via* Michael addition reaction with nitromethane and a diethylamine base. In the third step, the nitro derivative of chalcone undergoes chemical transformation in the presence of an ammonium source (ammonium acetate) to produce aza-dipyrrromethene, which further undergoes the fourth and final step, BF₂-complexation with boron trifluoride etherate (BF₃.OEt₂) and gives aza-BODIPY (**6**). This is a simple route with mild reaction conditions and gives a low yield (20–50%).



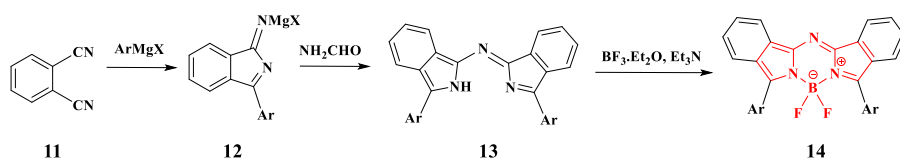
Scheme 1.1. O'Shea's method for aza-BODIPY (**6**) synthesis.

Later in 2006, Carreira and co-workers developed a synthetic method for the synthesis of symmetrical and asymmetrical aza-BODIPY (**10**), which includes a direct cyclization of substituted pyrrole followed by boron trifluoride complexation (Scheme 1.2.).^[48] This route provides higher yield (50%) compared to an earlier route by O'shea and co-workers. In this method the fused pyrrole molecular starting precursor was used to extend the π -conjugation.



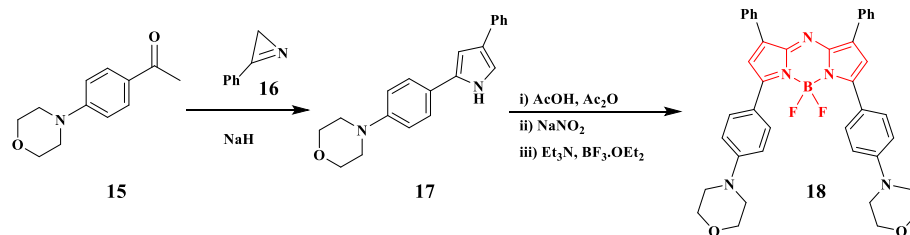
Scheme 1.2. Carreira's method for the synthesis of aza-BODIPY **10**.

Another method was provided by Lukyanets and co-workers in 2008 for the synthesis of symmetrical aza-BODIPY (**14**), which includes the reaction of aryl magnesium bromide with phthalonitrile followed by the boron trifluoride complexation (Scheme 1.3.).^[49] The main drawback with this route was the low yield (10–30%).



Scheme 1.3. Lukyanet's method for the synthesis of aza-BODIPY **14**.

In 2019, Jiang and co-workers has given a synthetic route for the preparation of aza-BODIPY (**18**) as shown in Scheme 1.4.^[50] The morpholino containing pyrrole (**17**) was obtained by the reaction of 1-(4-morpholinophenyl) ethanone with 3-phenyl-2H-azirine in the presence of sodium hydride. The morpholino containing pyrrole (**17**) was reacted with AcOH in acetone and then with NaNO₂, followed by complexation with BF₃.Et₂O to produce aza-BODIPY **18** in 42% yield.



Scheme 1.4. Jiang's synthesis of the morpholino-containing aza-BODIPY **18**.

There are several methods available in the literature to synthesize aryl substituted aza-BODIPYs, however the O'Shea's method is the most efficient method used for the synthesis of various aza-BODIPY based materials.

1.5. Photophysical Properties

Since last couple of decades, the chemistry of dipyrromethene dyes has drawn attention due to their ability to form stable coordination complexes. The π -conjugated dipyrromethene systems (e.g. BODIPY dyes) exhibit excellent optical features, such as strong absorption in the visible region, high molar absorption coefficients and high fluorescence quantum yields. Aza-BODIPY is an appealing chromophore due to its red-shifted absorption and emission spectra in comparison to the BODIPY core and also retains excellent optical features of the BODIPY.^[51–54] The presence of a nitrogen atom at the *meso*-position perturbs the energy levels, which leads to stabilization of the energy levels compared to BODIPY.^[55,56] This causes a bathochromic shift in the absorption spectrum in the 650–850 nm region, and the molar extinction coefficients in the range 7.5×10^4 – $9.5 \times 10^4 \text{ M}^{-1} \text{ cm}^{-1}$. Similar to BODIPY dyes, aza-BODIPY dyes also exhibit high molar extinction coefficients and moderate fluorescence quantum yields (ca. 0.20–0.40).^[46] The straightforward synthesis of the aza-BODIPY core and its red-shifted absorption, in contrast to its carbon analogue, present numerous possibilities for utilization in various optoelectronic applications.

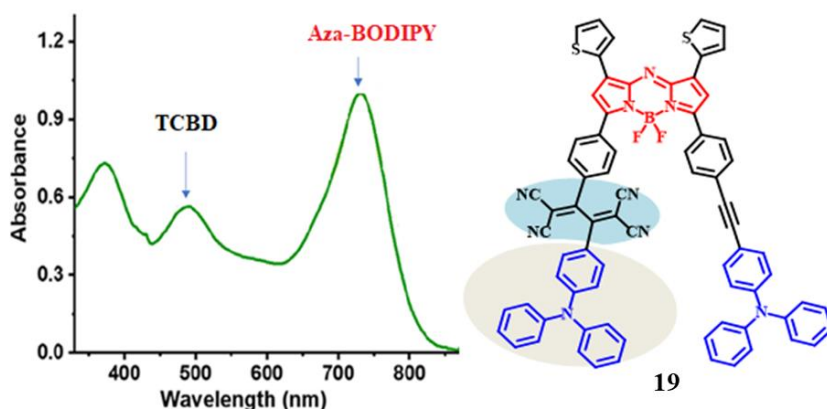


Figure 1.3. Absorption spectra of donor/acceptor based aza-BODIPY dye **19**.

Aza-BODIPY dyes have been widely used as NIR-emitting chemosensors, imaging probes, and fluorescent labels due to their high absorbance, attractive emission, and ease of structural modification.^[27,57] In addition, it has been found that the significant red shift in the absorption and emission into the NIR region can be effectively achieved by extension of π -conjugation *via* attachment of donor or/and acceptor groups to the phenyl rings, and replacement of F-atoms with alkynyl/aryl groups.^[41,58,59] Recently we have reported triphenylamine substituted tetracyanobutadiene (TCBD) bridged aza-BODIPY by [2 + 2] cycloaddition-retroelectrocyclization reaction (Figure 1.3).^[60] The introduction of TCBD between triphenylamine and aza-BODIPY results in panchromatic absorption owing to the absorption of TCBD at lower wavelength region (400–600 nm) and aza-BODIPY at longer wavelength region (650–850 nm). The molecules with panchromatic absorption covering Vis-NIR region and low band gap are of great interest for photovoltaic applications.^[30,61–63]

1.6. Applications of Near-Infrared Absorbing Aza-BODIPYs

1.6.1 In Organic Photovoltaics

Photovoltaic is one of the most rapidly expanding fields of electricity generation worldwide. Silicon solar cells grabbed the solar cell market due to higher efficiencies compared to organic solar cells. The Si-solar cells suffer from limitations of high fabrication and installation cost. Recently organic solar cells have attracted a great deal of attention by overcoming these limitations and emerging as a suitable alternative to silicon solar cells in the near future.

In recent years organic small molecules have attracted attention over polymers for their use in solar cell owing to their characteristic properties such as high purity, batch to batch reproducibility, stability, and scalable synthetic routes. The organic materials having broad absorption in the Vis-NIR region with low bandgap are considered as promising materials for solar cell. Hence conjugated organic dyes have been widely used for organic solar cells. The characteristic absorption of functionalized aza-BODIPY dyes towards NIR region with low HOMO-LUMO gap exhibits its potential to use in organic solar cells. The chemical structures of the aza-BODIPY dyes used in solar cells are provided in Chart 1.3. and their power conversion efficiencies (PCEs) are given in Table 1.1.

Ma and co-workers first time reported BF_2 -chelated azadipyrrromethene dyes **20** and **21** for planar heterojunction solar cells.^[64] The aza-BODIPYs (**20** and **21**) showed broad absorption in visible to NIR region with their absorption maxima at 656 nm and 724 nm respectively. These NIR dyes **20** and **21** were used as electron donors along with fullerene C_{60} as the acceptor in order to make efficient planar heterojunction organic solar cells (OSCs). The solar cell devices of aza-BODIPY **20** and **21** with fullerene C_{60} exhibited power conversion efficiencies up to 1.32 and 2.63% respectively.

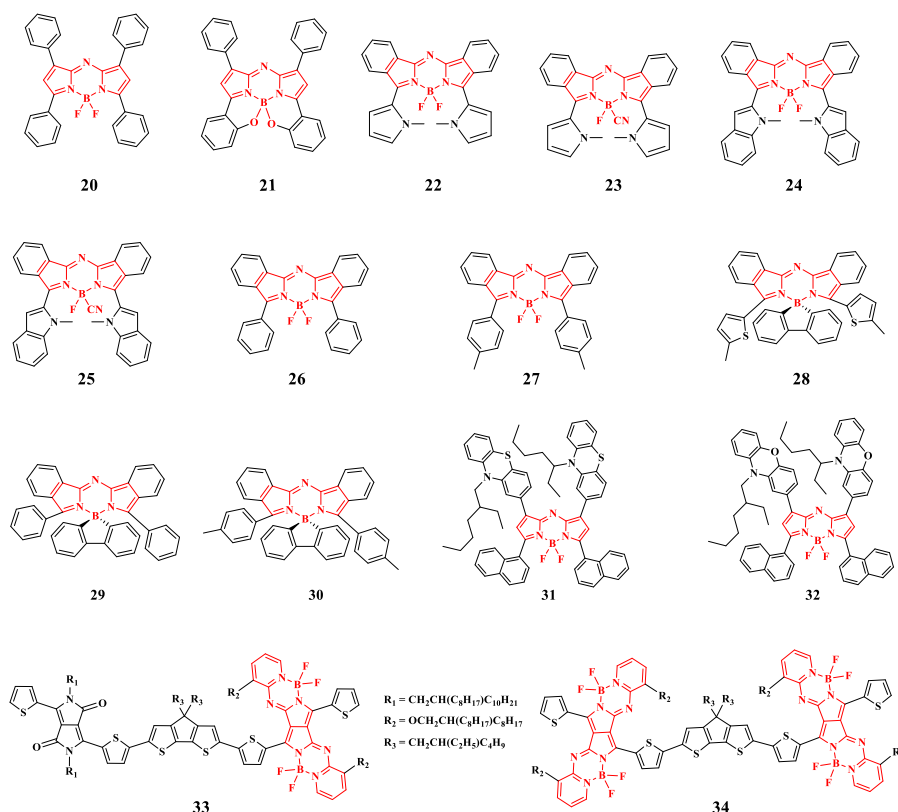


Chart 1.3. Chemical structures of aza-BODIPY dyes **20–34** used in organic solar cells.

Benzannulated aza-BODIPY dyes **22–25** with heterocyclic substituents, namely N-methyl pyrrole and N-methyl indole were synthesized by Li and co-workers. The photophysical properties of benzannulated aza-BODIPY dyes **22–25** exhibited absorption in the 690–795 nm regions with molar extinction coefficient between 65100–104500 L mol⁻¹ cm⁻¹. The cyclic voltammetry and DFT studies indicated aza-BODIPY dyes **22–25** could act as donor materials along with C₆₀ as the acceptor in solar cell. The HOMO and LUMO energy levels in these aza-BODIPY derivatives were tuned by replacing the cyano group by the fluorine atom. The aza-BODIPY **22–25** have excellent thermal stabilities, making them suitable for vacuum processing devices. The PCEs obtained for aza-BODIPYs **22–25** were 0.8 to 2.2% with highest PCE of 2.2% with V_{oc} of 0.67 V for **25**.

Leo and co-workers synthesized the benzannulated aza-BODIPY dyes **26–30** with a fluorene moiety connected to the boron atom.^[51] They showed absorption in 670–715 nm in solution (705–842 nm in thin film). Aza-BODIPY dyes **26–30** were used as donor materials along

with fullerene acceptor has showed efficiencies up to 4.5% for an optimized device using C₆₀ as an acceptor). Sharma and co-workers reported NIR absorbing aza-BODIPY dyes with covalently linked phenothiazine (in **31** AZA-PTZ-BOD) and phenoxazine (in **32** AZA-POZ-BOD) moieties as terminal groups and aza-BODIPY as a central core moiety and reported as donor materials along with PC₇₁BM acceptor for bulk heterojunction (BHJ) solar cell application.^[65] The absorption spectra of **31** and **32** showed absorption maxima in dichloromethane solvent at 655 nm and 652 nm, respectively. The film state absorption in **31** and **32** exhibited red shift of around 40 nm compared to the solution state which is related to the strong π - π interactions in the solid state (Figure 1.4.).^[66] The solution-processed bulk-heterojunction (BHJ) solar cell devices showed high PCE of 8.23% for the **31**:PC₇₁BM blend compared to that for the **32**:PC₇₁BM counterpart (7.24%).

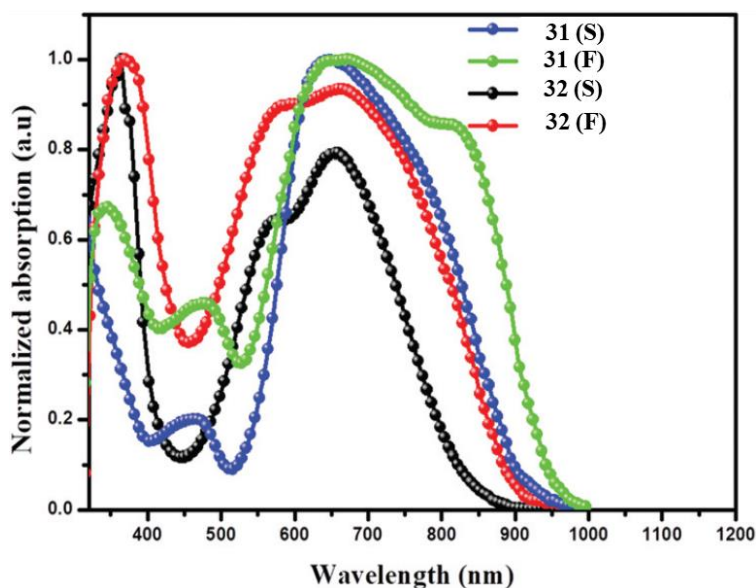


Figure 1.4. UV-visible absorption of **31** and **32** in dichloromethane solution (S) and thin film (F).

Shimizu and co-workers developed the aza-BODIPY dyes **33** and **34** by the Stille cross-coupling reaction.^[67] The aza-BODIPY dyes **33** and **34** exhibited broad absorption in the UV-Vis-NIR region with a absorption maxima at 783 and 827 nm with molar absorption

coefficient $1.08 \times 10^5 \text{ M}^{-1} \text{ cm}^{-1}$ and $1.17 \times 10^5 \text{ M}^{-1} \text{ cm}^{-1}$ respectively. The aza-BODIPY dyes **33** and **34** were used as donor materials along with PC₇₁BM acceptor for solar cell application. The symmetrical aza-BODIPY dye **34** exhibited higher PCE (3.88%) than the unsymmetrical dye **33** (1.49%) owing to the panchromatic absorption.

Table 1.1. Solar cell power conversion efficiencies of aza-BODIPY dyes **20–34**.

Aza-BODIPY	PCE (%)
20	1.3
21	2.63
22	0.8
23	0.8
24	1.6
25	0.8
26	1.1
27	2.7
28	3.7
29	4.5
30	2.6
31	8.23
32	7.24
33	1.49
34	3.88

1.6.2. Boron Neutron Capture Therapy

Cancer is currently one of the most dangerous diseases with highest fatality rate followed by cardiovascular disease. So far cancer treatments are suffering from toxic side effects of chemical drugs. Among the potential solutions, boron neutron capture therapy (BNCT) is most promising, highly selective targeted radiotherapy in the treatment of cancer. BNCT treatment is based on the nuclear capture and fission reaction in between non-toxic thermal neutron beam and ^{10}B atoms. This treatment is used to treat solid cancer tumors, including those found in the brain, neck, and head. BODIPY and aza-BODIPY fluorophores possess a boron atom and are interesting candidates for BNCT.

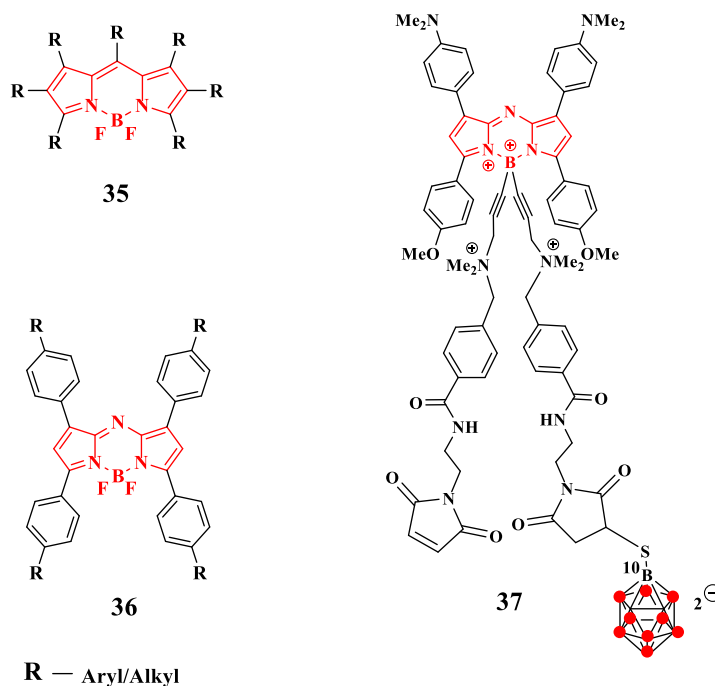


Chart 1.4. Chemical structure of BODIPY (35), aza-BODIPY (36), and aza-BODIPY (37) used in BNCT.

Sancey and co-workers reported the short wave infrared (SWIR) region emitting BODIPY 35, aza-BODIPY 36, and 37 aggregate in treating tumors *via* enhanced permeability and retention (EPR) with a high and sustainable tumor/healthy muscle ratio without the need for

anchoring vectors.^[68] Here, the fluorescence properties of aza-BODIPY useful to vectorize the small ^{10}B -BSH molecule at the target tissue. The dyes **35**, **36** and **37** were well absorbed by tumor cells and determined its biodistribution in mice with tumors. They demonstrated the BNCT potential of these compounds by exposing glioblastoma xenografts that included chorioallantoic membrane to slow neutrons.

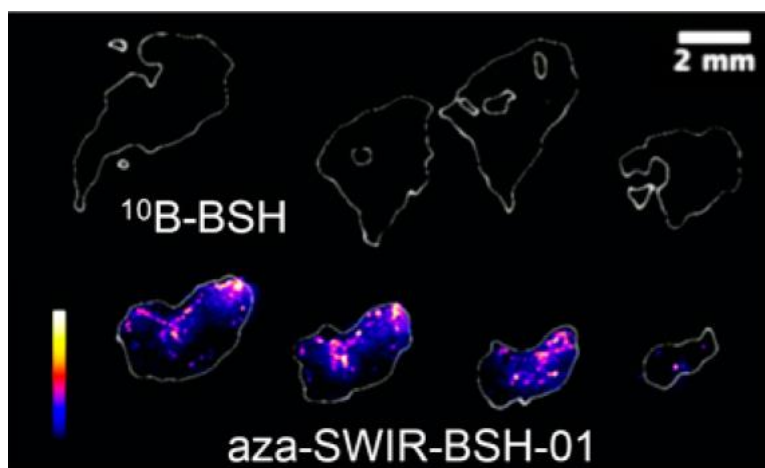


Figure 1.5. Laser-induced breakdown spectroscopy (LIBS) elemental imaging of boron from tumor sections collected at day 16 showing the presence of remaining boron in tumors treated with aza-SWIR-BSH-01 (**37**).

The optical imaging and elemental imaging based on the laser-induced breakdown spectroscopy (LIBS) were used to demonstrate tumor accumulation of the compound in real-time (Figure 1.5.). Overall, the fluorescent aza-BODIPY/ ^{10}B -BSH compounds has a greater theranostic potential for an effective BNCT approach since it can vectorize along with image ^{10}B -BSH in the tumor area. The authors confirmed the presence of boron at the tumor site under boron-containing conditions to enhance comprehension of the obtained findings. Consequently, tumors excised on day 16 underwent slicing and analysis using LIBS imaging for elemental examination. The analysis focused on phosphorus and the boron content and distribution. Phosphorus, found in every cell, was chosen because its distribution reflects the tissue area. In Figure 1.5., phosphorus was utilized to

outline the tissue sections (in white). As depicted in Figure 1.5., tumors treated with aza-SWIR-BSH-01 (**37**) exhibited observable boron in all sections, contrasting with the absence of boron in the ^{10}B -BSH condition. While ^{10}B -BSH might accumulate at the tumor site, it likely does so to a lesser extent, or it may be released from the tumor site over an extended period, falling below the detection limits of the LIBS system. Conversely, aza-SWIR-BSH-01 (**37**) accumulated significantly in the tumor region (Figure 1.5.) and remained in the tissues for 6 days post-administration.

1.6.3. Photodynamic therapy (for cancer treatment)

The use of reactive oxygen species, including $^1\text{O}_2$, $\text{O}_2^{\cdot-}$, OH^{\cdot} , etc., in photodynamic therapy has garnered significant interest in cancer treatment.^[69–71] This therapeutic approach relies on photosensitizers, light irradiation, and molecular oxygen as key components. There has been extensive development of organic or inorganic photosensitizers with exceptional reactive oxygen species generation efficiency for use in photodynamic therapy. This treatment modality is known for its non-invasiveness and reduced toxicity when compared to traditional therapies.

Consequently, researchers have been investigating new photosensitizers with optimal physicochemical properties to enhance the effectiveness of tumor photodynamic therapy. Aza-BODIPY is known for its strong NIR absorption, high extinction coefficient, and excellent photostability, all of which contribute to its remarkable photothermal conversion efficiency.

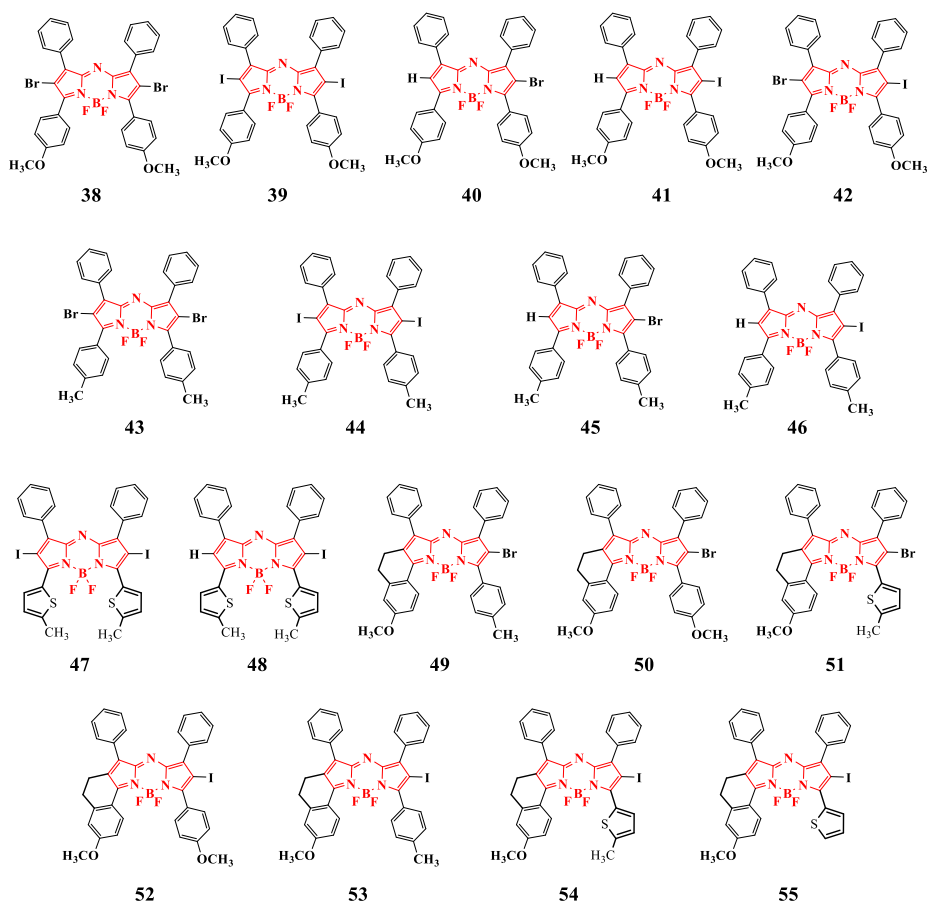


Chart 1.5. Chemical structures of aza-BODIPY derivatives **38–55** used in photothermal therapy and photodynamic therapy.

One of the best strategies in the development of efficient novel photosensitizer is to substitute the heavy atoms such as halogens (Bromine, Iodine) and metal ions which enhances the spin orbit coupling.^[72,73] In 2020, Zhao and co-workers used this strategy and systematically investigated the effect of halogens (Br, I) substitution on the performance of aza-BODIPY through synthesizing 18 different mono- or di-halogenated aza-BODIPY derivatives **38–55** (Chart 1.5).^[74] They found that all the halogen substituted aza-BODIPYs were capable of producing reactive oxygen species under light illumination. The mono-iodo substituted aza-BODIPY **41** showed the best photodynamic efficiency with a ¹O₂ quantum yield of 0.52.

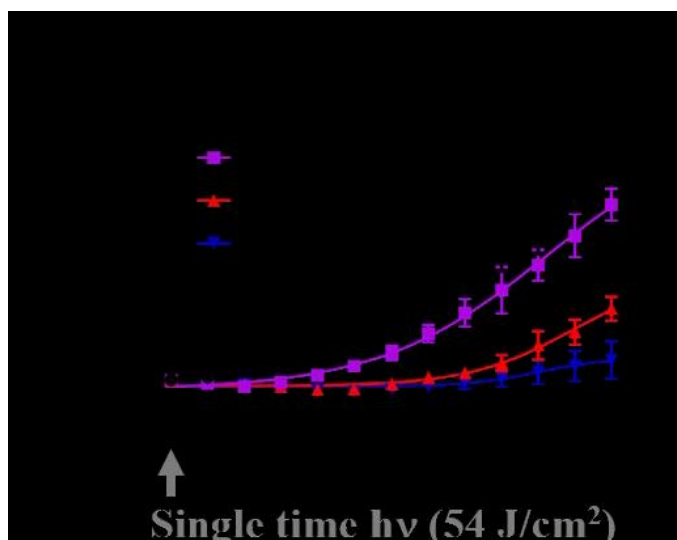


Figure 1.6. Tumor growth curves in evaluation of tumor growth inhibition in HeLa-tumor bearing xenograft model mediated by PDT.

The singlet oxygen quantum yield for aza-BODIPYs **38–55** are given in Table 1.2. These results demonstrated that the mono-iodo substituted aza-BODIPY **41** show selective tumor accumulation with a retention time up to the 10 hours, while it was eliminated from other major organs. Subsequent *vivo* antitumor investigations supported that the growth of compound aza-BODIPY **41** treated tumors were slower compared to that of tumors treated with the conventional photosensitizer chlorin e6 (Ce6) even at low drug dosage and the once-off irradiation (Figure 1.6.).

Table 1.2. Singlet oxygen quantum yields for aza-BODIPY derivatives 38–55.

Aza-BODIPY	Singlet oxygen quantum yield (Φ_{Δ}^a)
38	0.14
39	0.24
40	0.10
41	0.52
42	0.29
43	0.10
44	0.12
45	0.05
46	0.14
47	0.14
48	0.17
49	0.08
50	0.08
51	0.11
52	0.51
53	0.16
54	0.25
55	0.19

^aMeasured in DMF using ZnPc ($\Phi_{\Delta} = 0.56$ in DMF) as the standard.

^aSinglet oxygen quantum yield (Φ_{Δ}) with reference to ZnPc ($\Phi_{\Delta} = 0.56$) in DMF.

The merging of photodynamic and photothermal therapies could create greater sensitivity to improve the sensitivity of photodynamic therapy treatment at lower temperatures and under hypoxic conditions hence growing considerable interest in the field of oncological therapy.^[75] Aza-BODIPY derivatives exhibit higher absorption coefficients in the NIR range (>700 nm) compared to conventional BODIPY dyes and show greater photothermal conversion efficiency.

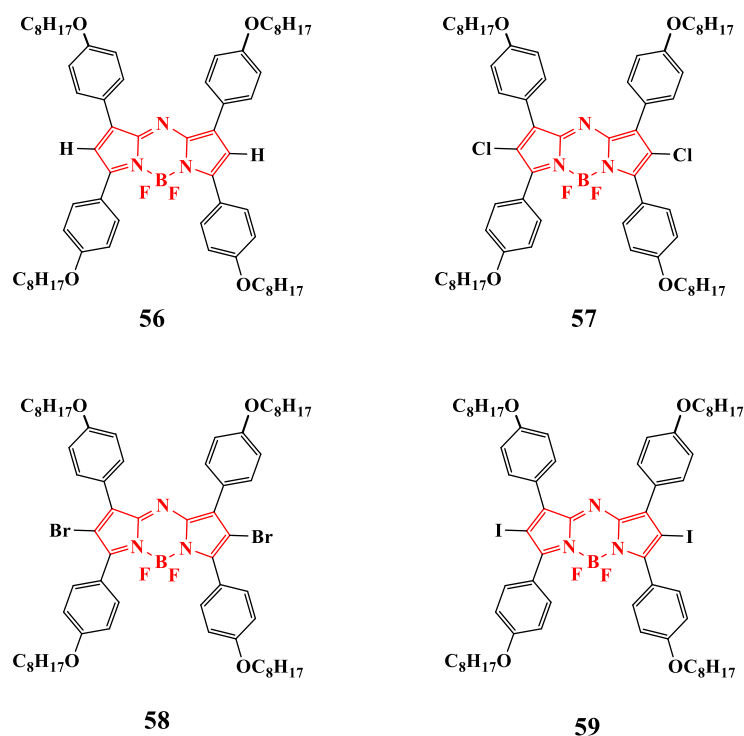


Chart 1.6. Chemical structures of aza-BODIPY derivatives **56–59** used in photothermal therapy and photodynamic therapy.

Zhao and co-workers in 2018 explored a range of halogenated aza-BODIPYs derivatives **56–59** and studied the impact of heavy atom on the performance of PDT/PTT. Aza-BODIPY was substituted with various moieties such as two chlorine (**57**), two bromine (**58**), or two iodine (**59**) atoms (Chart 1.6).^[76] The four alkoxy substituents (-OC₈H₁₇) were used to enhance the solubility of the compounds in organic solvents and also to improve the self-assembling ability of DSPE-PEG5000. These derivatives **56–59** were used as PDT/PTT agents and found that the **59** is the best PDT/PTT agent compared to others.

1.6.4. Fluorescence sensors

Ring-fused aza-BODIPY dyes have been used as fluorescent probes in the biological systems related to their desirable photophysical characteristics. Kobayashi and co-workers synthesized fluorescent probes based on ring-fused aza-BODIPY structures.^[27] They investigated the pH dependence on the optical properties of aza-

BODIPY **60** in dichloromethane by sequentially adding trifluoroacetic acid (TFA). The dye exhibited a blue shift in absorption by TFA addition, with decrease in intensity of peaks. The emission band also experienced a blue shift, while the emission intensity increased due to the elimination of electron-donating properties from the dimethylamino substituent. Due to its pH-dependent photophysical properties, aza-BODIPY **60** could serve as a turn-on fluorescence sensor. Liu and co-workers investigated the fluorescent probe performance of aza-BODIPY **61**. Here aza-BODIPY **61** was used as a turn-off fluorescent probe in ammonium ion detection. The addition of ammonium ion resulted in a quenching of the dye's emission intensity and colour change from green to red-pink corresponds to the H-aggregation.

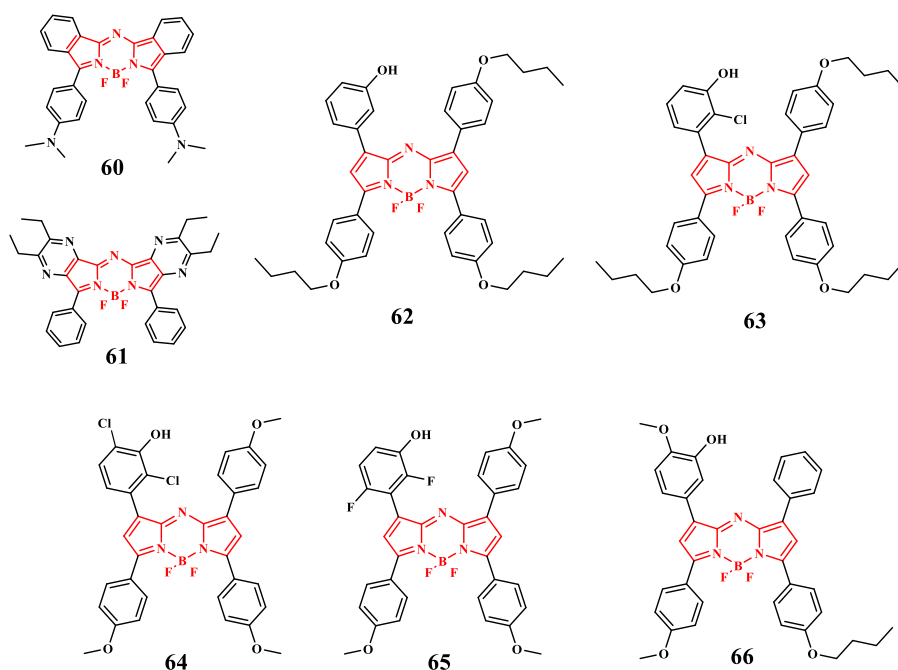


Chart 1.7. Chemical structures of aza-BODIPY derivatives **60–66** used as fluorescence sensors.

Boriso and co-workers in 2019 synthesized five Aza-BODIPY based acid–base indicator probes **62–66** (Chart 1.7.), and their spectral properties were tuned solely by photoinduced electron transfer.^[77] These dyes were made in such a way that the pH sensitive hydroxyl unit is placed at the *meta*-position of the phenyl substituent placed on

Aza-BODIPY core. Figure 1.7. shows the absorption and emission behaviour of aza-BODIPY **64** with pH indicates the quenching of fluorescence. However, absorption spectra were unaffected after the deprotonation of the hydroxyl group. Hence the hydroxyl groups are not in conjugation with the aza-BODIPY chromophore which makes these dyes **62–66** useful quenchers for photoinduced charge transfer. These aza-BODIPY probes **62–66** exhibit reversible “on”–“off” fluorescence response after deprotonation of the receptor. However, the absorption spectrum remains unchanged that is in contrast to state-of-the-art indicators of the aza-BODIPY dyes. This eliminates the significant changes in the efficiency of the inner filter effect and FRET efficiency which make these probes **62–66** suitable as viable acceptors in light harvesting systems applicable for ratiometric pH imaging. The substitution of electron accepting or electron donating moiety to dye provides suitable materials for measurements from pH 7 to very alkaline pH 13. The pKa values in the range between 7.5 and 11.7 facilitate measurements from physiological conditions (pH 7) to very alkaline pH. Herein the probe carrying two chlorine units in ortho-position of phenyl (aza-BODIPY **64**) ideally matches the seawater pH, however the other dyes possess higher pKa values due to the non-conjugation with electron withdrawing aza-BODIPY unit.

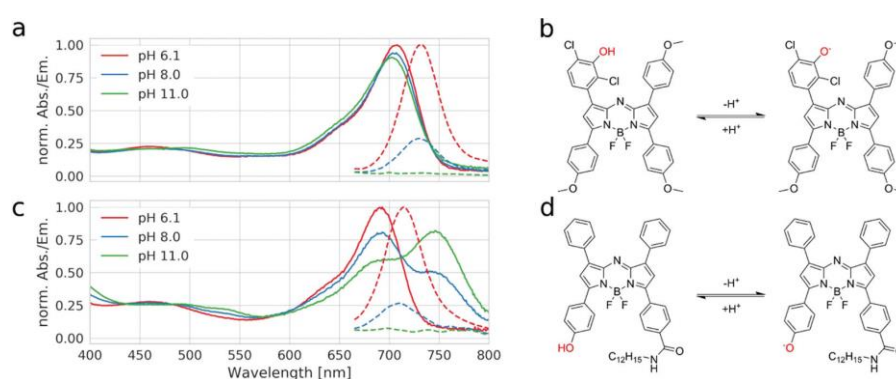


Figure 1.7. The pH dependence of absorption (solid lines) and emission spectra (dashed lines) of indicator **64** (a) and the state-of-the-art hydroxy-aza-BODIPY pH indicator (c) in hydrogel D4; (b) and (d) show the pH equilibria for the respective dyes.

1.6.5. Photo-redox catalysis

In recent years, photoredox catalytic organic reactions have attracted considerable attention.^[39,78,79] Various synthetic methods have been employed to prepare highly functionalized organic compounds in good yield and selectivity under mild reaction conditions.^[80–83] BODIPY dyes has shown immense potential as excellent sensitizer due to their favorable properties, including strong absorption within 500–600 nm range, significant fluorescence quantum yields, and excellent photostability. Aza-BODIPY exhibit a bathochromic shift of approximately 100 nm in their absorption compared to BODIPY; however, they have received relatively less exploration and investigation. Recently numbers of aza-BODIPY based derivatives have been reported in literature for photo redox catalysis.

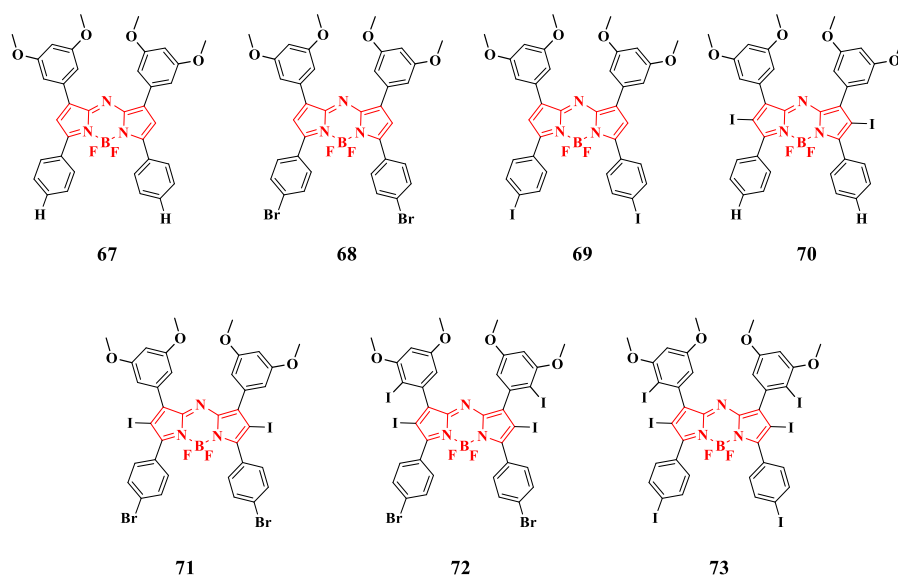
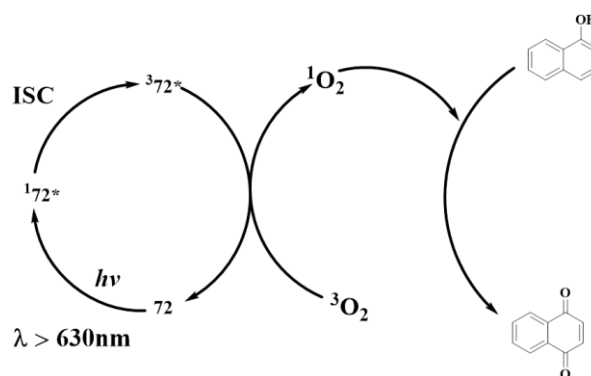


Chart 1.8. Chemical structures of aza-BODIPY derivatives **67–73** used in photo-redox catalysis.

Ramaiah and co-workers investigated the photocatalytic activity of aza-BODIPY dyes **67–73** (Chart 1.8.), which possess strong NIR absorption.^[84] They introduced heavy atoms (halogens) to modify both the core structure and the periphery of the dyes. Aza-BODIPY dyes **67–73** exhibited robust absorption in the NIR region, characterized by high molar-extinction coefficients. The introduction of heavy atoms at the core as well as at the periphery of these derivatives led to a

substantial improvement in their intersystem-crossing efficiency. It was demonstrated that 2,6-disubstituted dyes generate singlet oxygen with greater efficiency, which could be attributed to the heavy atom effect induced by the presence of iodides. Moreover, aza-BODIPY **72** and aza-BODIPY **73**, with six halogen atoms attached to both the core and the periphery, exhibited notably higher singlet oxygen quantum yields (Φ_{Δ}) of 80% and 70%, respectively. The authors successfully achieved a 100% conversion of 1-naphthol to 1,4-naphthoquinone through photoirradiation, employing aza-BODIPY **72** as the triplet photosensitizer (Scheme 1.5.). This high conversion was attributed to the excellent singlet oxygen quantum yield (Φ_{Δ}), photostability, and solubility exhibited by aza-BODIPY **73**.



Scheme 1.5. Photooxygenation of 1-naphthol by using aza-BODIPY **72**.

1.6.6. Photoacoustic probes

Photoacoustic imaging is a rapidly growing field and is a potential alternative to MRI and X-ray scans in the clinical practice because of its ability to provide high resolution images of tissues at depths (in the cm range). Photoacoustic probes have been widely studied for their ability to visualize and selectively target specific cancers, blood vessels, and metabolic processes. Aza-BODIPY dyes have a unique combination of photostability, brightness, and high absorption coefficients in the near-infrared region, making them ideal candidates for various medical imaging applications.

For the first time, Chan and co-workers developed small molecule based photoacoustic probes aza-BODIPY **74** and **75** (Chart 1.9.) for ratiometric imaging of Cu^{2+} .^[85] These molecules were constructed by attaching a 2-picolinic ester to phenyl of aza-BODIPY, which is easily hydrolyzed by $\text{Cu}(\text{II})$, but it cannot be hydrolyzed by other divalent metal ions. Aza-BODIPY **75** show two absorption bands, first below 700 nm (697 nm) which is related to the capped 2-picolinic ester attachment and the second above 700 nm (767 nm), relates to uncapped phenoxide product. Irradiating an aza-BODIPY probe **74** at the blue-shifted absorbance maxima at 680 nm as well as the red-shifted absorbance maxima at 755 nm gives two corresponding PA signals. The aza-BODIPY **75** is very selective for $\text{Cu}(\text{II})$ as compared to other metal ions. These results provided importance of photoacoustic imaging to carry out imaging experiments in the cm range and also this technique provides the imaging depth in cm range which is greater than that with optical methods.

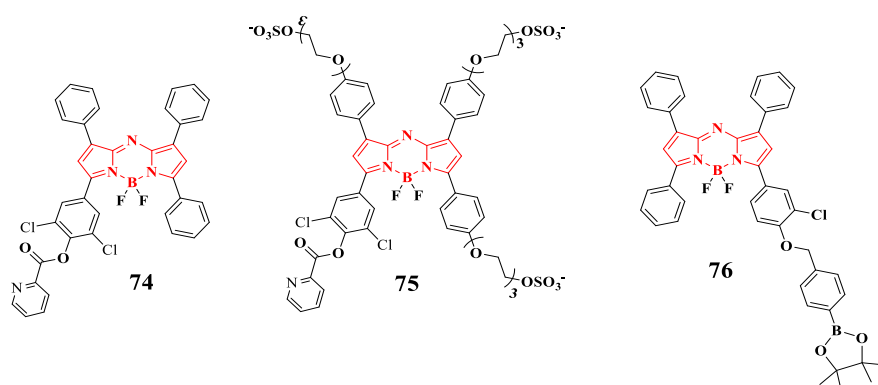


Chart 1.9. Chemical structures of aza-BODIPY derivatives **74–76** used in photoacoustic probe applications.

The peroxynitrite (ONOO^-) is recognized as a highly reactive oxidizing agent within biological systems, and its close association with tumors has been established. Consequently, it becomes crucial to promptly detect the presence of ONOO^- in tumors to gain insights into the underlying mechanisms and enhance therapeutic interventions. In 2017, Pu and co-workers introduced organic semiconductor nanoprobe incorporated with significant quantities of borane for in

vivo ratiometric photoacoustic imaging of ONOO^- . The main sensing component chosen was boronate-caged aza-BODIPY **76**. In the presence of ONOO^- , the boronate group could be eliminated, leading to the formation of a phenoxide product with the red shift in the absorption towards NIR region. The phenoxide product generated was utilized for ratiometric photoacoustic imaging. The boronate component exhibits reactivity towards both ONOO^- and H_2O_2 . To address these concerns, bulky boranes were introduced possessing properties of optical inactivation and heightened chemical activity. This modification rendered the nanoparticles with no response to H_2O_2 and pH variations, thereby improved the specificity for detecting ONOO^- .

A lack of oxygen occurs hypoxia which can cause damage to the body's functions. This is common in various diseases, such as cancer and ischemia. Hence identifying tumor hypoxia can help in treatment of patients with respect to their response. Chan and co-workers developed the ratiometric hypoxia probes aza-BODIPYs **77** (**rHyP-1**) and **78** (**red-rHyP-1**), which is a hypoxia responsive small molecule probe used for reliable hypoxia detection using photoacoustic imaging.^[86] In the absence of oxygen, *N*-oxide group is reduced which results in a red-shift in absorption of probe aza-BODIPY **78** from 749 to 818 nm. The normalized absorption spectra (in chloroform) and photoacoustic spectra of **77** and **78** are as shown in Figure 1.8.). In hypoxic conditions, in vitro photoacoustic imaging experiments of aza-BODIPY **78** exhibited the $\text{PA}_{820}/\text{PA}_{770}$ ratio of 2-fold than that of under normoxic conditions.

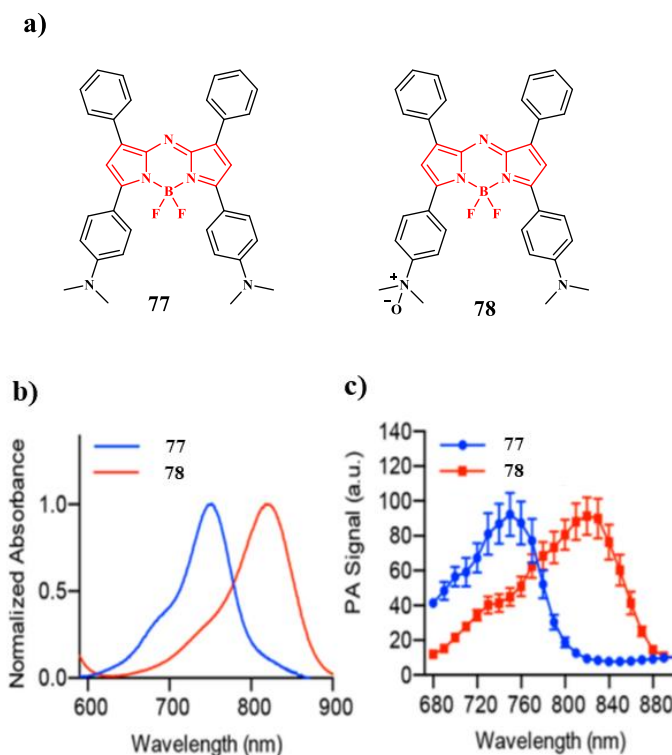


Figure 1.8. a) Chemical structures of aza-BODIPY derivatives **77** (**rHyP-1**) and **78** (**red-rHyP-1**) used in photoacoustic imaging; (b) Normalized absorption spectra of **77** and **78** in chloroform. (c) PA spectra of **77** and **78** in chloroform.

1.6.7. Energy-transferring chromophores in optoelectronics

There are number of literature reports available on aza-BODIPY derivatives showing fluorescence resonance energy transfer (FRET) phenomena and their applications in energy transfer cassettes.^[87–94] FRET is a mechanism of having transfer of energy in between two chromophores, in which donor possesses high quantum yield and there is significant overlap between emission band observed from donor and absorption band of acceptor. FRET operates within the distance range of around 10 nm between two chromophores.

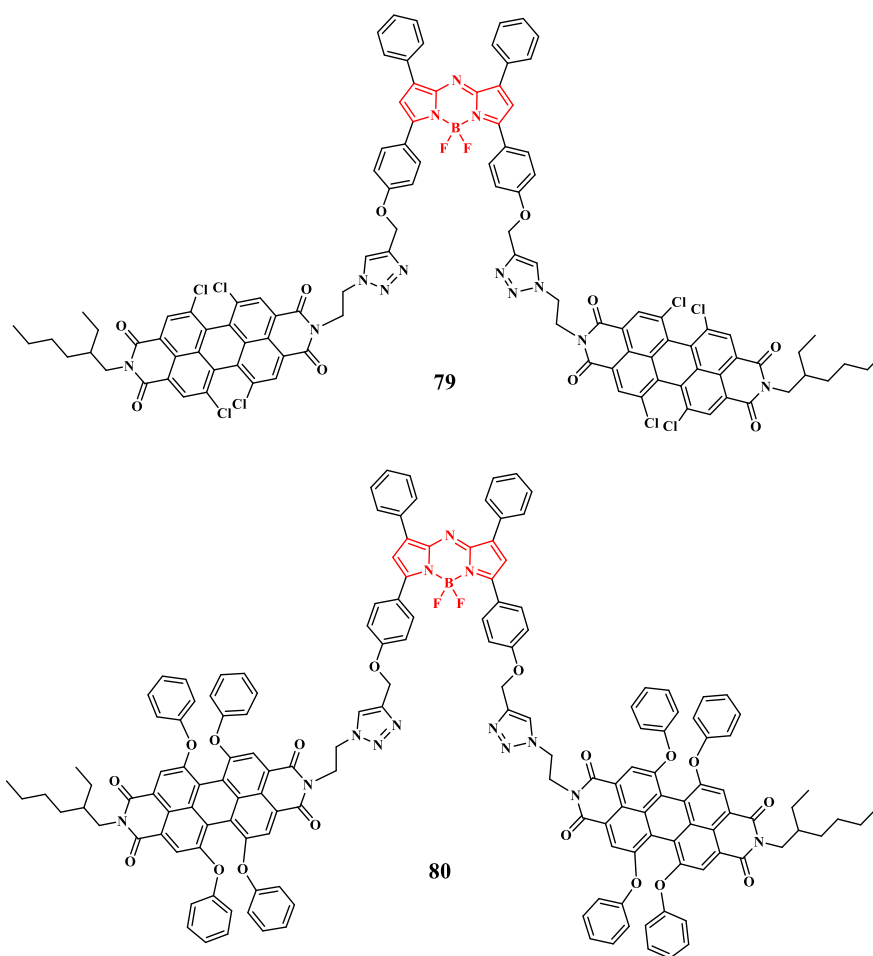


Chart 1.10. Chemical structures of aza-BODIPY derivatives **79** and **80** used in (Energy-transferring chromophores in) optoelectronics applications.

Sengupta and co-workers synthesized multichromophoric triads composed of central aza-BODIPY core and bay substituted (tetrachloro- and tetraphenoxy-) perylenediimides (PDI) as end chromophores **79** and **80** via copper catalyzed azide-alkyne cycloaddition reaction.^[95] These triads showed around 99% FRET from the end chromophore PDIs to central core aza-BODIPY and are having panchromatic absorption and near infrared (NIR) emission. The absorption spectrum of triad **79** in CHCl_3 displayed two absorption bands at 520 nm ($\epsilon = 72951 \text{ M}^{-1} \text{ cm}^{-1}$) and 688 nm ($\epsilon = 68828 \text{ M}^{-1} \text{ cm}^{-1}$) corresponding to the PDI and aza-BODIPY moieties respectively (Figure 1.9.). In the similar fashion, the triad **80** exhibited absorption maximum at 580 nm ($\epsilon = 99795 \text{ M}^{-1} \text{ cm}^{-1}$) and 688 nm ($\epsilon = 88612 \text{ M}^{-1}$

cm^{-1}). Upon excitation of the triad **79** at 520 nm, the emission intensity of the PDI donor at 550 nm was significantly quenched by approximately 98% compared to free PDI moiety and the emission intensity of the aza-BODIPY core was improved by ~15% at 717 nm (Figure 1.9.), exhibits excitation energy transfer from the PDI unit to aza-BODIPY core. Likewise, upon excitation of triad **80** at 580 nm decrease the fluorescence intensity of donor unit by about ~99%, accompanied by an associated increase in the intensity of aza-BODIPY core by ~16% at 688 nm. The lower values of fluorescence quantum yield in both aza-BODIPY triads **79** and **80** confirm the FRET phenomena between donor PDI and acceptor aza-BODIPY units.

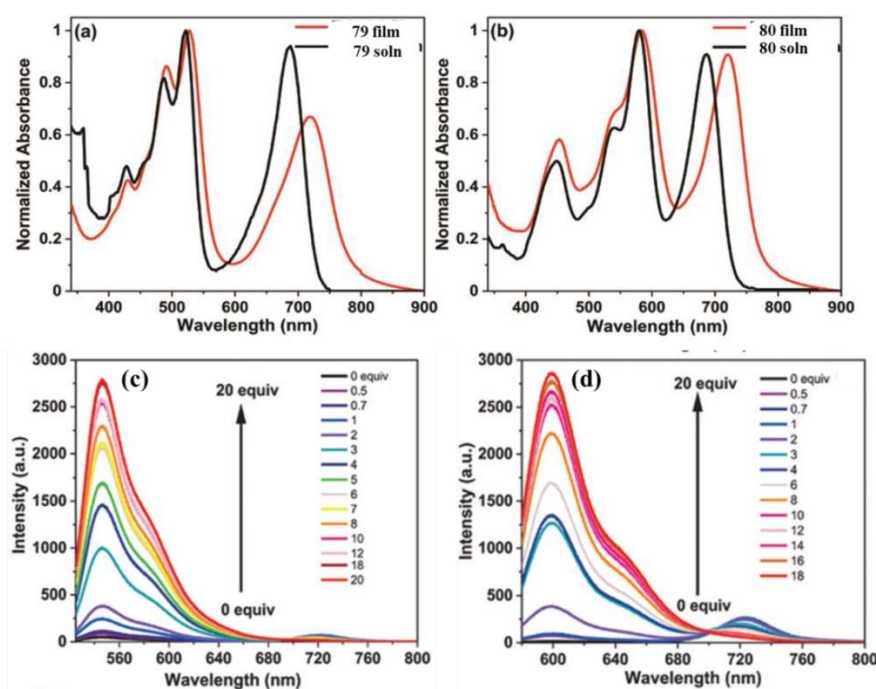


Figure 1.9. Thin film UV–Vis spectra for (a) **79** and (b) **80** spin-coated from CHCl_3 solution. Fluorescence spectral changes of (c) **79** (5 mM) and (d) **80** (5 mM) upon incremental addition of Co^{2+} (0 to 20 equiv.) in THF solution.

The electrochemical investigation showed the strong electron accepting character of these triads. Hence the electron mobilities were measured to be appreciable $2.44 \pm 1.70 \times 10^{-3} \text{ cm}^2 \text{ V}^{-1} \text{ s}^{-1}$ and $4.00 \pm 1.50 \times 10^{-3} \text{ cm}^2 \text{ V}^{-1} \text{ s}^{-1}$ respectively using space charge limited current (SCLC) method. These electron mobility values are higher than

reported aza-BODIPY based derivatives in the literature. These triads **79** and **80** showed the remarkable ratiometric FRET-off sensing when reacted with metal cations Co^{2+} and Fe^{3+} .

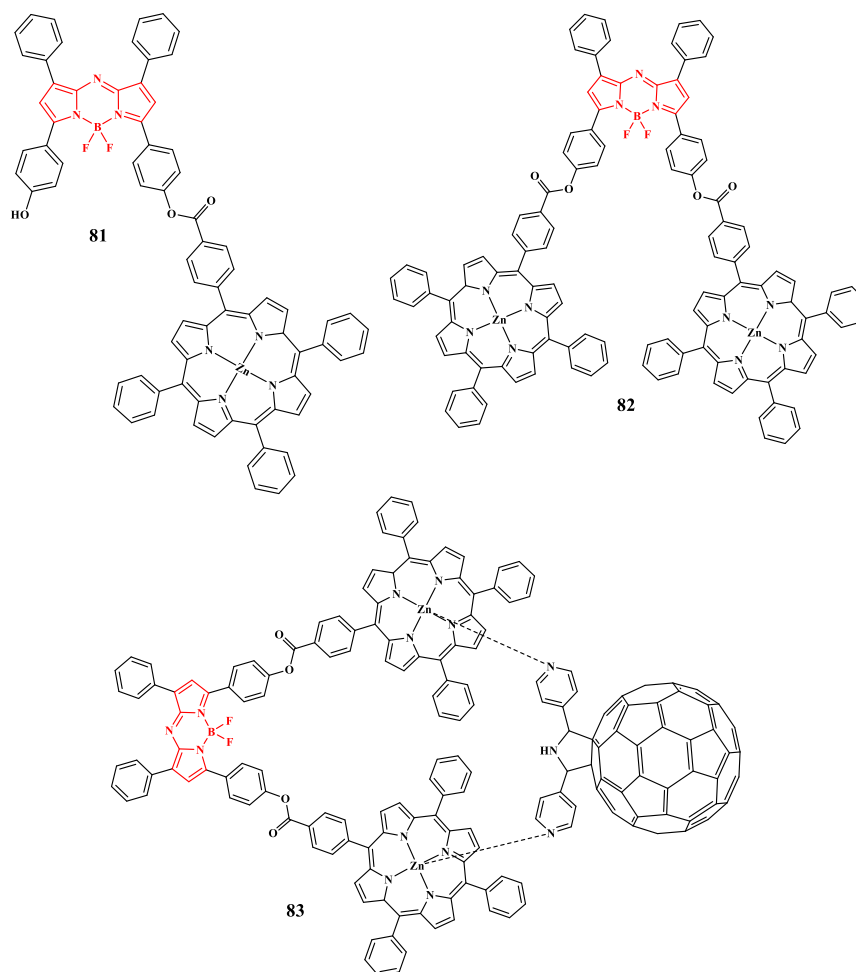


Chart 1.11. Chemical structures of aza-BODIPY derivatives **81**, **82** and **83** used in (Energy-transferring chromophores in) optoelectronics applications.

D'Souza and co-workers developed a molecular clip that contains BF₂-chelated tetraaryl aza-BODIPYs as a near-IR emitting fluorophores **81** (ZnP-azaBODIOPY) and **82** ((MP)₂-azaBODIOPY).^[96] Here the aza-BODIPY is covalently linked to one and two porphyrin rings (MP, M = 2H or Zn) in 'molecular clip' to host fullerene. The two Zn based triad **83** (C₆₀Py₂:(ZnP)₂-azaBODIOPY) is spatially arranged in a 'molecular clip' structure to accommodate the bispyridine functionalized fullerene through a 'two-point' metal-ligand axial coordination which forms supramolecular tetrad **83**.

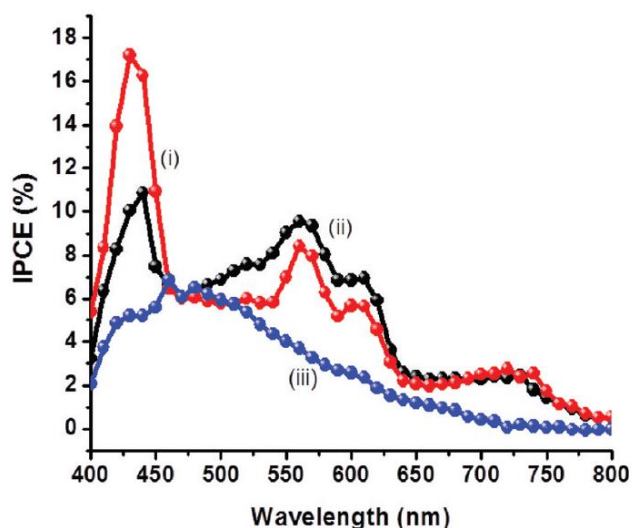


Figure 1.10. IPCE (%) curves of (i) **83** ($C_{60}py_2:(ZnP)_2$ -azaBODIPY tetrad), (ii) **82** ($(ZnP)_2$ -azaBODIPY triad), and (iii) $C_{60}py_2:(ZnP)_2$ donor-acceptor systems electrophoretically deposited on the surface in acetonitrile solution containing (0.25 M LiI, 0.25 M butyl methyl imidazolium iodide (BMII), 0.05 M I_2) for I^-/I_3^- redox mediator.

The introduction of second acceptor fullerene in molecular assembly helps electron transfer from the singlet excited metal porphyrin (MP) to the fullerene in order to generate charge-separated $C_{60}(py)_2^{\bullet-}:(ZnP)_2^{\bullet+}$ -azaBODIPY in nonpolar solvent. Therefore, the formation of a non-covalent assembly of building blocks helps in the formation of photo/electroactive materials with desired features which were not possible to attain in a single molecule. Photoelectrochemical cells were made by electrophoretic deposition of these systems on FTO/SnO₂ modified surface (Figure 1.10.). The higher IPCE of around 17% (nearly at the peak maxima) was observed for compound **83** modified electrode in comparison with compound **82** modified electrode (~11%).

1.7. References

- (1) (a) Liangwab, M., Chen, J. (2013). Arylamine organic dyes for dye sensitized solar cells, *Chem. Soc. Rev.*, 42, 3453-3488 (DOI: 10.1039/C3CS35372A). (b) Mishra, A., Fischer, M. K. R., Bauerle, P. (2009). Metal-free organic dyes for dye-sensitized

solar cells: from structure: property relationships to design rules, *Angew. Chem., Int. Ed.*, 48, 2474-2499 (DOI: 10.1002/anie.200804709).

- (2) (a) Thomas, K. R. J., Lin J. T., Velusamy, M., Tao, Y. T., Chuen, C. H. (2004). Color tuning in benzo[1,2,5]thiadiazole-based small molecules by amino conjugation/deconjugation: bright red-light-emitting diodes, *Adv. Funct. Mater.*, 14, 83-90 (DOI: 10.1002/adfm.200304486). (b) Omer, K. M., Ku, S. Y., Wong, K. T., Bard, A. J. (2009). Green electrogenerated chemiluminescence of highly fluorescent benzothiadiazole and fluorene derivatives, *J. Am. Chem. Soc.*, 131, 10733-10741 (DOI: 10.1021/ja904135y). (c) Yasuda, T., Shinohara, Y., Matsuda, T., Han, L., Ishi-i, T. (2012). Improved power conversion efficiency of bulk-heterojunction organic solar cells using a benzothiadiazole–triphenylamine polymer, *J. Mater. Chem.*, 22, 2539-2544 (DOI: 10.1039/c2jm14671a).
- (3) Ostroverkhova, O. (2016). Organic Optoelectronic Materials: Mechanisms and Applications, *Chem. Rev.*, 116, 13279–13412 (DOI: 10.1021/acs.chemrev.6b00127).
- (4) (a) Mochida, T., Yamazaki, S. (2002). Mono- and diferrocenyl complexes with electron-accepting moieties formed by the reaction of ferrocenylalkynes with tetracyanoethylene, *J. Chem. Soc. Dalton Trans.*, 0, 3559-3564 (DOI: 10.1039/B204168E.) (b) Michinobu, T. (2010). Click synthesis of donor–acceptor-type aromatic polymers, *Pure Appl. Chem.*, 82, 1001 (DOI: 10.1351/PAC-CON-09-09-09). (c) Maligaspe, E., Pundsack, T. J., Albert, L. M., Zatsikha, Y. V., Solntsev, P. V., Blank, D. A., Nemykin, V. N. (2015). Synthesis and charge-transfer dynamics in a ferrocene-containing organoboryl aza-BODIPY donor-acceptor triad with boron as the hub, *Inorg. Chem.*, 54, 4167–4174 (DOI: 10.1021/acs.inorgchem.5b00494).

- (5) (a) Michinobu, T., Satoh, N., Cai, J., Lia, Y., Han, L. (2014). Novel design of organic donor–acceptor dyes without carboxylic acid anchoring groups for dye-sensitized solar cells, *J. Mater. Chem. C*, 2, 3367 (DOI: 10.1039/c3tc32165g). (b) Leliège, A., Blanchard, P., Rousseau, T., Roncali, J. (2011). Triphenylamine/Tetracyanobutadiene-Based D-A-D π -Conjugated Systems as Molecular Donors for Organic Solar Cells, *Org. Lett.*, 13, 3098–3101 (DOI: 10.1021/ol201002j).
- (6) Zhang, L., Zeng S., Yin L., Ji C., Li, K., Li Y., Wang Y. (2013). The synthesis and photovoltaic properties of A–D–A-type small molecules containing diketopyrrolopyrrole terminal units, *New J. Chem.*, 37, 632. (DOI: 10.1039/C2NJ40963A).
- (7) (a) Liangwab, M., Chen, J. (2013). Arylamine organic dyes for dyesensitized solar cells, *Chem. Soc. Rev.*, 42, 3453–3488 (DOI: 10.1039/C3CS35372A). (b) Thomas, K. R. J., Lin, J. T., Velusamy, M., Tao, Y. T., Chuen, C. H. (2004). Color tuning in benzo[1,2,5]thiadiazole-based small molecules by amino conjugation/deconjugation: bright red-light-emitting diodes, *Adv. Funct. Mater.*, 14, 83–90 (DOI: 10.1002/adfm.200304486).
- (8) Mishra, A., Fischer, M. K. R., Bauerle, P. (2009). Metal-free organic dyes for dye-sensitized solar cells: from structure: property relationships to design rules, *Angew. Chem., Int. Ed.*, 48, 2474–2499 (DOI: 10.1002/anie.200804709).
- (9) Omer, K. M., Ku, S. Y., Wong, K. T., Bard, A. J. (2009). Green electrogenerated chemiluminescence of highly fluorescent benzothiadiazole and fluorene derivatives, *J. Am. Chem. Soc.*, 131, 10733–10741 (DOI: 10.1021/ja904135y).
- (10) Zhao, Y., Luo, Y., Wu, S., Wang, C., Ahmidayi, N., Lévêque, G., ... & Xu, T. (2023). Enhanced near-infrared photoresponse for efficient organic solar cells using hybrid plasmonic nanostructures. *Physica E: Low-dimensional Systems and*

Nanostructures, 146, 115534. (DOI: 10.1016/j.physe.2022.115534).

- (11) Khan, M. U., Hussain, R., Yasir Mehboob, M., Khalid, M., Shafiq, Z., Aslam, M., ... & Janjua, M. R. S. A. (2020). In silico modeling of new “Y-Series”-based near-infrared sensitive non-fullerene acceptors for efficient organic solar cells. *ACS omega*, 5(37), 24125-24137. (DOI: 10.1021/acsomega.0c03796).
- (12) Bellier, Q., Pégaz, S., Aronica, C., Guennic, B. L., Andraud, C., & Maury, O. (2011). Near-infrared nitrofluorene substituted aza-boron-dipyrromethenes dyes. *Organic Letters*, 13(1), 22-25. (DOI: 10.1021/ol102701v).
- (13) Liu, K., Ouyang, B., Guo, X., Guo, Y., & Liu, Y. (2022). Advances in flexible organic field-effect transistors and their applications for flexible electronics. *npj Flexible Electronics*, 6(1), 1. (DOI: 10.1038/s41528-022-00133-3).
- (14) Qi, J., Qiao, W., & Wang, Z. Y. (2016). Advances in organic near-infrared materials and emerging applications. *The Chemical Record*, 16(3), 1531-1548. (DOI: 10.1002/tcr.201600013).
- (15) Zampetti, A., Minotto, A., & Cacialli, F. (2019). Near-infrared (NIR) organic light-emitting diodes (OLEDs): challenges and opportunities. *Advanced Functional Materials*, 29(21), 1807623. (DOI: 10.1002/adfm.201807623).
- (16) Liu, W., Deng, S., Zhang, L., Ju, C. W., Xie, Y., Deng, W., ... & Cao, Y. (2023). Short-wavelength Infrared Organic Light-emitting Diodes from A-D-A'-D-A type Small Molecules with Emission Beyond 1100 nm. *Advanced Materials*, 2302924. (DOI: 10.1002/adma.202302924).
- (17) Gut, A., Ciejka, J., Makuszewski, J., Majewska, I., Brela, M., & Łapok, Ł. (2022). Near-Infrared fluorescent unsymmetrical aza-

- BODIPYs: Synthesis, photophysics and TD-DFT calculations. *Spectrochimica Acta Part A: Molecular and Biomolecular Spectroscopy*, 271, 120898. (DOI: 10.1016/j.saa.2022.120898).
- (18) Jiang, X. D., Fu, Y., Zhang, T., & Zhao, W. (2012). Synthesis and properties of NIR aza-BODIPYs with aryl and alkynyl substituents on the boron center. *Tetrahedron Letters*, 53(42), 5703-5706. (DOI: 10.1016/j.tetlet.2012.08.056)
- (19) Zhang, L., Zhao, L., Wang, K., & Jiang, J. (2016). Chiral benzo-fused Aza-BODIPYs with optical activity extending into the NIR range. *Dyes and Pigments*, 134, 427-433. (DOI: 10.1016/j.dyepig.2016.07.039).
- (20) Virgili, T., Ganzer, L., Botta, C., Squeo, B. M., & Pasini, M. (2022). Asymmetric AZA-BODIPY with Optical Gain in the Near-Infrared Region. *Molecules*, 27(14), 4538. (DOI: 10.3390/molecules27144538).
- (21) Sharma, R., Maragani, R., & Misra, R. (2016). Ferrocenyl aza-dipyrromethene and aza-BODIPY: synthesis and properties. *Journal of Organometallic Chemistry*, 825, 8-14. (DOI: 10.1016/j.jorganchem.2016.10.019).
- (22) Gawale, Y., & Sekar, N. (2018). Investigating the excited state optical properties and origin of large stokes shift in Benz [c, d] indole N-Heteroarene BF₂ dyes with ab initio tools. *Journal of Photochemistry and Photobiology B: Biology*, 178, 472-480. (DOI: 10.1016/j.jphotobiol.2017.12.006).
- (23) Schafer, C., Mony, J., Olsson, T., & Borjesson, K. (2022). Effect of the Aza-N-Bridge and Push–Pull Moieties: A Comparative Study between BODIPYs and Aza-BODIPYs. *The Journal of Organic Chemistry*, 87(5), 2569-2579. (DOI: 10.1021/acs.joc.1c02525).

- (24) Swamy, P. C. A., Sivaraman, G., Priyanka, R. N., Raja, S. O., Ponnuvel, K., Shanmugpriya, J., & Gulyani, A. (2020). Near Infrared (NIR) absorbing dyes as promising photosensitizer for photo dynamic therapy. *Coordination Chemistry Reviews*, 411, 213233. (DOI: 10.1016/j.ccr.2020.213233).
- (25) Wagner, R. W., & Lindsey, J. S. (1996). Boron-dipyrromethene dyes for incorporation in synthetic multi-pigment light-harvesting arrays. *Pure and applied chemistry*, 68(7), 1373-1380. (DOI: 10.1351/pac199668071373).
- (26) Sathyamoorthi, G., Soong, M. L., Ross, T. W., & Boyer, J. H. (1993). Fluorescent tricyclic β -azavinamidine-BF₂ complexes. *Heteroatom Chemistry*, 4(6), 603-608. (DOI: 10.1002/hc.520040613).
- (27) Shukla, V. K., Chakraborty, G., Ray, A. K., & Nagaiyan, S. (2023). Red and NIR emitting ring-fused BODIPY/aza-BODIPY dyes. *Dyes and Pigments*, 111245. (DOI: 10.1016/j.dyepig.2023.111245).
- (28) Shamova, L. I., Zatsikha, Y. V., & Nemykin, V. N. (2021). Synthesis pathways for the preparation of the BODIPY analogues: aza-BODIPYs, BOPHYs and some other pyrrole-based acyclic chromophores. *Dalton Transactions*, 50(5), 1569-1593. (DOI: 10.1039/D0DT03964K).
- (29) Zhu, L., Xie, W., Zhao, L., Zhang, Y., & Chen, Z. (2017). Tetraphenylethylene-and fluorene-functionalized near-infrared aza-BODIPY dyes for living cell imaging. *RSC advances*, 7(88), 55839-55845. (DOI: 10.1039/C7RA10820F).
- (30) Rana, P., Singh, N., Majumdar, P., & Singh, S. P. (2022). Evolution of BODIPY/aza-BODIPY dyes for organic photoredox/energy transfer catalysis. *Coordination Chemistry Reviews*, 470, 214698. (DOI: 10.1016/j.ccr.2022.214698).

- (31) Jiang, X. D., Guan, J., Zhao, J., Le Guennic, B., Jacquemin, D., Zhang, Z., ... & Xiao, L. (2017). Synthesis, structure and photophysical properties of NIR aza-BODIPYs with F/N3/NH2 groups at 1, 7-positions. *Dyes and Pigments*, 136, 619-626. (DOI: 10.1016/j.dyepig.2016.09.019).
- (32) Strobl, M., Rappitsch, T., Borisov, S. M., Mayr, T., & Klimant, I. (2015). NIR-emitting aza-BODIPY dyes—new building blocks for broad-range optical pH sensors. *Analyst*, 140(21), 7150-7153. (DOI: 10.1039/C5AN01389E).
- (33) Gut, A., Łapok, Ł., Jamróz, D., Gorski, A., SolarSKI, J., & Nowakowska, M. (2017). Photophysics and redox properties of aza-BODIPY dyes with electron-withdrawing groups. *New Journal of Chemistry*, 41(20), 12110-12122. (DOI: 10.1039/C7NJ02757E).
- (34) Gupta, I., & Kesavan, P. E. (2019). Carbazole Substituted BODIPYs. *Frontiers in Chemistry*, 7, 841. (DOI: 10.3389/fchem.2019.00841)
- (35) Antina, E., Bumagina, N., Marfin, Y., Guseva, G., Nikitina, L., Sbytov, D., & Telegin, F. (2022). BODIPY Conjugates as Functional Compounds for Medical Diagnostics and Treatment. *Molecules*, 27(4), 1396. (DOI: 10.3390/molecules27041396).
- (36) Swamy P, C. A., Priyanka, R. N., Mukherjee, S., & Thilagar, P. (2015). Panchromatic Borane–aza-BODIPY Conjugate: Synthesis, Intriguing Optical Properties, and Selective Fluorescent Sensing of Fluoride Anions. *European Journal of Inorganic Chemistry*, 2015(13), 2338-2344. (DOI: 10.1002/ejic.201500089).
- (37) Avellanal-Zaballa, E., Prieto-Castañeda, A., García-Garrido, F., Agarrabeitia, A. R., Rebollar, E., Bañuelos, J., ... & Ortiz, M. J. (2020). Red/NIR Thermally Activated Delayed Fluorescence

from Aza-BODIPYs. *Chemistry–A European Journal*, 26(68), 16080-16088. (DOI: 10.1002/chem.202002916).

- (38) Yao, Y., Xiao, X., Liu, S., Tian, B., & Zhang, J. (2023). Syntheses, optical properties, and bioimaging application of near-infrared aza-BODIPY dyes with electronic push–pull system. *Research on Chemical Intermediates*, 1-14. (DOI: 10.1007/s11164-023-05028-0).
- (39) Loudet, A., & Burgess, K. (2007). BODIPY dyes and their derivatives: syntheses and spectroscopic properties. *Chemical reviews*, 107(11), 4891-4932. (DOI: 10.1021/cr078381n).
- (40) Obłóza, M., Łapok, Ł., Pędziński, T., Stadnicka, K. M., & Nowakowska, M. (2019). Synthesis, photophysics and redox properties of aza-BODIPY dyes with electron-donating groups. *ChemPhysChem*, 20(19), 2482-2497. (DOI: 10.1002/cphc.201900689).
- (41) Lu, H., Mack, J., Yang, Y., & Shen, Z. (2014). Structural modification strategies for the rational design of red/NIR region BODIPYs. *Chemical Society Reviews*, 43(13), 4778-4823. (DOI: 10.1039/C4CS00030G).
- (42) Bessette, A., & Hanan, G. S. (2014). Design, synthesis and photophysical studies of dipyrromethene-based materials: insights into their applications in organic photovoltaic devices. *Chemical Society Reviews*, 43(10), 3342-3405. (DOI: 10.1039/C3CS60411J).
- (43) Khan, T. K., Sheokand, P., & Agarwal, N. (2014). Synthesis and Studies of Aza-BODIPY-Based π -Conjugates for Organic Electronic Applications. *European Journal of Organic Chemistry*, 2014(7), 1416-1422. (DOI: 10.1002/ejoc.201301300).

- (44) David, S., Chang, H. J., Lopes, C., Brännlund, C., Le Guennic, B., Berginc, G., ... & Maury, O. (2021). Benzothiadiazole-Substituted Aza-BODIPY Dyes: Two-Photon Absorption Enhancement for Improved Optical Limiting Performances in the Short-Wave IR Range. *Chemistry–A European Journal*, 27(10), 3517-3525. (DOI: 10.1002/chem.202004899).
- (45) Ipek, O. S., Topal, S., & Ozturk, T. (2021). Synthesis, characterization and sensing properties of donor-acceptor systems based Dithieno [3, 2-b; 2', 3'-d] thiophene and boron. *Dyes and Pigments*, 192, 109458. (DOI: 10.1016/j.dyepig.2021.109458).
- (46) Çetindere, S. (2021). Photophysics of BODIPY Dyes: Recent Advances. *Photophysics, Photochem. Substit. React.-Recent Adv*, 2021, 31-50. (DOI: 10.5772/intechopen.92609).
- (47) Killoran, J., Allen, L., Gallagher, J. F., Gallagher, W. M., & O'Shea, D. F. (2002). Synthesis of BF₂ Chelates of Tetraarylazadipyrrromethenes and Evidence for Their Photodynamic Therapeutic Behavior. *ChemInform*, 33(51), 177-177. (DOI: 10.1039/B204317C).
- (48) Zhao, W., & Carreira, E. M. (2006). Conformationally restricted aza-BODIPY: highly fluorescent, stable near-infrared absorbing dyes. *Chemistry–A European Journal*, 12(27), 7254-7263. (DOI: 10.1002/chem.200600527).
- (49) Donyagina, V. F., Shimizu, S., Kobayashi, N., & Lukyanets, E. A. (2008). Synthesis of N, N-difluoroboryl complexes of 3, 3'-diarylazadiisindolylmethenes. *Tetrahedron Letters*, 49(42), 6152-6154. (DOI: 10.1016/j.tetlet.2008.08.026).
- (50) Jiang, X. D., Jia, L., Su, Y., Li, C., Sun, C., & Xiao, L. (2019). Synthesis and application of near-infrared absorbing morpholino-

containing aza-BODIPYs. *Tetrahedron*, 75(33), 4556-4560. (DOI: 10.1016/j.tet.2019.06.046).

- (51) Gresser, R., Hummert, M., Hartmann, H., Leo, K., & Riede, M. (2011). Synthesis and characterization of near-infrared absorbing benzannulated aza-BODIPY dyes. *Chemistry–A European Journal*, 17(10), 2939-2947. (DOI: 10.1002/chem.201002941).
- (52) Gresser, R., Hummert, M., Hartmann, H., Leo, K., & Riede, M. (2011). Synthesis and characterization of near-infrared absorbing benzannulated aza-BODIPY dyes. *Chemistry–A European Journal*, 17(10), 2939-2947. (DOI: 10.1016/j.jlumin.2023.120099).
- (53) Ni, Y., & Wu, J. (2014). Far-red and near infrared BODIPY dyes: synthesis and applications for fluorescent pH probes and bio-imaging. *Organic & biomolecular chemistry*, 12(23), 3774-3791. (DOI: 10.1039/C3OB42554A).
- (54) Saha, S., Kanaparthi, R. K., & Soldatovic, T. (Eds.). (2021). Photophysics, Photochemical and Substitution Reactions: Recent Advances.
- (55) Zarcone, S. R., Yarbrough, H. J., Neal, M. J., Kelly, J. C., Kaczynski, K. L., Bloomfield, A. J., ... & Chase, D. T. (2022). Synthesis and photophysical properties of nitrated aza-BODIPYs. *New Journal of Chemistry*, 46(9), 4483-4496. (DOI: 10.1039/D1NJ05976A).
- (56) Karatay, A., Miser, M. C., Cui, X., Küçüköz, B., Yılmaz, H., Sevinç, G., ... & Elmali, A. (2015). The effect of heavy atom to two photon absorption properties and intersystem crossing mechanism in aza-boron-dipyrromethene compounds. *Dyes and Pigments*, 122, 286-294. (DOI: 10.1016/j.dyepig.2015.07.002).

- (57) Jiang, X. D., Li, S., Guan, J., Fang, T., Liu, X., & Xiao, L. J. (2016). Recent advances of the near-infrared fluorescent aza-BODIPY dyes. *Current Organic Chemistry*, 20(16), 1736-1744. (DOI: 10.2174/1385272820666160229224354)
- (58) Gresser, R., Hartmann, H., Wrackmeyer, M., Leo, K., & Riede, M. (2011). Synthesis of thiophene-substituted aza-BODIPYs and their optical and electrochemical properties. *Tetrahedron*, 67(37), 7148-7155. (DOI: 10.1016/j.tet.2011.06.100).
- (59) Balsukuri, N., Lone, M. Y., Jha, P. C., Mori, S., & Gupta, I. (2016). Synthesis, Structure, and Optical Studies of Donor–Acceptor-Type Near-Infrared (NIR) Aza–Boron-Dipyrromethene (BODIPY) Dyes. *Chemistry–An Asian Journal*, 11(10), 1572-1587. (DOI: 10.1002/asia.201600167).
- (60) Pinjari, D., Alsaleh, A. Z., Patil, Y., Misra, R., & D'Souza, F. (2020). Interfacing High-Energy Charge-Transfer States to a Near-IR Sensitizer for Efficient Electron Transfer upon Near-IR Irradiation. *Angewandte Chemie International Edition*, 59(52), 23697-23705. (DOI: 10.1002/anie.202013036).
- (61) Qian, G., & Wang, Z. Y. (2010). Near-infrared organic compounds and emerging applications. *Chemistry–An Asian Journal*, 5(5), 1006-1029. (DOI: 10.1002/asia.200900596).
- (62) Mueller, T., Gresser, R., Leo, K., & Riede, M. (2012). Organic solar cells based on a novel infrared absorbing aza-bodipy dye. *Solar energy materials and solar cells*, 99, 176-181. (DOI: 10.1016/j.solmat.2011.11.006).
- (63) Fan, G., Yang, L., & Chen, Z. (2014). Water-soluble BODIPY and aza-BODIPY dyes: synthetic progress and applications. *Frontiers of Chemical Science and Engineering*, 8, 405-417. (DOI: 10.1007/s11705-014-1445-7).

- (64) Leblebici, S. Y., Catane, L., Barclay, D. E., Olson, T., Chen, T. L., & Ma, B. (2011). Near-infrared azadipyrromethenes as electron donor for efficient planar heterojunction organic solar cells. *ACS applied materials & interfaces*, 3(11), 4469-4474. (DOI: 10.1021/am201157d).
- (65) Rao, R. S., Yadagiri, B., Sharma, G. D., & Singh, S. P. (2019). Butterfly architecture of NIR Aza-BODIPY small molecules decorated with phenothiazine or phenoxazine. *Chemical Communications*, 55(83), 12535-12538. (DOI: 10.1039/C9CC06300E).
- (66) Baranovskii, S. D., Wiemer, M., Nenashev, A. V., Jansson, F., & Gebhard, F. (2012). Calculating the efficiency of exciton dissociation at the interface between a conjugated polymer and an electron acceptor. *The Journal of Physical Chemistry Letters*, 3(9), 1214-1221. (DOI: 10.1021/jz300123k).
- (67) Feng, R., Sato, N., Yasuda, T., Furuta, H., & Shimizu, S. (2020). Rational design of pyrrolopyrrole-aza-BODIPY-based acceptor–donor–acceptor triads for organic photovoltaics application. *Chemical Communications*, 56(20), 2975-2978. (DOI: 10.1039/D0CC00398K).
- (68) Kalot, G., Godard, A., Busser, B., Pliquett, J., Broekgaarden, M., Motto-Ros, V., ... & Sancey, L. (2020). Aza-BODIPY: A new vector for enhanced theranostic boron neutron capture therapy applications. *Cells*, 9(9), 1953. (DOI: 10.3390/cells9091953).
- (69) Yang, B., Chen, Y., & Shi, J. (2019). Reactive oxygen species (ROS)-based nanomedicine. *Chemical reviews*, 119(8), 4881-4985. (DOI: 10.1021/acs.chemrev.8b00626).
- (70) Wei, W., Rosenkrans, Z. T., Luo, Q. Y., Lan, X., & Cai, W. (2019). Exploiting Nanomaterial-Mediated Autophagy for

- Cancer Therapy. *Small Methods*, 3(2), 1800365. (DOI: 10.1002/smtd.201800365).
- (71) Yan, K. C., Sedgwick, A. C., Zang, Y., Chen, G. R., He, X. P., Li, J., ... & James, T. D. (2019). Sensors, imaging agents, and theranostics to help understand and treat reactive oxygen species related diseases. *Small Methods*, 3(7), 1900013. (DOI: 10.1002/smtd.201900013).
- (72) Xie, J., Wang, Y., Choi, W., Jangili, P., Ge, Y., Xu, Y., ... & Kim, J. S. (2021). Overcoming barriers in photodynamic therapy harnessing nano-formulation strategies. *Chemical Society Reviews*, 50(16), 9152-9201. (DOI: 10.1039/D0CS01370F).
- (73) Du, J., Shi, T., Long, S., Chen, P., Sun, W., Fan, J., & Peng, X. (2021). Enhanced photodynamic therapy for overcoming tumor hypoxia: From microenvironment regulation to photosensitizer innovation. *Coordination Chemistry Reviews*, 427, 213604. (DOI: 10.1016/j.ccr.2020.213604).
- (74) Yu, Z., Zhou, J., Ji, X., Lin, G., Xu, S., Dong, X., & Zhao, W. (2020). Discovery of a monoiodo aza-BODIPY near-infrared photosensitizer: in vitro and in vivo evaluation for photodynamic therapy. *Journal of Medicinal Chemistry*, 63(17), 9950-9964. (DOI: 10.1021/acs.jmedchem.0c00882).
- (75) Shin, J., Xu, Y., Koo, S., Lim, J. H., Lee, J. Y., Sharma, A., ... & Kim, J. S. (2021). Mitochondria-targeted nanotheranostic: Harnessing single-laser-activated dual phototherapeutic processing for hypoxic tumor treatment. *Matter*, 4(7), 2508-2521. (DOI: 10.1016/j.matt.2021.05.022).
- (76) Zhao, M., Xu, Y., Xie, M., Zou, L., Wang, Z., Liu, S., & Zhao, Q. (2018). Halogenated Aza-BODIPY for imaging-guided synergistic photodynamic and photothermal tumor therapy.

Advanced healthcare materials, 7(18), 1800606. (DOI: 10.1002/adhm.201800606).

- (77) Staudinger, C., Breininger, J., Klimant, I., & Borisov, S. M. (2019). Near-infrared fluorescent aza-BODIPY dyes for sensing and imaging of pH from the neutral to highly alkaline range. *Analyst*, 144(7), 2393-2402. (DOI: 10.1039/C9AN00118B).
- (78) Ozlem, S., & Akkaya, E. U. (2009). Thinking outside the silicon box: molecular and logic as an additional layer of selectivity in singlet oxygen generation for photodynamic therapy. *Journal of the American Chemical Society*, 131(1), 48-49. (DOI: 10.1021/ja808389t).
- (79) Gorman, A., Killoran, J., O'Shea, C., Kenna, T., Gallagher, W. M., & O'Shea, D. F. (2004). In vitro demonstration of the heavy-atom effect for photodynamic therapy. *Journal of the American Chemical Society*, 126(34), 10619-10631. (DOI: 10.1021/ja047649e).
- (80) Wood, T. E., & Thompson, A. (2007). Advances in the chemistry of dipyrrens and their complexes. *Chemical reviews*, 107(5), 1831-1861. (DOI: 10.1021/cr050052c).
- (81) Bergström, F., Mikhalyov, I., Hägglöf, P., Wortmann, R., Ny, T., & Johansson, L. B. Å. (2002). Dimers of dipyrrometheneboron difluoride (BODIPY) with light spectroscopic applications in chemistry and biology. *Journal of the American Chemical Society*, 124(2), 196-204. (DOI: 10.1021/ja010983f).
- (82) Bonardi, L., Kanaan, H., Camerel, F., Jolinet, P., Retailleau, P., & Ziessel, R. (2008). Fine-tuning of yellow or red photo- and electroluminescence of functional difluoro-boradiazaindacene films. *Advanced Functional Materials*, 18(3), 401-413. (DOI: 10.1002/adfm.200700697).

- (83) Byrne, A. T., O'connor, A. E., Hall, M., Murtagh, J., O'Neill, K., Curran, K. M., ... & Gallagher, W. M. (2009). Vascular-targeted photodynamic therapy with BF₂-chelated Tetraaryl-Azadipyrrromethene agents: a multi-modality molecular imaging approach to therapeutic assessment. *British journal of cancer*, 101(9), 1565-1573. (DOI: 10.1038/sj.bjc.6605247).
- (84) Adarsh, N., Shanmugasundaram, M., Avirah, R. R., & Ramaiah, D. (2012). Aza-BODIPY Derivatives: Enhanced Quantum Yields of Triplet Excited States and the Generation of Singlet Oxygen and their Role as Facile Sustainable Photooxygenation Catalysts. *Chemistry—A European Journal*, 18(40), 12655-12662. (DOI: 10.1002/chem.201202438).
- (85) Li, H., Zhang, P., Smaga, L. P., Hoffman, R. A., & Chan, J. (2015). Photoacoustic probes for ratiometric imaging of copper (II). *Journal of the American Chemical Society*, 137(50), 15628-15631. (DOI: 10.1021/jacs.5b10504).
- (86) Knox, H. J., Kim, T. W., Zhu, Z., & Chan, J. (2018). Photophysical tuning of N-oxide-based probes enables ratiometric photoacoustic imaging of tumor hypoxia. *ACS chemical biology*, 13(7), 1838-1843. (DOI: 10.1021/acscchembio.8b00099).
- (87) Tian, Y., Zhou, H., Cheng, Q., Dang, H., Qian, H., Teng, C., ... & Yan, L. (2022). Stable twisted conformation aza-BODIPY NIR-II fluorescent nanoparticles with ultra-large Stokes shift for imaging-guided phototherapy. *Journal of Materials Chemistry B*, 10(5), 707-716. (DOI: 10.1039/D1TB02066H).
- (88) Loudet, A., Bandichhor, R., Wu, L., & Burgess, K. (2008). Functionalized BF₂ chelated azadipyrrromethene dyes. *Tetrahedron*, 64(17), 3642-3654. (DOI: 10.1016/j.tet.2008.01.117).

- (89) Chang, H. J., Bondar, M. V., Munera, N., David, S., Maury, O., Berginc, G., ... & Van Stryland, E. W. (2022). Femtosecond Spectroscopy and Nonlinear Optical Properties of aza-BODIPY Derivatives in Solution. *Chemistry–A European Journal*, 28(17), e202104072. (DOI: 10.1002/chem.202104072).
- (90) Amin, A. N., El-Khouly, M. E., Subbaiyan, N. K., Zandler, M. E., Supur, M., Fukuzumi, S., & D'Souza, F. (2011). Syntheses, electrochemistry, and photodynamics of ferrocene–azadipyrrromethane donor–acceptor dyads and triads. *The Journal of Physical Chemistry A*, 115(35), 9810-9819. (DOI: 10.1021/jp205236n).
- (91) Zhu, X., Wang, J. X., Niu, L. Y., & Yang, Q. Z. (2019). Aggregation-induced emission materials with narrowed emission band by light-harvesting strategy: fluorescence and chemiluminescence imaging. *Chemistry of Materials*, 31(9), 3573-3581. (DOI: 10.1021/acs.chemmater.9b01338).
- (92) Bhat, G., Kielar, M., Rao, H., Gholami, M. D., Mathers, I., Larin, A. C., ... & Sonar, P. (2022). Versatile aza-BODIPY-based low-bandgap conjugated small molecule for light harvesting and near-infrared photodetection. *InfoMat*, 4(12), e12345. (DOI: 10.1002/inf2.12345).
- (93) Zhou, J., Gai, L., Zhou, Z., Yang, W., Mack, J., Xu, K., ... & Shen, Z. (2016). Rational Design of Emissive NIR-Absorbing Chromophores: RhIII Porphyrin-Aza-BODIPY Conjugates with Orthogonal Metal–Carbon Bonds. *Chemistry–A European Journal*, 22(37), 13201-13209. (DOI: 10.1002/chem.201602670).
- (94) Koch, A., & Ravikanth, M. (2019). Monofunctionalized 1, 3, 5, 7-TetraarylazaBODIPYs and Their Application in the Synthesis of AzaBODIPY Based Conjugates. *The Journal of Organic*

Chemistry, 84(17), 10775-10784. (DOI: 10.1021/acs.joc.9b01311).

- (95) Rani, K., Pandey, U. K., & Sengupta, S. (2021). Efficient electron transporting and panchromatic absorbing FRET cassettes based on aza-BODIPY and perylenediimide towards multiple metal FRET-Off sensing and ratiometric temperature sensing. *Journal of Materials Chemistry C*, 9(13), 4607-4618. (DOI: 10.1039/D1TC00068C).
- (96) D'Souza, F., Amin, A. N., El-Khouly, M. E., Subbaiyan, N. K., Zandler, M. E., & Fukuzumi, S. (2012). Control over photoinduced energy and electron transfer in supramolecular polyads of covalently linked azaBODIPY-bisporphyrin 'molecular clip'hosting fullerene. *Journal of the American Chemical Society*, 134(1), 654-664. (DOI: 10.1021/ja209718g).

Chapter 2

Materials and experimental techniques

2.1. Introduction

In this chapter the materials used, general synthetic procedures, characterization techniques and the instrumentation employed in this thesis are discussed.

2.2. Chemicals for synthesis

Common solvents used for syntheses were purified according to known procedures.^[1] Benzaldehyde, acetophenone, nitromethane, ethanol, methanol, potassium hydroxide, ammonium acetate, phosphorus oxychloride, dimethylformamide, and boron trifluoride etherate were obtained from Spectrochem India. Triethylamine, *N,N*-diisopropylethylamine, were obtained from S.D.Fine chem. Ltd. *N,N*-Dimethylethylamine, fullerene (C₆₀), sarcosine, hydroxylamine hydrochloride, CuI, Pd(PPh₃)₄, PdCl₂(PPh₃)₂, and tetrabutylammonium hexafluorophosphate (TBAF₆) were procured from Aldrich chemicals USA. Aluminum oxide (neutral) and silica gel (100–200 mesh and 230–400 mesh) were purchased from Rankem chemicals, India. TLC pre-coated silica gel plates (Kieselgel 60F254, Merck) were obtained from Merck, India.

Dry solvents dichloromethane, chloroform, tetrahydrofuran (THF), *N,N*-dimethylformamide (DMF), dioxane and methanol were obtained from spectrochem and S.D.Fine chem. Ltd. All oxygen or moisture sensitive reactions were performed under nitrogen/argon atmosphere using standard schlenk method.

The solvents and reagents were used as received unless otherwise indicated. Photophysical and electrochemical studies were performed with spectroscopic grade solvents.

2.3. Spectroscopic Measurements

2.3.1. NMR Spectroscopy

^1H NMR (400/500 MHz), ^{13}C NMR (100/125 MHz), ^{11}B NMR (128.37 MHz), and ^{19}F NMR (376.49 MHz) spectra were recorded on the Bruker Avance (III) 400/500 MHz, using CDCl_3 as solvent. Chemical shifts in ^1H , ^{13}C , ^{11}B and ^{19}F NMR spectra were reported in parts per million (ppm). In ^1H NMR chemical shifts are reported relative to the residual solvent peak (CDCl_3 , 7.26 ppm). Multiplicities are given as: s (singlet), d (doublet), t (triplet), q (quartet), dd (doublet of doublets), m (multiplet), and the coupling constants J , are given in Hz. ^{13}C NMR chemical shifts are reported relative to the solvent residual peak (CDCl_3 , 77.36 ppm).

2.3.2. Mass Spectrometry

High resolution mass spectra (HRMS) were recorded on Bruker-Daltonics, micrOTOF-Q II mass spectrometer using positive and negative mode electrospray ionizations.

2.3.3. UV-Vis Spectroscopy

UV-Vis absorption spectra were recorded using a Varian Cary100 Bio UV-Vis and PerkinElmer LAMBDA 35 UV/Vis spectrophotometer.

2.4. Electrochemical Studies

Cyclic voltamograms (CVs) and Differential Pulse Voltamograms (DPVs) were recorded on CHI620D electrochemical analyzer using Glassy carbon as working electrode, Pt wire as the counter electrode, and Saturated Calomel Electrode (SCE)/ Ag/AgCl as the reference electrode. The scan rate was 100 mVs^{-1} . A solution of tetrabutylammonium hexafluorophosphate (TBAPF_6) in DCM (0.1 M) was employed as the supporting electrolyte.

2.5. Elemental Analysis

Elemental analyses for elements carbon, hydrogen, nitrogen and sulphur were performed on the Thermo Scientific FLASH 2000 (formerly the Flash EA1112) elemental analyser.

2.6. Computational Calculations

The density functional theory (DFT) calculation were carried out at the B3LYP/6-31G (d, p) level for B, F, S, C, N, O, H in the Gaussian 09 program.^[2]

2.7. References

- [1] (a) Vogel, A. I., Tatchell, A. R., Furnis, B. S., Hannaford, A. J., & Smith, P. W. G. (1996). *Vogel's Textbook of Practical Organic Chemistry (5th Edition)* (5th ed.); (b) Wei Ssberger, A. Proskraner, E. S. Riddick, J. A. Toppos Jr., E. F. (1970). *Organic Solvents in Techniques of Organic Chemistry*, Vol. IV, 3rd Edition, Inc. New York.
- [2] (a) Frisch, M. J.; Trucks, G. W.; Schlegel, H. B.; Scuseria, G. E.; Robb, M. A.; Cheeseman, J. R.; Scalmani, G.; Barone, V.; Mennucci, B.; Petersson, G. A.; Nakatsuji, H.; Caricato, M.; Li, X.; Hratchian, H. P.; Izmaylov, A. F.; Bloino, J.; Zheng, G.; Sonnenberg, J. L.; Hada, M.; Ehara, M.; Toyota, K.; Fukuda, R.; Hasegawa, J.; Ishida, M.; Nakajima, T.; Honda, Y.; Kitao, O.; Nakai, H.; Vreven, T.; Montgomery, J. A. Jr.; Peralta, J. E.; Ogliaro, F.; Bearpark, M.; Heyd, J. J.; Brothers, E.; Kudin, K. N.; Staroverov, V. N.; Kobayashi, R.; Normand, J.; Raghavachari, K.; Rendell, A.; Burant, J. C.; Iyengar, S. S.; Tomasi, J.; Cossi, M.; Rega, N.; Millam, N. J.; Klene, M.; Knox, J. E.; Cross, J. B.; Bakken, V.; Adamo, C.; Jaramillo, J.; Gomperts, R.; Stratmann, R. E.; Yazyev, O.; Austin, A. J.; Cammi, R.; Pomelli, C.; Ochterski, J. W.; Martin, R. L.; Morokuma, K.; Zakrzewski, V. G.; Voth, G. A.; Salvador, P.;

Dannenberg, J. J.; Dapprich, S.; Daniels, A. D.; Farkas, O.; Foresman, J. B.; Ortiz, J. V.; Cioslowski, J.; Fox, D. J. (2009). *Gaussian 09, revision A.02*; Gaussian, Inc.: Wallingford, CT. (b) Lee, C., Yang, W., & Parr, R. G. (1988). Development of the Colle-Salvetti correlation-energy formula into a functional of the electron density. *Physical Review B*, 37(2), 785–789. **DOI:** 10.1103/PhysRevB.37.785; (c) A.D. Becke (1993). A new mixing of Hartree-Fock and local density-functional theories. *J. Chem. Phys.* 98 (2), 1372–377. **DOI:** 10.1063/1.464304.

Chapter 3

NIR absorbing donor-acceptor functionalized aza-BODIPYs: synthesis, photophysical and electrochemical properties

3.1. Introduction

The π -conjugated organic chromophores with near-infrared (NIR) absorption has grabbed considerable attention due to their excellent photophysical properties and widespread applications in optoelectronics.^[1–5] These dyes have become the preferred choice for various biological applications due to their optical properties including high quantum yield, low photobleaching, and deep tissue penetration.^[6–10] Aza-BODIPY is an important class of boron family which offers an exceptional structural adaptability and can be easily functionalized at all positions on the core.^[11–16] The introduction of a nitrogen atom at the meso position of the boron dipyrromethene (BODIPY) leads to a significant bathochromic shift of the absorption and emission in resulting aza-BODIPY chromophore.^[17–22] Since the last decade, significant progress has been seen in the chemistry of aza-BODIPY dyes by substituting various aryl moieties at 1, 7-positions, 3, 5-positions or 2, 6-positions.^[23–28] The donor and acceptor functionalized chromophores based on aza-BODIPY have been reported for various optoelectronic applications such as solar cells, organic light emitting diodes and in bioimaging.^[29–35]

The functionalization of the aza-BODIPY core with a donor substituent will result in a donor–acceptor (D–A) molecular system with absorption extending towards NIR region, and the strength of this D–A interaction can be tuned by varying the nature and number of the donor substituents.^[36–40] The literature shows that the simple change in donor substituent on aza-dipyrromethene or aza-BODIPY leads to

huge redshift in the absorption spectra.^[41] We have recently reported different donor functionalized aza-BODIPY dyes and studied their photophysical and electrochemical properties.^[42]

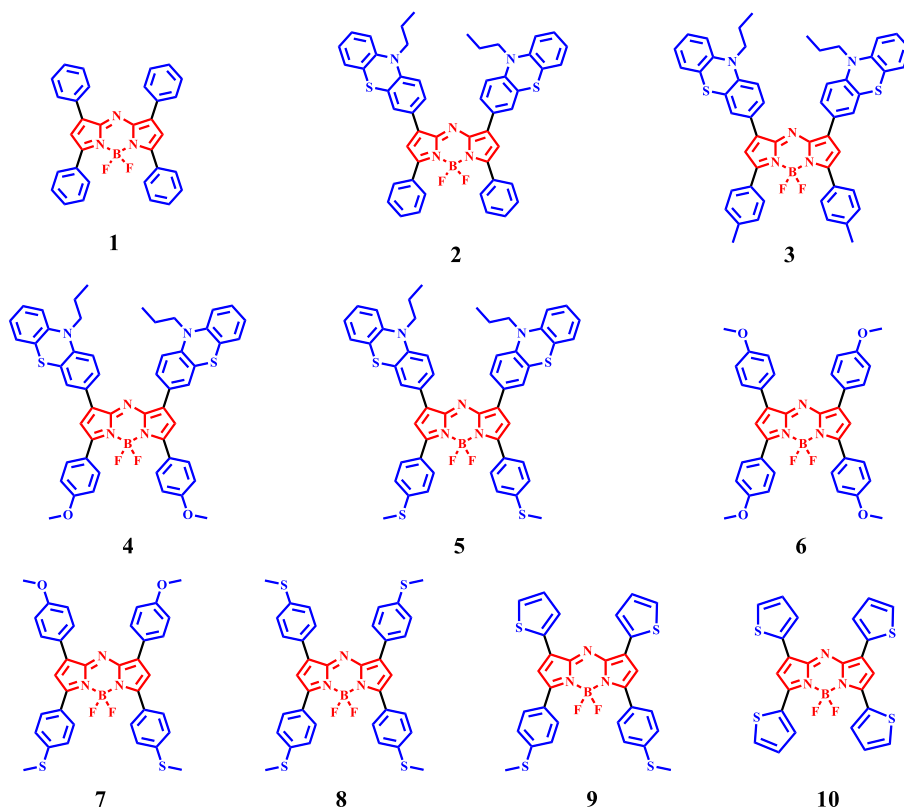
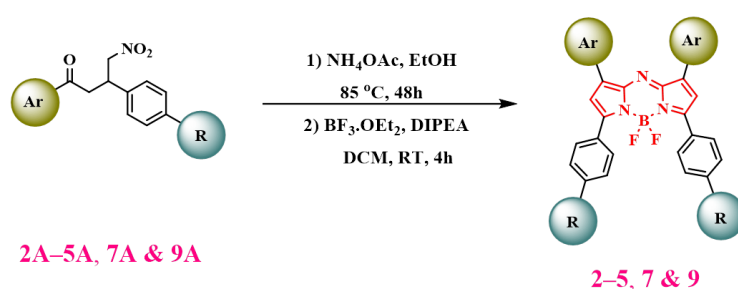


Figure 3.1. Chemical structures of tetra-aryl functionalized aza-BODIPYs **1–10**.

Herein, we report the design and synthesis of tetra-aryl substituted aza-BODIPY dyes **2–5**, **7** and **9** using condensation reaction followed by complexation with boron trifluoride diethyl etherate ($\text{BF}_3 \cdot \text{OEt}_2$). The optical and electrochemical properties of the aza-BODIPYs **1–10** were investigated, along with the computational calculations. The primary aim of this study was to explore and compare the effect of aryl functionalization (such as phenyl, tolyl, anisole, phenothiazine, thioanisole, thiophene) on the photophysical and electrochemical properties of aza-BODIPY.

3.2. Results and Discussion

The synthesis of tetra-phenyl, tetra-anisole, tetra-thioanisole, and tetra-thiophene functionalized aza-BODIPYs **1**, **6**, **8**, and **10** are previously reported in the literature.^[13,43–45] The synthesis of different donor substituted aza-BODIPY dyes **2–5**, **7** and **9** are shown in Scheme 3.1. These aza-BODIPY derivatives were synthesized by reacting intermediates **2A–5A**, **7A** and **9A** with ammonium acetate in ethanol solvent at 85 °C for 48 hours followed by complexation without purifying at this stage by using boron trifluoride diethyl etherate (BF₃.OEt₂) at room temperature. The intermediate precursors **2A–5A**, **7A** and **9A** were synthesized by reacting different aryl benzaldehydes with different aryl acetophenones at room temperature for 24 hours followed by reaction with nitromethane, diethylamine at 60 °C for 24 hours.^[46]



Aza-BODIPY	2	3	4	5	7	9
	-H	-CH ₃	-OCH ₃	-SCH ₃	-SCH ₃	-SCH ₃
Yield %	80%	78%	75%	70%	80%	65%

Scheme 3.1. Synthetic route for aryl functionalized aza-BODIPY dyes **2–5**, **7** and **9**.

The aza-BODIPY dyes **2–5**, **7** and **9** were purified by column chromatography, using silica gel. The aza-BODIPY dyes **2–5**, **7** and **9** exhibited excellent solubility in common organic solvents namely, dichloromethane, chloroform, toluene, and are well characterized using

^1H NMR, ^{13}C NMR, ^{11}B NMR, ^{19}F NMR and HRMS characterization techniques.

3.3. Photophysical Properties

The electronic absorption spectra of the aza-BODIPY dyes **2–5**, **7** and **9** were recorded in dichloromethane solvent at room temperature (Figure 3.2.) and the corresponding data are listed in Table 3.1. The absorption spectra of tetra-aryl functionalized aza-BODIPY dyes **1–10** exhibited two absorption bands covering absorption in the visible and near-infrared region. They show one intense broad absorption band in the visible region from 400–520 nm due to $\pi \rightarrow \pi^*$ transition, and another absorption band covering the visible to NIR region from 520–1000 nm due to intermolecular charge transfer (ICT) transition. Notably, the intense band in the longer wavelength region showed a broad absorption in phenothiazine functionalized aza-BODIPY dyes **2–5**.

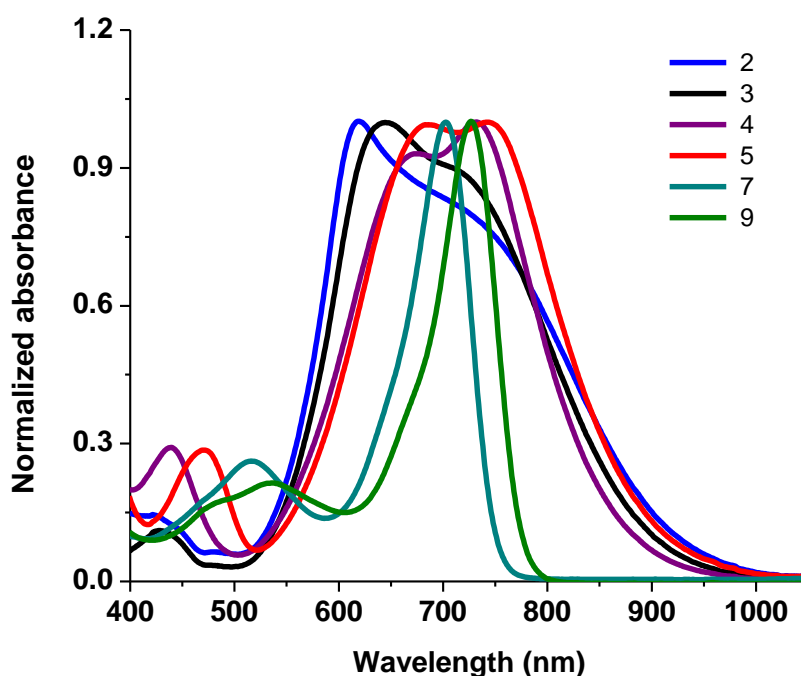


Figure 3.2. Normalized electronic absorption spectra of aryl functionalized aza-BODIPYs **2–5**, **7** and **9** ($1 \times 10^{-5}\text{M}$).

The tetra-aryl functionalized aza-BODIPY dyes **1–10** show absorption maxima at 650,^[43] 620, 644, 732, 744, 690,^[44] 702, 717,^[45] 727 and 742,^[13] nm respectively. The molar absorption coefficients (ϵ_{max}) for tetra-aryl functionalized aza-BODIPYs were observed at: 66,000 M⁻¹cm⁻¹ for **1**, 36,000 M⁻¹cm⁻¹ for **2**, 35,000 M⁻¹cm⁻¹ for **3**, 53,000 M⁻¹cm⁻¹ for **4**, and 41,000 M⁻¹cm⁻¹ for **5**, 66,000 M⁻¹cm⁻¹ for **6**, 58,000 M⁻¹cm⁻¹ for **7**, 93,000 M⁻¹cm⁻¹ for **8**, 43,000 M⁻¹cm⁻¹ for **9**, and 110,000 M⁻¹cm⁻¹ for **10**. The phenothiazine substituted di-anisole and di-thioanisole functionalized aza-BODIPYs **4** and **5** exhibited red shifted absorption bands in the longer wavelength region, owing to the stronger electron donating ability of the anisole and thioanisole units compared to the phenyl and tolyl substituents in aza-BODIPYs **1–3**. Similarly, the di and tetra-thiophene functionalized aza-BODIPYs **9** and **10** exhibited red shifted absorption bands in the longer wavelength region compared to the anisole and thioanisole functionalized aza-BODIPYs **6–8**, due to the presence of stronger donating ability of the thiophene unit.

The aza-BODIPY dyes **4**, **5** and **7–10** show a red-shifted absorption compared to other aza-BODIPY dyes **1–3** and **6** due to presence of strong donating phenothiazine, thioanisole, and thiophene units. The phenothiazine functionalized aza-BODIPY with tolyl substituent **3** shows bathochromic shift of 24 nm compared to aza-BODIPY with phenyl substituent **2** indicating that the methyl substituent on phenyl moieties has a pronounced effect. The change of substituent from tolyl to anisole and thioanisole in phenothiazine functionalized aza-BODIPY **3** exhibited red shift of 88 and 100 nm in aza-BODIPY **4** and **5** respectively due to better communication between anisole/thioanisole donor and aza-BODIPY acceptor respectively. The change of electron donating anisole units in tetra-anisole substituted aza-BODIPY **6** shows red shift of the absorption by 37 nm in aza-BODIPY **9** with two thiophene and two thioanisole substituents.

Table 3.1. Photophysical properties of tetra-aryl functionalized aza-BODIPY dyes **1–10**.

Dyes	λ_{max} (nm) ^a	$\epsilon \times 10^4$ (M ⁻¹ .cm ⁻¹) ^a
1 ^[43]	650	6.6
2	620	3.6
3	644	3.5
4	732	5.3
5	744	4.1
6 ^[44]	690	6.6
7	702	5.8
8 ^[45]	717	9.3
9	727	4.3
10 ^[13]	742	11.0

^aAbsorbance measured in dichloromethane at 1×10^{-5} M concentration, ϵ : molar extinction coefficient.

The replacement of two electron donating units in two thiophene and two thioanisole functionalized aza-BODIPY **9** with tetra-thiophene units in aza-BODIPY **10** led to a red shift in absorption by 15 nm. The absorption data in Table 1 showed that the simple change in aryl substituent has a significant impact on absorption, as donating strength of aryl substituent on aza-BODIPY increases, the red shift in the absorption maxima was observed.

3.4. Electrochemical Properties

The oxidation and reduction potentials of the tetra-aryl functionalized aza-BODIPY dyes **2–5**, **7** and **9** were investigated by using cyclic voltammetry (CV) at 100 mV s⁻¹ scan rate in dichloromethane solvent with tetrabutylammonium hexafluorophosphate (Bu₄NPF₆) as a supporting electrolyte (0.1 M). Figure 3.3. and Figure 3.4. shows the CV plots, and the corresponding data are given in Table 3.2.

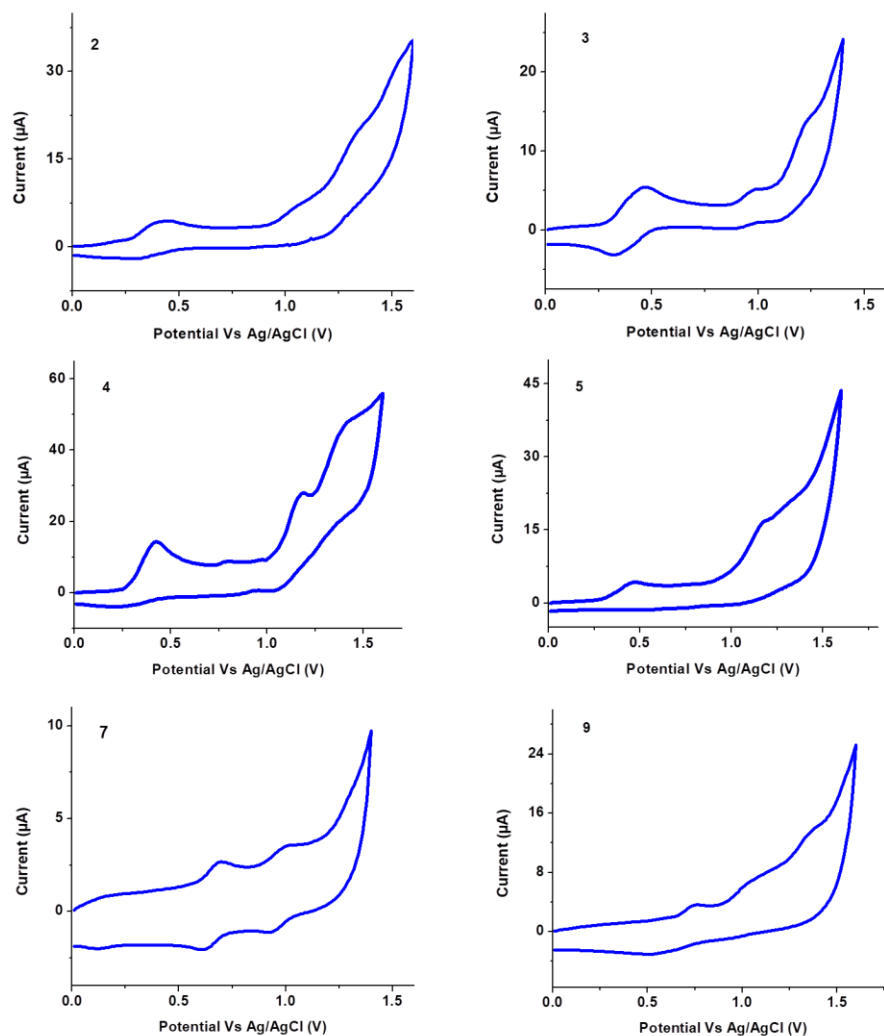


Figure 3.3. Oxidation CV curves of phenothiazine based azabodipyrromethanes **2–5, 7 and 9**.

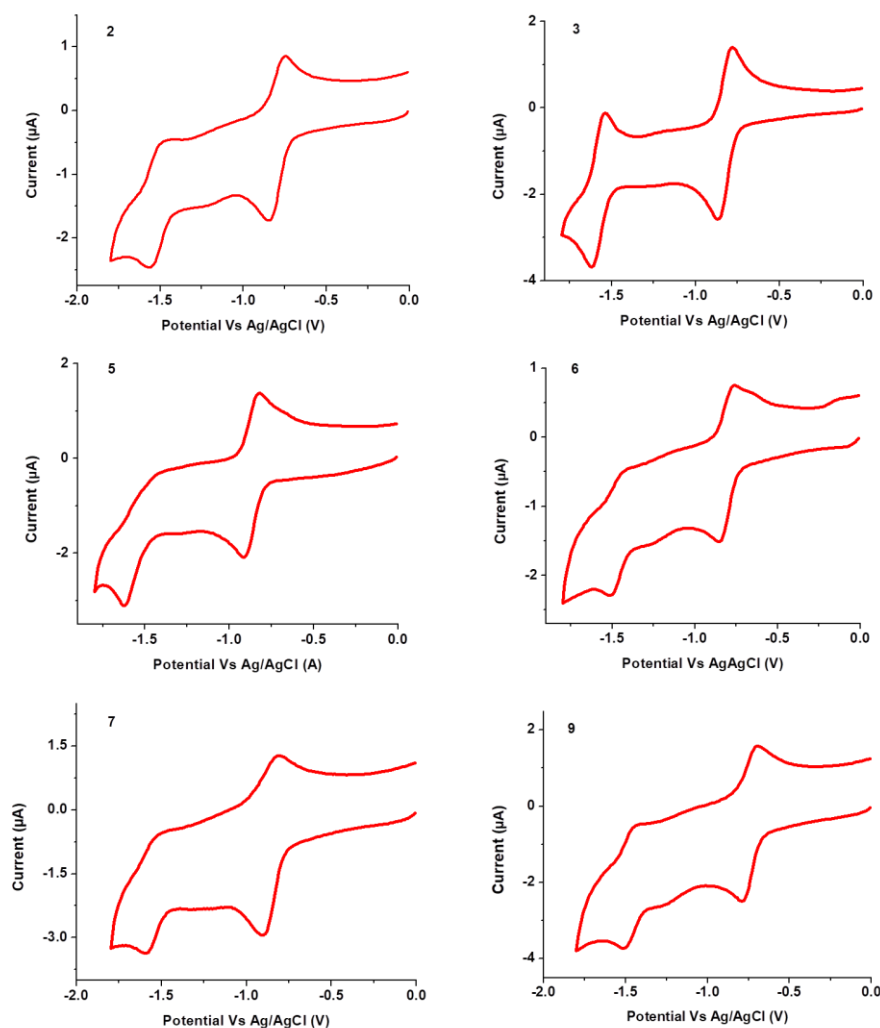


Figure 3.4. Reduction CV curves of tetra-aryl functionalized aza-BODIPYs **2–5**, **7** and **9**.

The phenothiazine functionalized aza-BODIPYs with phenyl, tolyl, anisole and thioanisole substitution **2–5** exhibited three oxidation potentials corresponding to phenothiazine and aza-BODIPY unit. The aza-BODIPYs **2–5** show oxidation potentials at 0.42 V, 1.06 V, 1.32 V; 0.47 V, 0.99 V, 1.23 V; 0.42 V, 1.18 V, 1.41 V; and 0.47 V, 1.16 V, 1.28 V respectively. The aza-BODIPYs with anisole and thiophene substitution **7** and **9** exhibited oxidation potentials at 0.65 V, 0.98 V, and 0.75 V, 1.05 V, 1.37 V respectively related to two thiophene and aza-BODIPY moieties in the molecule. The first oxidation potential of aza-BODIPYs **7** and **9** is anodically shifted as compared to other aza-BODIPYs (**2–5**). Notably, the first oxidation potential in phenothiazine

functionalized aza-BODIPYs with tolyl and thioanisole substitution (**3** and **5**) is anodically shifted compared to phenothiazine functionalized aza-BODIPYs with phenyl and anisole substitution (**2** and **4**), which made them difficult to oxidize.

Table 3.2. Electrochemical properties of tetra-aryl functionalized aza-BODIPYs **2–5**, **7** and **9**.

Dyes	E^1	E^2	E^3	E^1	E^2
	Oxid ^a	Oxid ^a	Oxid ^a	Red ^a	Red ^a
2	0.42	1.06	1.32	-0.85	-1.56
3	0.47	0.99	1.23	-0.87	-1.60
4	0.42	1.18	1.41	-0.91	-1.62
5	0.47	1.16	1.28	-0.86	-1.51
7	0.65	0.98	-	-0.91	-1.60
9	0.75	1.05	1.37	-0.79	-1.52

^aThe electrochemical analysis was performed with a 0.1 M Bu₄NPF₆ solution in dichloromethane at a scan rate of 100 mVs⁻¹ vs Ag/AgCl at 25 °C.

The tetra-aryl functionalized aza-BODIPYs **2–5**, **7** and **9** exhibit two reduction potentials owing to the electron withdrawing aza-BODIPY core. The reduction potentials of aza-BODIPY dyes **2**, **3**, **4** and **5** were found at -0.85 V, -1.56 V; -0.87 V, -1.60 V; -0.91 V, -1.62 V, and -0.86 V, -1.51 V respectively. The reduction potentials observed for aza-BODIPY **7** are at -0.91 V, -1.60 V and for aza-BODIPY **9** are at -0.79 V, and -1.52 V. The phenothiazine functionalized aza-BODIPYs with two phenyl substituents (in **2**) and with two thioanisole substituents (in **5**) exhibit easier reduction compared to aza-BODIPYs with two tolyl substituents (in **3**) and two anisole substitution (in **4**). The first reduction potential in case of aza-BODIPY **9** with two thienyl and two thioanisole substituents is anodically shifted compared to other aza-BODIPY dyes. The second reduction potential in case of aza-BODIPYs **3**, **4** and **7** is cathodically shifted compared to other aza-BODIPYs.

3.5. Theoretical calculations

In order to understand the geometry and electronic structures of the donor functionalized aza-BODIPY dyes **1–10**, DFT calculations were carried out using the Gaussian 09W program at the B3LYP/6-31G (d, p) level for C, H, N, S, and B. The structure optimization was performed in the gas phase and the corresponding frontier molecular orbitals with HOMO-LUMO gap of aza-BODIPYs **1–10** are shown in Figures 3.5., 3.6. and 3.7. The HOMOs and LUMOs of the tetra-phenyl and tetra-thienyl based aza-BODIPYs dyes **1** and **10** show electron density distributed on whole molecular backbone. The HOMO-LUMO gap values for aza-BODIPYs dyes **1** and **10** are 2.19 eV and 1.94 eV respectively (Figure 3.5.) which indicates substitution of stronger electron donating thienyl unit on aza-BODIPY decreases the HOMO-LUMO gap.

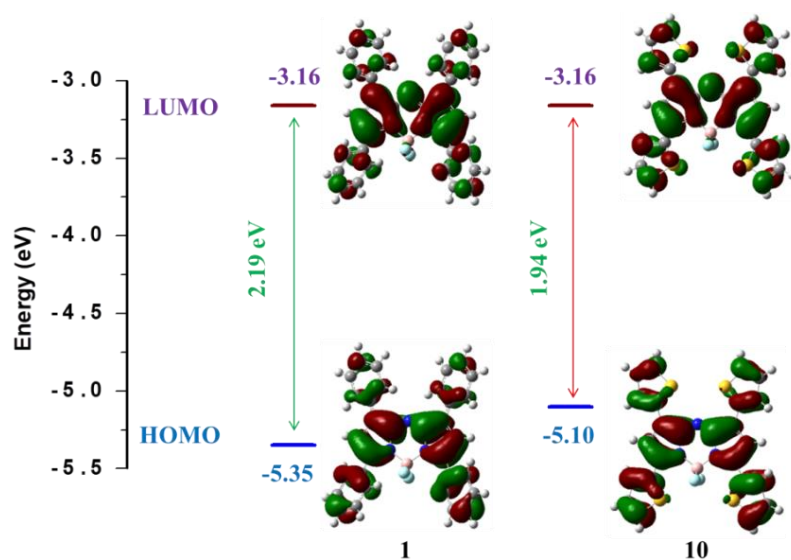


Figure 3.5. HOMO–LUMO energy level diagram of tetra-aryl substituted aza-BODIPYs **1** and **10**.

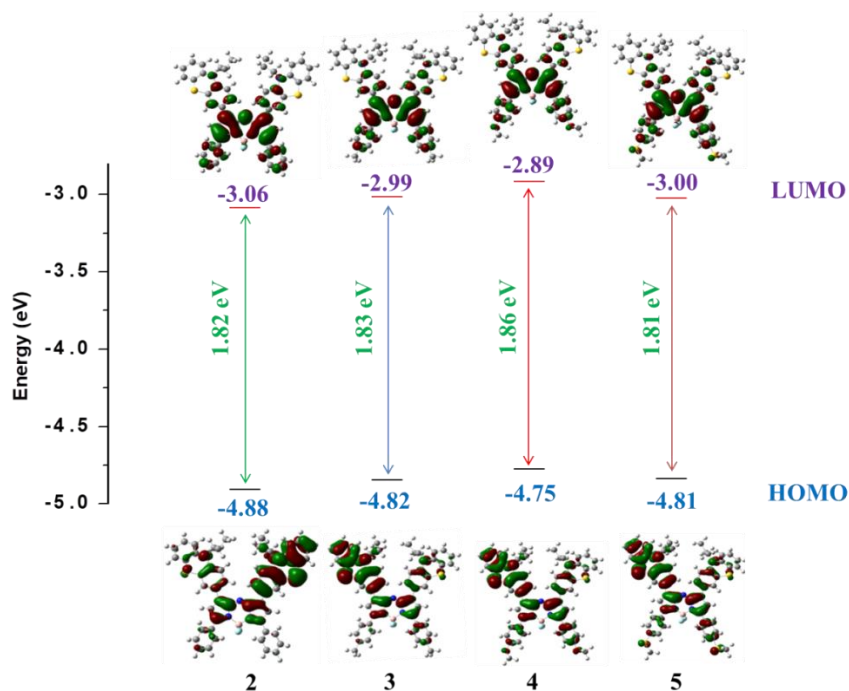


Figure 3.6. HOMO–LUMO energy level diagram of tetra-aryl substituted aza-BODIPYs **2–5**.

The frontier molecular orbitals (FMOs) of phenothiazine based aza-BODIPYs **2–5** (Figure 3.6.) shows that the electron density in HOMOs is mainly localized on phenothiazine donor unit, whereas electron density in LUMOs is mainly localized on aza-BODIPY acceptor core. This indicates intramolecular charge transfer (ICT) interaction. The HOMO-LUMO gap values for aza-BODIPYs dyes **2–5** were found to be 1.82 eV, 1.83 eV, 1.86 eV and 1.81 eV respectively (Figure 3.6.) which indicates substitution of stronger electron donating thioanisole moiety to aza-BODIPY decreases the HOMO-LUMO gap.

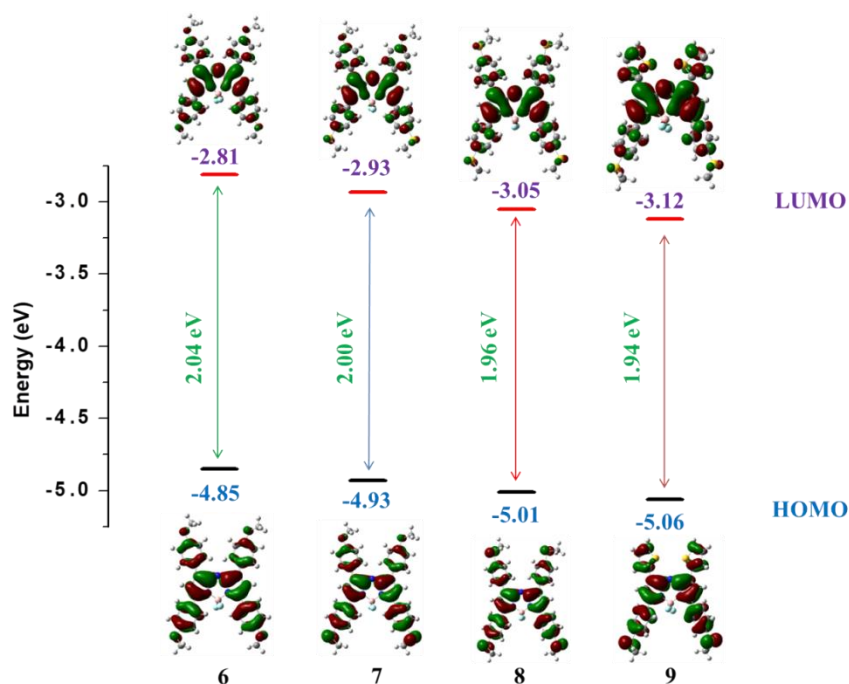


Figure 3.7. HOMO–LUMO energy level diagram of tetra-aryl substituted aza-BODIPYs **6–9**.

FMOs of aza-BODIPYs **6–9** in Figure 3.7. shows that the electron density in HOMOs is localized on whole molecular backbone whereas electron density in LUMOs is concentrated on aza-BODIPY acceptor core (Figure 3.7.). This indicates intramolecular charge transfer (ICT) interaction from donor to aza-BODIPY acceptor unit. As we go from **6** to **9** the HOMO and LUMO energy has been decreased. The HOMO–LUMO gap values for aza-BODIPYs **6–9** was found to be 2.04 eV, 2.00 eV, 1.96 eV and 1.96 eV respectively (Figure 3.7.) which indicates substitution of strong electron donating moiety on aza-BODIPY core decreases the HOMO-LUMO gap. The energy level diagram in tetra-aryl substituted aza-BODIPY dyes **1–10** show HOMO-LUMO gap values from the calculations are in between 2.19 eV and 1.81 eV. The di-phenothiazine substituted aza-BODIPYs **2–5** displayed lower HOMO-LUMO gap values compared to the other tetra-aryl substituted aza-BODIPYs. This indicates that the substitution of phenothiazine unit has a more prominent donating effect over other aryl moieties attached to aza-BODIPY core.

3.6. Experimental section

General methods

The chemicals were used as received unless otherwise indicated. All the moisture sensitive reactions were performed under argon atmosphere using the standard Schlenk method. ^1H NMR (500 MHz) and ^{13}C NMR (125 MHz) spectra were recorded by using CDCl_3 as the solvent. The ^1H NMR chemical shifts are reported in parts per million (ppm) relative to the solvent residual peak (CDCl_3 , 7.26 ppm). The multiplicities are given as: s (singlet), d (doublet), m (multiplet), and the coupling constants, J, are given in Hz. The ^{13}C NMR chemical shifts are reported with relative to the solvent residual peak (CDCl_3 , 77.0 ppm). HRMS was recorded on a mass spectrometer (ESI-TOF). The UV-visible absorption spectra recorded on UV-visible Spectrophotometer in dichloromethane. Cyclic voltammograms (CVs) were recorded on an electrochemical analyzer using glassy carbon as working electrode, Pt wire as the counter electrode, and Ag/AgCl as the reference electrode.

General method for the synthesis of aza-BODIPY dyes 2–5, 7 and 9:

In a 100 mL round bottom flask, **2A** (0.200 g, 0.46 mmol) and ammonium acetate (1.24 g, 16.1 mmol) were dissolved in 25 mL of ethanol. The reaction mixture was heated to 85 °C for 48 hours. After the completion of the reaction, the mixture was directly used in the next step. The reaction mixture (0.100 g, 0.13 mmol) was then dissolved in 25 mL of dichloromethane, and diisopropylethylamine (0.45 mL, 2.6 mmol) was added dropwise. The solution was stirred at room temperature for 15 minutes, following which $\text{BF}_3 \cdot \text{Et}_2\text{O}$ (0.32 mL, 2.6 mmol) was added. The solution was stirred at room temperature for 4 hours. The solvent was evaporated, and the crude product was purified on a silica gel column chromatography (dichloromethane/hexane, 3:2, v/v) to afford aza-BODIPY **2**. The

characterization data of aza-BODIPYs **2–5**, **7** and **9** are summarized below.

Aza-BODIPY 1:

Aza-BODIPY **1** was reported in literature.^[43]

Aza-BODIPY 2:

Yield: 48%; **¹H NMR** (500 MHz, CDCl₃, δ in ppm): 8.02 - 7.96 (m, 5 H), 7.89 (d, J = 2.0 Hz, 2 H), 7.49 - 7.44 (m, 6 H), 7.19 - 7.15 (m, 2 H), 7.11 (dd, J = 1.4, 7.5 Hz, 2 H), 7.03 (d, J = 8.5 Hz, 2 H), 6.97 - 6.86 (m, 7 H), 3.97 - 3.86 (t, J = 7.1 Hz, 4 H), 1.98 - 1.86 (m, 4 H), 1.05 (t, J = 7.4 Hz, 6 H); **¹³C NMR** (125 MHz, CDCl₃, δ in ppm): 158.8, 146.4, 145.5, 144.2, 142.5, 131.9, 130.6, 129.5, 128.9, 128.5, 127.7, 127.4, 127.3, 127.0, 124.6, 124.1, 122.9, 117.0, 115.6, 115.5, 49.5, 20.2, 11.3; **¹¹B NMR** (160 MHz, CDCl₃) δ 0.88 (t, J_{B-F} =31.6 Hz). **¹⁹F NMR** (471 MHz, CDCl₃) δ -130.64 (q, J_{F-B} =31.0 Hz); **HRMS** (ESI) m/z [M+nH]⁺ calcd for C₅₀H₄₁BF₂N₅S₂: 824.2867 found 824.2838.

Aza-BODIPY 3:

Yield: 41%; **¹H NMR** (500 MHz, CDCl₃, δ in ppm): 7.98 - 7.90 (m, 6 H), 7.87 (s, 2 H), 7.27 (s, 4 H), 7.16 (t, J = 7.8 Hz, 2 H), 7.10 (d, J = 7.5 Hz, 2 H), 7.01 (d, J = 8.5 Hz, 2 H), 6.95 - 6.84 (m, 6 H), 3.90 (t, J = 7.1 Hz, 4 H), 2.41 (s, 6 H), 1.95 - 1.86 (m, 4 H), 1.04 (t, J = 7.3 Hz, 6 H); **¹³C NMR** (125 MHz, CDCl₃, δ in ppm): 158.6, 146.2, 145.3, 144.2, 142.1, 141.1, 129.5, 129.3, 129.1, 128.8, 127.6, 127.4, 127.3, 127.1, 124.6, 124.1, 122.8, 116.9, 115.6, 115.5, 49.5, 21.6, 20.2, 11.4; **¹¹B NMR** (160 MHz, CDCl₃) δ 0.91 (t, J_{B-F} =31.9 Hz). **¹⁹F NMR** (471 MHz, CDCl₃) δ -130.88 (q, J_{F-B} =31.3 Hz); **HRMS** (ESI) m/z [M+nK]⁺ calcd for C₅₂H₄₄BF₂N₅S₂K⁺: 890.2740 found 890.2224.

Aza-BODIPY 4:

Yield: 43%; **¹H NMR** (500 MHz, CDCl₃, δ in ppm): 7.98 - 8.03 (m, 4 H), 7.92 (dd, J = 2.0, 8.5 Hz, 2 H), 7.81 (d, J = 2.0 Hz, 2 H), 7.10 - 7.16 (m, 2 H), 7.04 (dd, J = 1.4, 7.6 Hz, 2 H), 6.92 - 6.98 (m, 6 H), 6.86 - 6.91 (m, 2 H), 6.79 - 6.85 (m, 4 H), 3.85-3.82 (m, 10 H), 1.78 - 1.93 (m, 4 H), 1.00 (t, J = 7.3 Hz, 6 H). **¹³C NMR** (125 MHz, CDCl₃, δ in ppm) :161.6, 157.4, 145.9, 145.1, 144.2, 141.3, 131.5, 131.4, 129.0, 127.5, 127.3, 127.2, 127.0, 124.4, 124.3, 124.1, 116.6, 115.5, 115.4, 114.1 55.4, 49.4, 20.1, 11.3; **¹¹B NMR** (160 MHz, CDCl₃) δ 1.01 (t, J_{B-F} =32.7 Hz). **¹⁹F NMR** (471 MHz, CDCl₃) δ -131.13 (q, J_{F-B} =32.8 Hz); **HRMS** (ESI) m/z [M+nH]⁺ calcd for C₅₂H₄₅BF₂N₅O₂S₂: 884.3079 found 884.3056.

Aza-BODIPY 5:

Yield: 50%; **¹H NMR** (500 MHz, CDCl₃, δ in ppm): 8.00 - 7.92 (m, 6 H), 7.87 (d, J = 1.5 Hz, 2 H), 7.30 (d, J = 8.4 Hz, 4 H), 7.18 - 7.15 (m, 2 H), 7.10 (d, J = 7.5 Hz, 2 H), 7.02 (d, J = 8.7 Hz, 2 H), 6.95 - 6.87 (m, 6 H), 3.90 (t, J = 7.0 Hz, 4 H), 2.54 (s, 6 H), 1.94 - 1.86 (m, 4 H), 1.04 (t, J = 7.3 Hz, 6 H); **¹³C NMR** (125 MHz, CDCl₃, δ in ppm): 157.5, 146.3, 144.2, 142.9, 142.0, 141.9, 129.8, 128.8, 128.1, 127.6, 127.4, 127.3, 127.0, 125.5, 124.6, 124.1, 122.8, 116.8, 115.6, 115.5, 49.5, 20.2, 15.0, 11.4; **¹¹B NMR** (160 MHz, CDCl₃) δ 0.91 (t, J_{B-F} =31.9 Hz). **¹⁹F NMR** (471 MHz, CDCl₃) δ -130.88 (q, J_{F-B} =31.3 Hz); **HRMS** (ESI) m/z [M+nH]⁺ calcd for C₅₂H₄₅BF₂N₅S₄: 916.2622 found 916.2238.

Aza-BODIPY 6:

Aza-BODIPY **6** was reported in literature.^[44]

Aza-BODIPY 7:

Yield: 47%; **¹H NMR** (500 MHz, CDCl₃, δ in ppm): 8.07 - 7.98 (m, 8 H), 7.32-7.31 (d, J = 8.5 Hz, 4 H), 7.01 - 6.94 (m, 6 H), 3.90 (s, 6 H), 2.54 (s, 6 H); **¹³C NMR** (125 MHz, CDCl₃, δ in ppm) :160.9, 157.8,

145.5, 143.2, 143.0, 130.8, 129.8, 128.0, 125.5, 125.4, 117.3, 114.2, 55.5, 15.0; **¹¹B NMR** (160 MHz, CDCl₃) δ 1.02 (t, J_{B-F} =32.4 Hz). **¹⁹F NMR** (471 MHz, CDCl₃) δ -131.04 (q, J_{F-B} =32.3 Hz); **HRMS** (ESI) m/z [M+nH]⁺ calcd for C₃₆H₃₁BF₂N₃O₂S₂: 650.1920 found 650.1985.

Aza-BODIPY 8:

Aza-BODIPY **8** was reported in literature.^[45]

Aza-BODIPY 9:

Yield: 44%; **¹H NMR** (500 MHz, CDCl₃, δ in ppm): 7.99-7.98 (d, J = 8.5 Hz, 4 H), 7.93-7.92 (d, J = 2.9 Hz, 2 H), 7.57-7.56 (d, J = 4.4 Hz, 2 H), 7.32-7.30 (d, J = 8.5 Hz, 4 H), 7.22- 7.20 (m, 2 H), 6.94 (s, 2 H), 2.54 (s, 6 H); **¹³C NMR** (125 MHz, CDCl₃, δ in ppm) : 158.2, 143.3, 134.8, 130.0, 129.9, 129.8, 129.8, 129.5, 128.3, 127.7, 125.4, 116.5, 14.9; **¹¹B NMR** (160 MHz, CDCl₃) δ 0.95 (t, J_{B-F} =31.7 Hz). **¹⁹F NMR** (471 MHz, CDCl₃) δ -130.74 (q, J_{F-B} =31.4 Hz); **HRMS** (ESI) m/z [M+nNa]⁺ calcd for C₃₀H₂₂BF₂N₃S₄Na⁺: 624.0655 found 624.0572.

Aza-BODIPY 10:

Aza-BODIPY **10** was reported in literature.^[13]

3.7. Conclusion

In conclusion, we designed and synthesized different donor functionalized tetra-aryl substituted aza-BODIPY dyes **2–5**, **7**, and **9**. Further we studied their photophysical and electrochemical properties and compared with reported aza-BODIPYs **1**, **6**, **8**, and **10**. The electronic absorption spectra of the aza-BODIPYs **1–10** exhibited a broad absorption covering visible to near-infrared region. The diphenothiazine and di-thioanisole based aza-BODIPY **5** as well as tetra-thiophene based aza-BODIPY **10**, exhibited red-shifted absorption maximum as compared to tetra-aryl aza-BODIPY dyes. The cyclic voltammetry investigation show multiple oxidation and reduction

potentials in aza-BODIPYs **1–10** related to corresponding donor and acceptor (aza-BODIPY) moieties. The intramolecular charge transfer (ICT) from different aryl donors to aza-BODIPY acceptor leads to the decrease in HOMO-LUMO gap. The results obtained in this work demonstrated that simple electron donating substitution on aza-BODIPY core can induce huge bathochromic shift in their absorption and hence this will be a useful strategy to develop NIR dyes. A broad absorption in the vis-NIR range, multiple redox peaks, and low HOMO-LUMO gap values in these aza-BODIPY derivatives indicate the suitability as a potential candidate for organic photovoltaics and bioimaging.

3.8. References

- [1] Perzon, E., Zhang, F., Andersson, M., Mammo, W., Inganäs, O., Andersson, M. R. (2007). A Conjugated Polymer for Near Infrared Optoelectronic Applications. *Advanced Materials*, 19(20), 3308–3311. (DOI: 10.1002/adma.200700557).
- [2] Zhang, Y., Wei, Q., He, Z., Wang, Y., Shan, T., Fu, Y., Guo, X., Zhong, H. (2022). Efficient Optoelectronic Devices Enabled by Near-Infrared Organic Semiconductors with a Photoresponse beyond 1050 Nm. *ACS Appl. Mater. Interfaces*, 14(27), 31066–31074. (DOI: 10.1021/acsami.2c06277).
- [3] Cherumukkil, S., Vedhanarayanan, B., Das, G., Praveen, V. K., Ajayaghosh, A. (2018). Self-Assembly of Bodipy-Derived Extended π -Systems. *BCSJ*, 91(1), 100–120. (DOI: 10.1246/bcsj.20170334).
- [4] Aderne, R., Strassel, K., Jenatsch, S., Diethelm, M., Hany, R., Nüesch, F., Carvalho, R. dos S., Legnani, C., Cremona, M. (2019). Near-Infrared Absorbing Cyanine Dyes for All-Organic Optical Upconversion Devices. *Organic Electronics*, 74, 96–102. (DOI: 10.1016/j.orgel.2019.07.002).

- [5] Xu, M., Li, X., Liu, S., Zhang, L., Xie, W. (2023). Near-Infrared Organic Light-Emitting Materials, Devices and Applications. *Materials Chemistry Frontiers*. (DOI: 10.1039/D3QM00585B).
- [6] Ghoroghchian, P. P., Therien, M. J., Hammer, D. A. (2009). In Vivo Fluorescence Imaging: A Personal Perspective. *Wiley Interdiscip Rev Nanomed Nanobiotechnol*, 1(2), 156–167. (DOI: 10.1002/wnan.7).
- [7] Cassette, E., Helle, M., Bezdetnaya, L., Marchal, F., Dubertret, B., Pons, T. (2013). Design of New Quantum Dot Materials for Deep Tissue Infrared Imaging. *Advanced Drug Delivery Reviews*, 65(5), 719–731. (DOI: 10.1016/j.addr.2012.08.016).
- [8] Chang, X. H., Zhang, J., Wu, L. H., Peng, Y. K., Yang, X. Y., Li, X. L., Ma, A. J., Ma, J. C., Chen, G.-Q. (2019). Research Progress of Near-Infrared Fluorescence Immunoassay. *Micromachines*, 10(6), 422. (DOI: 10.3390/mi10060422).
- [9] Lesani, P., Mohamad Hadi, A. H., Lu, Z., Palomba, S., New, E. J., Zreiqat, H. (2021). Design Principles and Biological Applications of Red-Emissive Two-Photon Carbon Dots. *Commun Mater*, 2(1), 1–12. (DOI: 10.1038/s43246-021-00214-2).
- [10] Zhang, N., Lu, C., Chen, M., Xu, X., Shu, G., Du, Y., Ji, J. (2021). Recent Advances in Near-Infrared II Imaging Technology for Biological Detection. *Journal of Nanobiotechnology*, 19(1), 132. (DOI: 10.1186/s12951-021-00870-z).
- [11] Shi, Z., Han, X., Hu, W., Bai, H., Peng, B., Ji, L., Fan, Q., Li, L., Huang, W. (2020). Bioapplications of Small Molecule Aza-BODIPY: From Rational Structural Design to in Vivo Investigations. *Chem. Soc. Rev.*, 49(21), 7533–7567. (DOI: 10.1039/D0CS00234H).

- [12] Sheng, W., Wu, Y., Yu, C., Bobadova-Parvanova, P., Hao, E., Jiao, L. (2018). Synthesis, Crystal Structure, and the Deep near-Infrared Absorption/Emission of Bright azaBODIPY-Based Organic Fluorophores. *Organic letters*, 20(9), 2620–2623. (DOI: 10.1021/acs.orglett.8b00820).
- [13] Gresser, R., Hartmann, H., Wrackmeyer, M., Leo, K., Riede, M. (2011). Synthesis of Thiophene-Substituted Aza-BODIPYs and Their Optical and Electrochemical Properties. *Tetrahedron*, 67(37), 7148–7155. (DOI: 10.1016/j.tet.2011.06.100).
- [14] David, S., Chang, H.-J., Lopes, C., Brännlund, C., Le Guennic, B., Berginc, G., Van Stryland, E., Bondar, M. V., Hagan, D., Jacquemin, D., Andraud, C., Maury, O. (2021). Benzothiadiazole-Substituted Aza-BODIPY Dyes: Two-Photon Absorption Enhancement for Improved Optical Limiting Performances in the Short-Wave IR Range. *Chemistry – A European Journal*, 27(10), 3517–3525. (DOI: 10.1002/chem.202004899).
- [15] Balsukuri, N., Boruah, N. J., Kesavan, P. E., Gupta, I. (2018). Near Infra-Red Dyes Based on Pyrene Aza-BODIPYs. *New J. Chem.*, 42(8), 5875–5888. (DOI: 10.1039/C7NJ03408C).
- [16] Wang, J., Yu, C., Hao, E., Jiao, L. (2022). Conformationally Restricted and Ring-Fused Aza-BODIPYs as Promising near Infrared Absorbing and Emitting Dyes. *Coordination Chemistry Reviews*, 470, 214709. (DOI: 10.1016/j.ccr.2022.214709).
- [17] Lu, P., Chung, K.-Y., Stafford, A., Kiker, M., Kafle, K., A. Page, Z. (2021). Boron Dipyrromethene (BODIPY) in Polymer Chemistry. *Polymer Chemistry*, 12(3), 327–348. (DOI: 10.1039/D0PY01513J).
- [18] Łapok, Ł., Cieślak, I., Pędziniński, T., Stadnicka, K. M., Nowakowska, M. (2020). Near-Infrared Photoactive Aza-BODIPY: Thermally Robust and Photostable Photosensitizer and

- Efficient Electron Donor. *ChemPhysChem*, 21(8), 725–740. (DOI: 10.1002/cphc.202000117).
- [19] Wang, Y., Zhang, D., Xiong, K., Shang, R., Jiang, X.-D. (2022). Near-Infrared Absorbing (>700 Nm) Aza-BODIPYs by Freezing the Rotation of the Aryl Groups. *Chinese Chemical Letters*, 33(1), 115–122. (DOI: 10.1016/j.cclet.2021.06.083).
- [20] Rana, P., Singh, N., Majumdar, P., Prakash Singh, S. (2022). Evolution of BODIPY/Aza-BODIPY Dyes for Organic Photoredox/Energy Transfer Catalysis. *Coordination Chemistry Reviews*, 470, 214698. (DOI: 10.1016/j.ccr.2022.214698).
- [21] Pino, Y. C., Aguilera, J. A., García-González, V., Alatorre-Meda, M., Rodríguez-Velázquez, E., Espinoza, K. A., Frayde-Gómez, H., Rivero, I. A. (2022). Synthesis of Aza-BODIPYs, Their Differential Binding for Cu(II), and Results of Bioimaging as Fluorescent Dyes of Langerhans β -Cells. *ACS Omega*, 7(47), 42752–42762. (DOI: 10.1021/acsomega.2c04151).
- [22] Gupta, I., Kesavan, P. E. (2019). Carbazole Substituted BODIPYs. *Frontiers in Chemistry*, 7. (DOI: 10.3389/fchem.2019.00841).
- [23] Shukla, V. K., Chakraborty, G., Ray, A. K., Nagaiyan, S. (2023). Red and NIR Emitting Ring-Fused BODIPY/Aza-BODIPY Dyes. *Dyes and Pigments*, 215, 111245. (DOI: 10.1016/j.dyepig.2023.111245).
- [24] Jiang, X. D., Guan, J., Zhao, J., Le Guennic, B., Jacquemin, D., Zhang, Z., Chen, S., Xiao, L. (2017). Synthesis, Structure and Photophysical Properties of NIR Aza-BODIPYs with F/N3/NH2 Groups at 1,7-Positions. *Dyes and Pigments*, 136, 619–626. (DOI: 10.1016/j.dyepig.2016.09.019).
- [25] Schäfer, C., Mony, J., Olsson, T., Börjesson, K. (2022). Effect of the Aza-N-Bridge and Push–Pull Moieties: A Comparative Study

- between BODIPYs and Aza-BODIPYs. *J. Org. Chem.*, 87(5), 2569–2579. (DOI: 10.1021/acs.joc.1c02525).
- [26] Kumar, S., Khan, T. K., Ravikanth, M. (2015). Synthesis and Properties of Hexaarylated AzaBODIPYs. *Tetrahedron*, 71(40), 7608–7613. (DOI: 10.1016/j.tet.2015.07.074).
- [27] Yılmaz, H., Sevinç, G., Hayvalı, M. (2021). 3, 3,5 and 2,6 Expanded Aza-BODIPYs Via Palladium-Catalyzed Suzuki-Miyaura Cross-Coupling Reactions: Synthesis and Photophysical Properties. *J Fluoresc*, 31(1), 151–164. (DOI: 10.1007/s10895-020-02646-4).
- [28] Pogonin, A. E., Shagurin, A. Y., Savenkova, M. A., Telegin, F. Y., Marfin, Y. S., Vashurin, A. S. (2020). Quantum Chemical Study Aimed at Modeling Efficient Aza-BODIPY NIR Dyes: Molecular and Electronic Structure, Absorption, and Emission Spectra. *Molecules*, 25(22), 5361. (DOI: 10.3390/molecules25225361).
- [29] Sadikogullari, B. C., Koramaz, I., Sütay, B., Karagoz, B., Özdemir, A. D. (2023). Application of Aza-BODIPY as a Nitroaromatic Sensor. *ACS Omega*, 8(28), 25254–25261. (DOI: 10.1021/acsomega.3c02349).
- [30] Merkushev, D., Vodyanova, O., Telegin, F., Melnikov, P., Yashtulov, N., Marfin, Y. (2022). Design of Promising Aza-BODIPYs for Bioimaging and Sensing. *Designs*, 6, 21. (DOI: 10.3390/designs6020021).
- [31] Liu, S., Shi, Z., Wenjuan, X., Yang, H., Xi, N., Liu, X., Zhao, Q., Huang, W.(2014). A Class of Wavelength-Tunable near-Infrared Aza-BODIPY Dyes and Their Application for Sensing Mercury Ion. *Dyes and Pigments*, 103, 145–153. (DOI: 10.1016/j.dyepig.2013.12.004).
- [32] Bodio, E., Denat, F., Goze, C. (2019). BODIPYS and Aza-BODIPY Derivatives as Promising Fluorophores for in Vivo

- Molecular Imaging and Theranostic Applications. *J. Porphyrins Phthalocyanines*, 23(11n12), 1159–1183. (DOI: 10.1142/S1088424619501268).
- [33] Fan, G., Yang, L., Chen, Z. (2015). Water-Soluble BODIPY and Aza-BODIPY Dyes: Synthetic Progress and Applications. *Front. Chem. Sci. Eng.*, 8(4), 405–417. (DOI: 10.1007/s11705-014-1445-7).
- [34] Parisotto, S., Lace, B., Artuso, E., Lombardi, C., Deagostino, A., Scudu, R., Garino, C., Medana, C., Prandi, C. (2017). Heck Functionalization of an Asymmetric Aza-BODIPY Core: Synthesis of Far-Red Infrared Probes for Bioimaging Applications. *Org. Biomol. Chem.*, 15(4), 884–893. (DOI: 10.1039/C6OB02602H).
- [35] Li, T., Meyer, T., Meerheim, R., Höppner, M., Körner, C., Vandewal, K., Zeika, O., Leo, K. (2017). Aza-BODIPY Dyes with Heterocyclic Substituents and Their Derivatives Bearing a Cyanide Co-Ligand: NIR Donor Materials for Vacuum-Processed Solar Cells. (DOI: 10.1039/c7ta02133j).
- [36] Kage, Y., Kang, S., Mori, S., Mamada, M., Adachi, C., Kim, D., Furuta, H., Shimizu, S. (2021). An Electron-Accepting Aza-BODIPY-Based Donor–Acceptor–Donor Architecture for Bright NIR Emission. *Chemistry – A European Journal*, 27(16), 5259–5267. (DOI: 10.1002/chem.202005360).
- [37] Baron, T., Maffei, V., Bucher, C., Le Guennic, B., Banyasz, A., Jacquemin, D., Berginc, G., Maury, O., Andraud, C. (2023). Tuning the Photophysical Properties of Aza-BODIPYs in the Near-Infrared Region by Introducing Electron-Donating Thiophene Substituents. *Chemistry – A European Journal*, 29(49), e202301357. (DOI: 10.1002/chem.202301357).
- [38] Liu, X., Zhang, J., Li, K., Sun, X., Wu, Z., Ren, A., Feng, J. (2013). New Insights into Two-Photon Absorption Properties of

- Functionalized Aza-BODIPY Dyes at Telecommunication Wavelengths: A Theoretical Study. *Phys. Chem. Chem. Phys.*, 15(13), 4666–4676. (DOI: 10.1039/C3CP44435J).
- [39] Zatsikha, Y. V., Blesener, T. S., Goff, P. C., Healy, A. T., Swedin, R. K., Herbert, D. E., Rohde, G. T., Chanawanno, K., Ziegler, C. J., Belosludov, R. V., Blank, D. A., Nemykin, V. N. (2018). 1,7-Dipyrene-Containing Aza-BODIPYs: Are Pyrene Groups Effective as Ligands To Promote and Direct Complex Formation with Common Nanocarbon Materials. *J. Phys. Chem. C*, 122 (49), 27893–27916. (DOI: 10.1021/acs.jpcc.8b09504).
- [40] Virgili, T., Ganzer, L., Botta, C., Squeo, B. M., Pasini, M. (2022). Asymmetric AZA-BODIPY with Optical Gain in the Near-Infrared Region. *Molecules*, 27(14), 4538. (DOI: 10.3390/molecules27144538).
- (41) Balsukuri, N., Lone, M. Y., Jha, P. C., Mori, S., Gupta, I. (2016). Synthesis, Structure, and Optical Studies of Donor–Acceptor-Type Near-Infrared (NIR) Aza–Boron-Dipyrromethene (BODIPY) Dyes. *Chemistry – An Asian Journal*, 11(10), 1572–1587. (DOI: 10.1002/asia.201600167).
- [42] Alsaleh, A. Z., Pinjari, D., Misra, R., D’Souza, F. (2023). Far-Red Excitation Induced Electron Transfer in Bis Donor-AzaBODIPY Push-Pull Systems, Role of Nitrogenous Donors in Promoting Charge Separation. *Chemistry – A European Journal*, 29(53), e202301659. (DOI: 10.1002/chem.202301659).
- [43] Mueller, T., Gresser, R., Leo, K., Riede, M. (2012). Organic Solar Cells Based on a Novel Infrared Absorbing Aza-Bodipy Dye. *Solar energy materials and solar cells*, 99, 176–181. (DOI: 10.1016/j.solmat.2011.11.006).
- [44] R. Zarccone, S., J. Yarbrough, H., J. Neal, M., C. Kelly, J., L. Kaczynski, K., J. Bloomfield, A., M. Bowers, G., D. Montgomery, T., T. Chase, D. (2022). Synthesis and

- Photophysical Properties of Nitrated Aza-BODIPYs. *New Journal of Chemistry*, 46(9), 4483–4496. (DOI: 10.1039/D1NJ05976A).
- [45] Markin, A., Ismael, A. K., Davidson, R. J., Milan, D. C., Nichols, R. J., Higgins, S. J., Lambert, C. J., Hsu, Y.-T., Yufit, D. S., Beeby, A. (2020). Conductance Behavior of Tetraphenyl-Aza-BODIPYs. *J. Phys. Chem. C*, 124(12), 6479–6485. (DOI: 10.1021/acs.jpcc.9b10232).
- [46] Rao, R. S., Yadagiri, B., Sharma, G. D., Singh, S. P. (2019). Butterfly Architecture of NIR Aza-BODIPY Small Molecules Decorated with Phenothiazine or Phenoxazine. *Chem. Commun.*, 55(83), 12535–12538. (DOI: 10.1039/C9CC06300E).

Chapter 4

NIR absorbing different donor functionalized ethyne bridged α -aza BODIPYs

4.1. Introduction

In recent years, the developments of near infrared (NIR) dyes garnered significant attention due to their potential applications in biomedical imaging and therapy techniques.^[1-3] These dyes have emerged as a preferred choice for biomedical imaging and diagnostic applications, primarily due to their optical properties, such as high quantum yield, low photobleaching, and deep tissue penetration.^[4-7] The boron-azadipyrrromethene (aza-BODIPY) dyes are one of the most remarkable class of NIR dyes.^[8] The aza-BODIPY is a dipyrromethene core in which the *meso*-carbon atom of BODIPY is replaced by a nitrogen atom.^[9] As compared to the parent BODIPY dyes, the absorption and emission of the aza-BODIPYs are considerably red-shifted.^[10] Recently, aza-BODIPY-based NIR absorbers have attracted significant interest because of their facile synthesis, high solubility, stability, absorption coefficients and fluorescence quantum yields.^[11-16] Aza-BODIPYs have been used in wide range of applications such as in photovoltaics, photodynamic therapies, and bioimaging.^[17-18] Our group is engaged in the development of donor-acceptor (D-A) organic dyes for various optoelectronic applications.^[19-20]

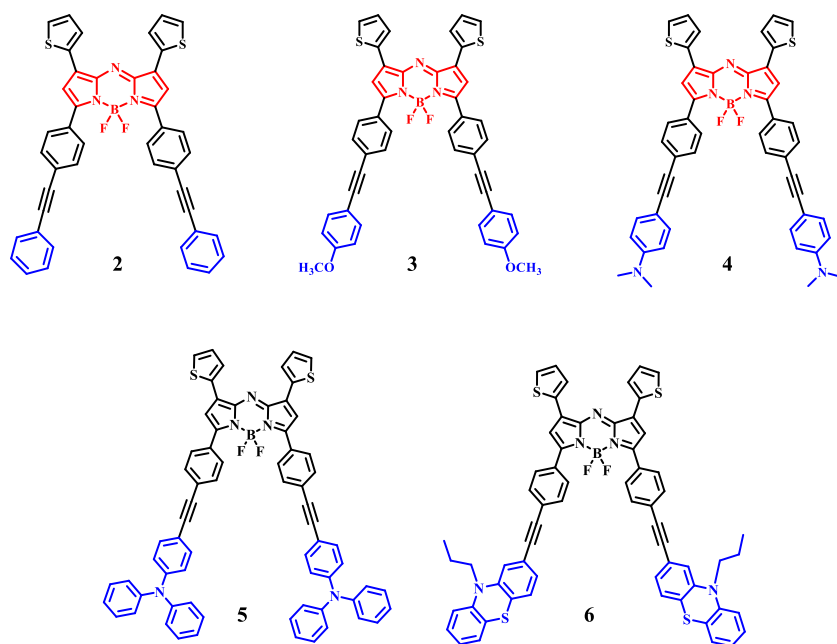


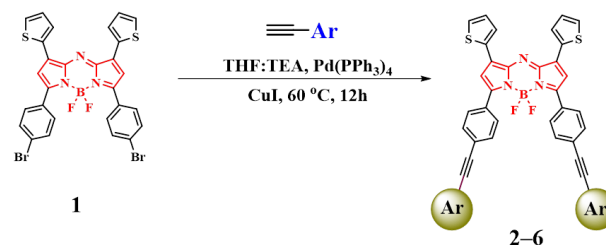
Figure 4.1. Chemical structures of donor functionalized aza-BODIPY dyes.

Herein, we describe the synthesis and characterization of five donor-based aza-BODIPY derivatives **2–6** using the Pd-catalyzed Sonogashira cross-coupling reaction. The optical and electrochemical properties of these derivatives were thoroughly investigated, and their computational studies were studied using the Gaussian 09W program for theoretical calculations to understand their geometries and electronic structures. The main objective of this study was to systematically investigate the effects of different donor groups attached to the aza-BODIPY core on the photophysical, electrochemical, and computational properties of the synthesized aza-BODIPY derivatives.

4.2. Results and Discussion

The synthesis of different donor-based aza-BODIPY dyes **2–6** are shown in Scheme 4.1. The dibromo-aza-dipyrromethene **1** was utilized in Sonogashira cross-coupling reactions with various donor-substituted ethynyl derivatives in solvents THF and TEA. The reaction mixture was heated at 60 °C for 12 hrs. Once the reaction was complete, the mixture was cooled, and then washed with water and brine. The organic layers were dried with anhydrous sodium sulfate, and

diisopropylethylamine was added dropwise, followed by boron trifluoride diethyl etherate ($\text{BF}_3 \cdot \text{Et}_2\text{O}$) at room temperature. This produced aza-BODIPY dyes **2–6** with a 75–85% yield.



Aza-BODIPY	2	3	4	5	6
Yield %	85%	80%	75%	82%	77%

Scheme 4.1. Synthetic route for donor functionalized aza-BODIPY dyes **2–6**.

The precursor for dibromo-aza-dipyrromethene **1** was synthesized using a reported procedure by reacting thiophene-2-carbaldehyde with 4-bromo-acetophenone.^[18] The various donor-based aza-BODIPY dyes **2–6** were purified by column chromatography, using neutral activated aluminium oxide. The aza-BODIPY dyes **2–6** are soluble in common organic solvents, such as chloroform, toluene, dichloromethane, and are well characterized using ^1H NMR, ^{13}C NMR, and HRMS techniques. Triphenylamine based aza-BODIPY dye **5** was prepared according to our earlier reported procedure.^[22]

4.3. Photophysical Properties

The absorption spectra of donor-functionalized aza-BODIPY dyes **2–6** were recorded in dichloromethane solvent at room temperature and are shown in Figure 4.2. The corresponding data are listed in Table 4.1.

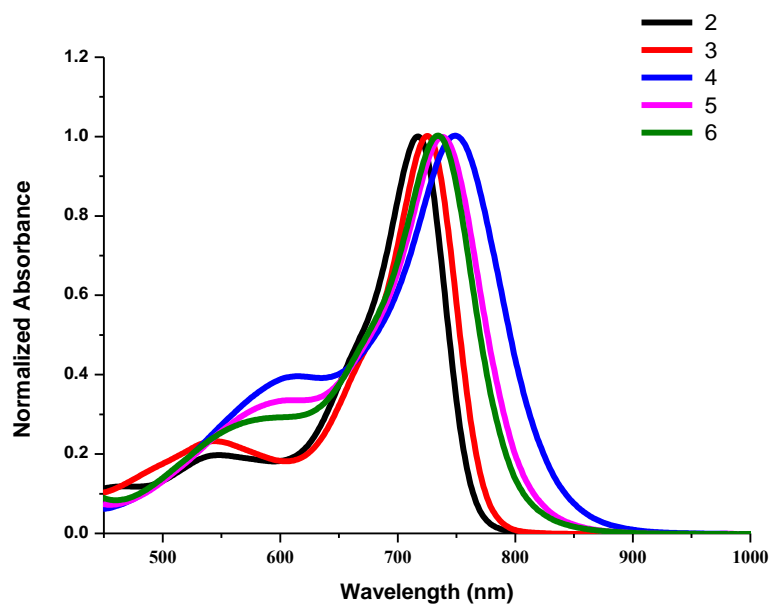


Figure 4.2. Normalized electronic absorption spectra of donor functionalized aza-BODIPYs **2–6** (1×10^{-5} M).

In the absorption spectrum, aza-BODIPY dyes **2–6** exhibit broad absorption bands covering the visible to NIR region from 450–900 nm. The aza-BODIPY dyes **2–6** show two major absorption bands; a higher energy absorption band around 540–602 nm due to $\pi \rightarrow \pi^*$ transition and a lower energy absorption band around 675–750 nm due to ICT (intramolecular charge transfer) transition. Among the five aza-BODIPY dyes, aza-BODIPY **4** exhibits a red-shifted absorption due to the presence of strong electron-donating *N,N*-dimethylaniline group compared to the other aza-BODIPY dyes **2**, **3**, **5**, and **6**. The absorption maxima of absorption bands at lower energy ICT transitions of aza-BODIPY dyes **2–6** follows the order: aza-BODIPY **4** > aza-BODIPY **5** > aza-BODIPY **6** > aza-BODIPY **3** > aza-BODIPY **2**.

Table 4.1. Photophysical and computational properties of aza-BODIPY dyes **2–6**.

Dyes	λ_{abs} (nm) ^a	$\epsilon/10^4$	E_g^b
		(M ⁻¹ .cm ⁻¹) ^a	(eV)
2	717	9.7	1.89
	540		
3	725	9.5	1.82
	542		
4	749	7.3	1.67
	602		
5	738	7.2	1.67
	592		
6	735	8.1	1.75
	578		

^aAbsorbance measured in dichloromethane at 1×10^{-5} M concentration, ϵ : molar extinction coefficient, ^bTheoretical HOMO–LUMO gap values calculated from DFT calculation.

Thus, compared to aza-BODIPY **4**, the absorption maxima (λ_{max}) are blue-shifted by 32 nm for aza-BODIPY **2**, 24 nm for aza-BODIPY **3**, 11 nm for aza-BODIPY **5**, and 14 nm for aza-BODIPY **6**. The molar absorption coefficients (ϵ_{max}) were observed as: 97,000 [M⁻¹cm⁻¹] for aza-BODIPY **2**, 95,000 [M⁻¹cm⁻¹] for aza-BODIPY **3**, 73,000 [M⁻¹cm⁻¹] for aza-BODIPY **4**, 72,000 [M⁻¹cm⁻¹] for aza-BODIPY **5**, and 81,000 [M⁻¹cm⁻¹] for aza-BODIPY **6**. Anisole functionalized aza-BODIPY **3** shows bathochromically shifted absorption compared to phenyl substituted aza-BODIPY **2** because of the presence of an anisole group, which is a stronger electron-donor than the phenyl group. In comparison of three aza-BODIPY dyes **4**, **5**, and **6**, aza-BODIPY **4** displays red-shifted absorption because of the strong electron-donating character of its *N*, *N*-dimethylamine unit, whereas phenothiazine substituted aza-BODIPY **6**, exhibits a slightly blue-shifted absorption in comparison to triphenylamine substituted aza-BODIPY **5**.

4.4. Electrochemical properties

The oxidation and reduction potentials of aza-BODIPY dyes **2–6** were investigated using differential pulse voltammetry (DPV) and cyclic voltammetry (CV) at 100 mV s^{-1} scan rate in dichloromethane solvent with tetrabutylammonium hexafluorophosphate (Bu_4NPF_6) as a supporting electrolyte (0.1 M). Figure 4.3. shows CV and DPV plots of the oxidation and reduction waves of aza-BODIPYs **2–6**, with data from Table 4.3. and 4.4.

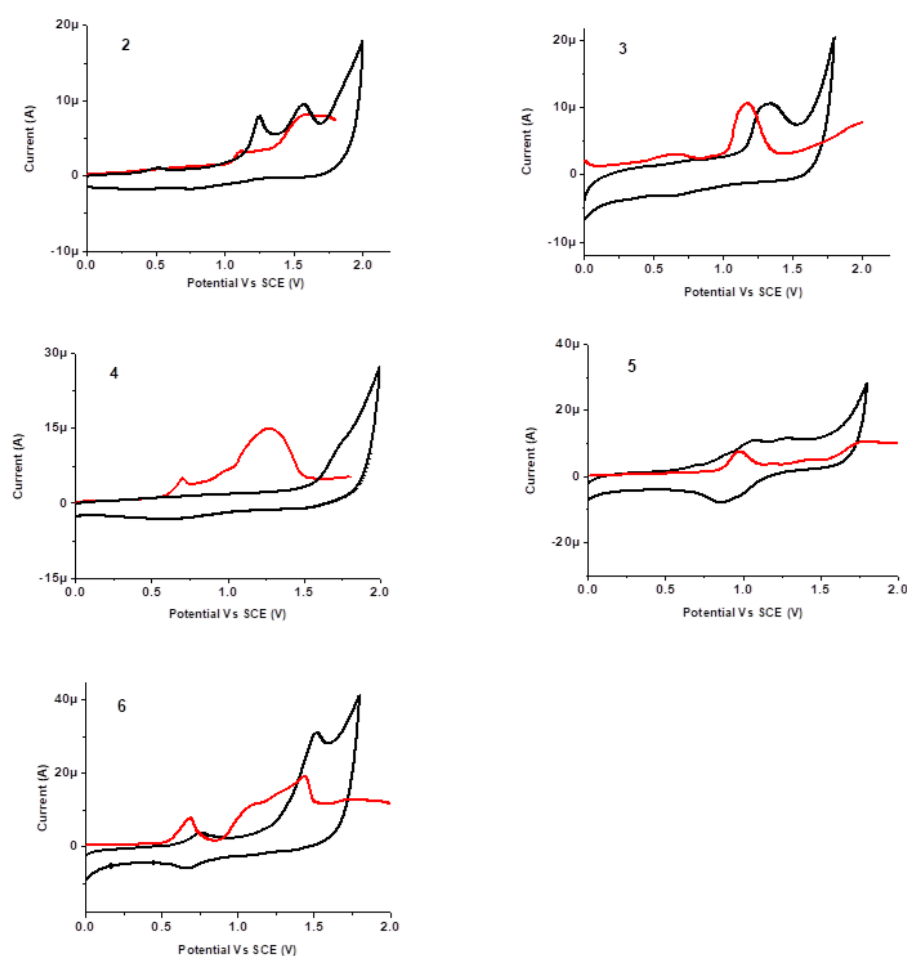


Figure 4.3. CV and DPV plot of aza-BODIPYs **2–6**.

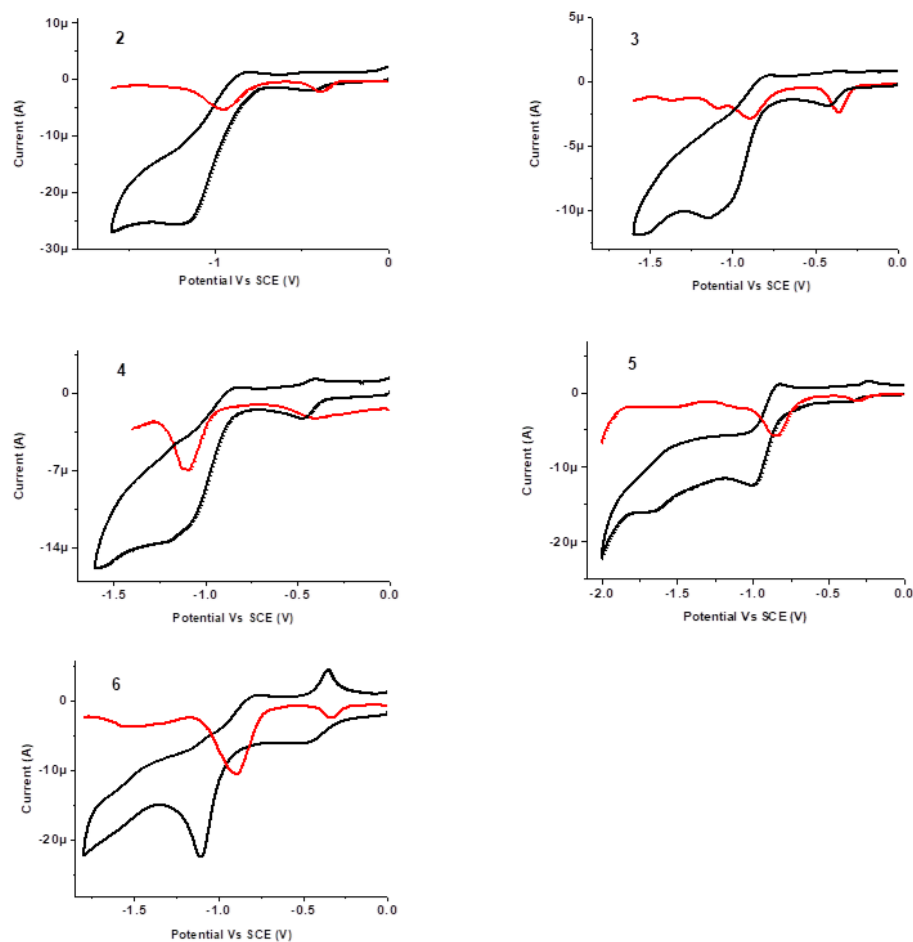


Figure 4.4. CV and DPV plot of aza-BODIPYs **2–6**.

Generally, aza-dipyrromethene and aza-BODIPY dyes exhibit one oxidation and two reduction potentials.^[23] However, in donor-substituted aza-BODIPYs **2–6** (Figure 4.3. and 4.4.), two oxidation potentials and two reduction potentials are illustrated due to the presence of donor and aza-BODIPY moiety. Specifically, the oxidation potentials are as follow; a) at 1.12 V and 1.55 V in aza-BODIPY **2**, b) at 0.64 V and 1.16 V in aza-BODIPY **3**, c) at 0.71 V and 1.28 V in aza-BODIPY **4**, d) at 0.97 V and 1.40 V in aza-BODIPY **5**, and e) at 0.69 V and 1.44 V in aza-BODIPY **6**. Aza-BODIPYs **2**, **4**, **5**, and **6** exhibited an anodic shift in their oxidation potentials when compared to aza-BODIPY **3**, indicating that they are relatively harder to oxidize.

Table 4.2. Electrochemical properties of aza-BODIPY dyes **2–6**.

Dyes	E^1 [V] Oxid ^a	E^2 [V] Oxid ^a	E^1 [V] Red ^a	E^2 [V] Red ^a
2	1.12	1.55	-0.40	-0.95
3	0.64	1.16	-0.37	-0.90
4	0.71	1.28	-0.43	-1.11
5	0.97	1.40	-0.32	-0.86
6	0.69	1.44	-0.34	-0.91

^aThe electrochemical analysis was performed with a 0.1 M Bu₄NPF₆ solution in dichloromethane at a scan rate of 100 mVs⁻¹ vs SCE at 25 °C.

The aza-BODIPY core has the following reduction potentials; a) -0.40 V and -0.95 V in aza-BODIPY **2**, b) -0.37 V and -0.90 V in aza-BODIPY **3**, c) -0.43 V and -1.11 V in aza-BODIPY **4**, d) -0.32 V and -0.86 V in aza-BODIPY **5**, and -0.34 V and -0.91 V in aza-BODIPY **6**. The first and second reduction potentials of aza-BODIPYs **2**, **3**, **5**, and **6** exhibited an anodic shift as compared to aza-BODIPY dye **4** due to the more donating nature of *N,N*-dimethylamine, which made them easier to reduce.

4.5. Computational Calculations

In order to understand the geometry and electronic structures of donor-functionalized aza-BODIPY dyes **2–6**, DFT calculations were carried out using the Gaussian 09W program at the B3LYP/6-31G (d, p) level for C, H, N, S, and B. Optimizations was carried out in the gas phase. Frontier molecular orbitals (FMOs) of aza-BODIPYs **2–6** obtained from these calculations were as shown below (Figure 4.5.).

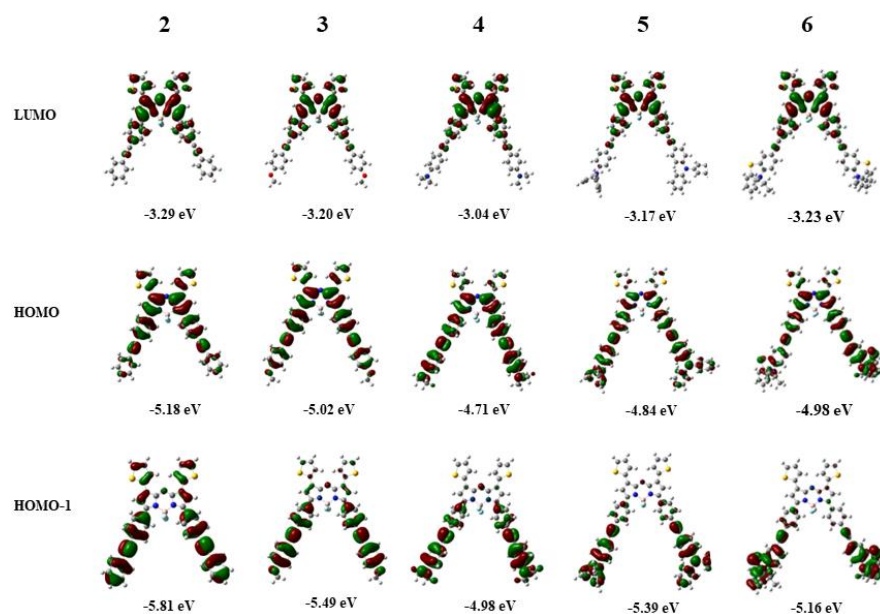


Figure 4.5. The FMOs of aza-BODIPY dyes **2–6** at B3LYP/6-31G (d, p) level.

The optimized structures of donor-functionalized aza-BODIPYs **2–6** have planar geometry. In aza-BODIPYs **2–6**, the electron density in highest occupied molecular orbital (HOMO) is predominantly located on the donor unit, whereas the electron density in lowest unoccupied molecular orbital (LUMO) is located on the aza-BODIPY moiety, indicating donor-acceptor interaction in donor substituted aza-BODIPY unit. The calculated HOMO energy level values for donor-substituted aza-BODIPY dyes **2–6** are -5.18, -5.02, -4.71, -4.84, and -4.98 eV, and the corresponding LUMO values are -3.29, -3.20, -3.04, -3.17, and -3.23 eV, respectively.

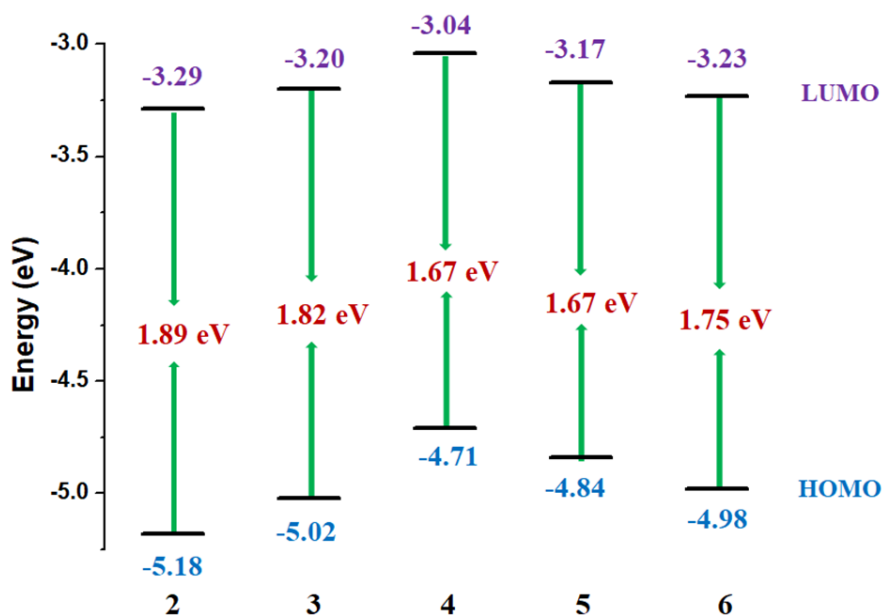


Figure 4.6. Energy level diagram for FMOs of aza-BODIPY dyes **2–6** estimated by DFT calculations.

Theoretical calculations reveal that aza-BODIPY dyes **4** and **5** exhibit a lower HOMO-LUMO gap than aza-BODIPY dyes **2**, **3**, and **6**, due to presence of strong electron donating units. The HOMO-LUMO gap (E_g) for aza-BODIPY dyes **2–6** lies between 1.67 eV and 1.89 eV, as shown in Figure 4.6. and listed in Table 4.1. The trend observed in the HOMO-LUMO gap values follows the order: aza-BODIPY **4** = aza-BODIPY **5** > aza-BODIPY **6** > aza-BODIPY **3** > aza-BODIPY **2**.

Table 4.3. Calculated major electronic transitions for aza-BODIPYs **2–6** in the gas phase.

Dyes	Wavelength (nm)	Composition	f^a
2	681	HOMO→LUMO (0.71)	0.89
	550	HOMO-1→LUMO (0.68)	0.66
3	716	HOMO→LUMO (0.70)	0.83
	597	HOMO-1→LUMO (0.70)	0.59
4	803	HOMO→LUMO (0.70)	0.68
	699	HOMO-1→LUMO (0.70)	0.50
5	825	HOMO→LUMO (0.70)	0.58
	747	HOMO-1→LUMO (0.70)	0.41
	615	HOMO-2→LUMO (0.69)	0.43
6	778	HOMO→LUMO (0.69)	0.56
	715	HOMO-1→LUMO (0.70)	0.25
	627	HOMO-2→LUMO (0.69)	0.53

TD-DFT calculations were performed on aza-BODIPY dyes **2–6** at the B3LYP/6-31G (d, p) level to achieve correlation with the absorption studies. The calculated electronic transitions, their composition and oscillator strength in different donor-substituted aza-BODIPY dyes **2–6** were obtained from TD-DFT calculations (Table 4.3.). The aza-BODIPY dyes **2–6** exhibit two main electronic transitions in the vis-NIR region, occurring from HOMO to LUMO and HOMO-1 to LUMO, as observed in the TD-DFT calculation. Charge transfer transitions from the donor to the aza-BODIPY unit were observed for the longer wavelength region.

4.6. Experimental section

General methods

The chemicals were used as received unless otherwise indicated. All the moisture sensitive reactions were performed under argon atmosphere using the standard Schlenk method. ^1H NMR (400 MHz)

and ^{13}C NMR (100 MHz) spectra were recorded by using CDCl_3 and CD_2Cl_2 as the solvent. The ^1H NMR chemical shifts are reported in parts per million (ppm) relative to the solvent residual peak (CDCl_3 , 7.26 ppm and CD_2Cl_2 , 5.32 ppm). The multiplicities are given as: s (singlet), d (doublet), m (multiplet), and the coupling constants, J , are given in Hz. The ^{13}C NMR chemical shifts are reported with relative to the solvent residual peak (CDCl_3 , 77.0 ppm and CD_2Cl_2 , 54.0 ppm). HRMS was recorded on a mass spectrometer (ESI-TOF). The UV-visible absorption spectra recorded on UV-visible Spectrophotometer in dichloromethane. Cyclic voltammograms (CVs) and differential pulse voltammograms (DPVs) were recorded on an electrochemical analyzer using glassy carbon as working electrode, Pt wire as the counter electrode, and SCE as the reference electrode.

Synthesis of aza-BODIPY 2:

In 100 ml round bottom flask, di-bromo aza-BODIPY **1** (0.500 g, 0.75 mmol), ethynylbenzene (0.153 g, 1.50 mmol) were dissolved in a THF/TEA mixture (v/v,1:1) and the solution was degassed with argon for 10 minutes. To this reaction mixture $\text{Pd}(\text{PPh}_3)_4$ (0.050 g), CuI (0.007 g) were added. After stirring 12 hrs at 60 °C, the solvent was removed under vacuum and the product was purified by column chromatography using neutral activated aluminum oxide (1: 1 dichloromethane: Hexane) as an eluent to yield 0.453 g (85%) of aza-BODIPY **2**. ^1H NMR (400 MHz, CDCl_3 , δ in ppm): 8.06-8.02 (4H, m), 7.95-7.94 (2H, d, $J = 4\text{Hz}$), 7.89-7.87 ((1H, d, $J = 8\text{Hz}$), 7.64-7.55 (10H, m), 7.37-7.36 (5H, m), 7.22-7.20 (2H, d, $J = 4\text{Hz}$), 6.97 (2H, s). ^{13}C NMR (100 MHz, CDCl_3 , δ in ppm): 158.3, 145.3, 138.3, 135.3, 135.2, 134.6, 132.2, 132.1, 131.9, 131.8, 131.7, 131.0, 130.6, 130.5, 130.4, 130.2, 130.0, 129.8, 129.5, 128.6, 128.4, 128.3, 127.7, 127.6, 126.0, 125.7, 123.0, 116.8, 92.5, 89.4. ^{11}B NMR (160 MHz, CDCl_3) δ 0.91 (t, $J_{\text{B-F}} = 30.9\text{ Hz}$). ^{19}F NMR (471 MHz, CDCl_3) δ -130.42 (q, $J_{\text{F-B}} = 31.1\text{ Hz}$). HRMS (ESI) m/z : $[\text{M} + \text{H}]^+$ calcd for $\text{C}_{44}\text{H}_{27}\text{BF}_2\text{N}_3\text{S}_2$: 710.1703; found 710.1709.

Synthesis of aza-BODIPY 3:

In 100 ml round bottom flask, di-bromo aza-BODIPY **1** (0.500 g, 0.75 mmol), 1-ethynyl-4-methoxybenzene (0.199 g (1.50 mmol) were dissolved in a THF/TEA mixture (v/v,1:1) and the solution was degassed with argon for 10 minutes. To this reaction mixture Pd(PPh₃)₄ (0.050 g), CuI (0.007 g) were added. After stirring 12 hrs at 60 °C, the solvent was removed under vacuum and the product was purified by column chromatography using neutral activated aluminum oxide (1: 1 dichloromethane : Hexane) as an eluent to yield 0.462 g (80%) aza-BODIPY **3**. ¹H NMR (400 MHz, CDCl₃, δ in ppm): 8.04-8.02 (4H, d, *J* = 8Hz), 7.93 (2H, s), 7.60-7.57 (6H, m), 7.51-7.48 (4H, d, *J* = 12Hz), 7.26 (2H, s), 6.96 (2H, s), 6.90-6.88 (4H, d, *J* = 8Hz), 3.84 (6H, s); ¹³C NMR (100 MHz, CDCl₃, δ in ppm): 159.9, 158.3, 149.3, 145.3, 138.2, 134.7, 133.3, 131.5, 130.6, 130.3, 129.8, 129.5, 128.3, 126.4, 116.8, 115.1, 114.1, 92.7, 88.3, 55.3. ¹¹B NMR (160 MHz, CDCl₃) δ 0.92 (t, *J*_{B-F} = 30.9 Hz). ¹⁹F NMR (471 MHz, CDCl₃) δ -130.46 (t, *J*_{F-B} = 31.0 Hz). HRMS (ESI) *m/z*: [M]⁺ calcd for C₄₆H₃₀BF₂N₃S₂O₂: 769.1844; found 769.1843.

Synthesis of aza-BODIPY 4:

In 100 ml round bottom flask, di-bromo aza-BODIPY **1** (0.500 g, 0.75 mmol), 4-ethynyl-*N*, *N*-dimethylaniline (0.218 g, 1.50 mmol) were dissolved in a THF/TEA mixture (v/v,1:1) and the solution was degassed with argon for 10 minutes. To this reaction mixture Pd(PPh₃)₄ (0.050 g), CuI (0.007 g) were added. After stirring 12 hrs at 60 °C, the solvent was removed under vacuum and the product was purified by column chromatography using neutral activated aluminium oxide (1: 1 dichloromethane : Hexane) as an eluent to yield 0.451 g (75%) aza-BODIPY **4**. ¹H NMR (400 MHz, CDCl₃, δ in ppm): 8.05-8.03 (4H, *J* = 8Hz), 7.94-7.93 (2H,d, *J* = 4Hz), 7.59-7.57 (6H, d, *J* = 8Hz), 7.45-7.42 (4H, d, *J* = 12Hz), 7.22-7.20 (2H, t, *J* = 4Hz), 6.98 (2H, s), 6.68-6.66 (4H,d, *J* = 8Hz), 3.01 (12H, s). ¹³C NMR (100 MHz, CDCl₃, δ in ppm): 158.2, 150.3, 145.3, 134.8, 133.0, 131.3,

130.1, 129.6, 129.5, 128.3, 127.1, 116.9, 111.8, 109.7, 94.5, 88.0. **¹¹B NMR** (160 MHz, CDCl₃) δ 0.96 (t, J_{B-F} = 31.0 Hz). **¹⁹F NMR** (471 MHz, CDCl₃) δ -130.57 (q, J_{F-B} = 31.1 Hz). **HRMS** (ESI) m/z : [M + H]⁺ calcd for C₄₈H₃₇BF₂N₅S₂: 796.2599; found 796.2554.

Synthesis of aza-BODIPY 5:

We successfully synthesized aza-BODIPY **5** by following the methodology described in our previous publication [22].

¹¹B NMR (160 MHz, CDCl₃) δ 1.12-0.73 (t, J_{B-F} = 30.9 Hz). **¹⁹F NMR** (471 MHz, CDCl₃) δ -130.50 (q, J_{F-B} = 31.0 Hz).

Synthesis of aza-BODIPY 6:

In 100 ml round bottom flask, di-bromo aza-BODIPY **1** (0.500 g, 0.75 mmol), 3-ethynyl-10-propyl-10H-phenothiazine (0.399 g, 1.50 mmol) were dissolved in a THF/TEA mixture (v/v,1:1) and the solution was degassed with argon for 10 minutes. To this reaction mixture Pd(PPh₃)₄ (0.050 g), CuI (0.007 g) were added. After stirring 12 hrs at 60 °C, the solvent was removed under vacuum and the product was purified by column chromatography using neutral activated aluminium oxide (1: 1 dichloromethane : Hexane) as an eluent to yield 0.600 g (77%) aza-BODIPY **6**. **¹H NMR** (400 MHz, CDCl₃, δ in ppm): 8.04-8.02 (4H, d, J = 8 Hz), 7.94 (2H, s), 7.59-7.57 (6H, d, J = 8 Hz), 7.34-7.30 (4H, m), 7.22-7.11 (6H, m), 6.96-6.79 (8H, m), 3.84-3.81 (4H, t, J = 8 Hz), 1.86-1.81 (4H, q), 1.04-1.00 (6H, t, J = 8 Hz). **¹³C NMR** (100 MHz, CDCl₃, δ in ppm): 158.2, 145.6, 145.3, 144.5, 138.1, 134.7, 131.5, 131.0, 130.7, 130.3, 130.3, 129.8, 129.5, 128.3, 127.5, 127.3, 126.2, 124.8, 124.2, 124.1, 122.8, 116.8, 116.7, 115.6, 115.0, 92.3, 89.5, 49.3, 31.6, 22.7, 20.1, 11.3, 11.2; **¹¹B NMR** (160 MHz, CDCl₃) δ 0.92 (t, J_{B-F} = 31.1 Hz). **¹⁹F NMR** (471 MHz, CDCl₃) δ -130.42 (q, J_{F-B} = 31.1 Hz). **HRMS** (ESI) m/z : [M + Na]⁺ calcd for C₆₂H₄₄BF₂N₅S₄Na: 1058.2409; found 1058.2443.

4.7. Conclusion

In conclusion, a series of donor-functionalized aza-BODIPY dyes (**2–6**) were successfully synthesized via the Pd-catalyzed Sonogashira cross-coupling reaction. In optical properties, the *N,N*-dimethylaniline-substituted aza-BODIPY dye **4** showed a red-shifted absorption compared to the other aza-BODIPY dyes (**2**, **3**, **5**, and **6**). Electrochemical studies exhibited multiple oxidation and reduction waves associated with the donor and acceptor groups. Computational calculations showed that the aza-BODIPY dyes (**2–6**) have low HOMO-LUMO gap values. These aza-BODIPY derivatives exhibit promising features such as their absorption in the visible-to-near-infrared (vis-NIR) range, multiple redox peaks, and low HOMO-LUMO gap values, which suggest their potential use in organic photovoltaics and bioimaging.

4.8. References

- [1] Chen, X., Yu, B., Wang, J., Luo, Z., Meng, H., Xie, B., Zhou, R., Liu, S., Zhao, Q. (2023). A Near-Infrared Organic Photodetector Based on an Aza-BODIPY Dye for a Laser Microphone System. *J. Mater. Chem. C*, 11(6), 2267–2272. (DOI: 10.1039/D2TC04274F).
- [2] Zhang, N., Lu, C., Chen, M., Xu, X., Shu, G., Du, Y., Ji, J. (2021). Recent Advances in Near-Infrared II Imaging Technology for Biological Detection. *J. Nanobiotechnology*, 19(1), 132. (DOI: 10.1186/s12951-021-00870-z).
- [3] Ding, F., Zhan, Y., Lu, X., Sun, Y. (2018). Recent Advances in Near-Infrared II Fluorophores for Multifunctional Biomedical Imaging. *Chem. Sci.*, 9(19), 4370–4380. (DOI: 10.1039/C8SC01153B)
- [4] Wang, S., Li, B., Zhang, F. (2020). Molecular Fluorophores for Deep-Tissue Bioimaging. *ACS Cent. Sci.*, 6(8), 1302–1316. (DOI: 10.1021/acscentsci.0c00544).

- [5] Liu, Y., Teng, L., Liu, H.-W., Xu, C., Guo, H., Yuan, L., Zhang, X.-B., Tan, W. (2019). Recent Advances in Organic-Dye-Based Photoacoustic Probes for Biosensing and Bioimaging. *Sci. China Chem.*, 62(10), 1275–1285. (DOI: 10.1007/s11426-019-9506-2).
- [6] Virgili, T., Ganzer, L., Botta, C., Squeo, B. M., Pasini, M. (2022). Asymmetric AZA-BODIPY with Optical Gain in the Near-Infrared Region. *Molecules*, 27(14), 4538. DOI: 10.3390/molecules27144538).
- [7] Yang, N., Song, S., Liu, C., Ren, J., Wang, X., Zhu, S., Yu, C. (2022). An Aza-BODIPY-Based NIR-II Luminogen Enables Efficient Phototheranostics. *Biomater. Sci.*, 10(17), 4815–4821. (DOI: 10.1039/D2BM00670G).
- [8] Zhu, L., Xie, W., Zhao, L., Zhang, Y., Chen, Z. (2017). Tetraphenylethylene- and Fluorene-Functionalized near-Infrared Aza-BODIPY Dyes for Living Cell Imaging. *RSC Adv.*, 7(88), 55839–55845. (DOI: 10.1039/C7RA10820F).
- [9] Balsukuri, N., Manav, N., Lone, M. Y., Mori, S., Das, A., Sen, P., Gupta, I. (2020). Donor-Acceptor Architectures of Tetraphenylethylene Linked Aza-BODIPYs: Synthesis, Crystal Structure, Energy Transfer and Computational Studies. *Dyes Pigments*, 176, 108249. (DOI: 10.1016/j.dyepig.2020.108249).
- [10] Balsukuri, N., Boruah, N. J., Kesavan, P. E., Gupta, I. (2018). Near Infra-Red Dyes Based on Pyrene Aza-BODIPYs. *New J. Chem.*, 42(8), 5875–5888. (DOI: 10.1039/C7NJ03408C).
- [11] Li, L., Wang, L., Tang, H., Cao, D. (2017). A Facile Synthesis of Novel Near-Infrared Pyrrolopyrrole Aza-BODIPY Luminogens with Aggregation-Enhanced Emission Characteristics. *Chem. Commun.*, 53(59), 8352–8355. (DOI: 10.1039/C7CC04568A).

- [12] Pliquett, J., Dubois, A., Racœur, C., Mabrouk, N., Amor, S., Lescure, R., Bettaïeb, A., Collin, B., Bernhard, C., Denat, F., Bellaye, P. S., Paul, C., Bodio, E., Goze, C. (2019). A Promising Family of Fluorescent Water-Soluble Aza-BODIPY Dyes for in Vivo Molecular Imaging. *Bioconj. Chem.*, 30(4), 1061–1066. (DOI: 10.1021/acs.bioconjchem.8b00795).
- [13] Xu, Y., Zhao, M., Zou, L., Wu, L., Xie, M., Yang, T., Liu, S., Huang, W., Zhao, Q. (2018). Highly Stable and Multifunctional Aza-BODIPY-Based Phototherapeutic Agent for Anticancer Treatment. *ACS Appl. Mater. Interfaces*, 10(51), 44324–44335. (DOI: 10.1021/acsami.8b18669).
- [14] Li, S., Lv, M., Wang, J., Zhang, D., Xu, Z., Jiang, X.-D. (2022). Near-Infrared Absorbing Aza-BODIPYs with 1,7-Di- Tert -Butyl Groups by Low-Barrier Rotation for Photothermal Application. *Mater. Adv.*, 3(2), 1254–1262. (DOI: 10.1039/D1MA01052B).
- [15] Jiang, X.-D., Liu, X., Fang, T., Sun, C. (2017). Synthesis and Application of Methylthio-Substituted BODIPYs/Aza-BODIPYs. *Dyes and Pigments*, 146, 438–444. (DOI: 10.1016/j.dyepig.2017.07.038).
- [16] Khan, T. K., Sheokand, P., Agarwal, N. (2014). Synthesis and Studies of Aza-BODIPY-Based π -Conjugates for Organic Electronic Applications: Synthesis and Studies of Aza-BODIPY-Based π -Conjugates. *Eur. J. Org. Chem.*, 2014(7), 1416–1422. (DOI: 10.1002/ejoc.201301300).
- [17] Squeo, B. M., Ganzer, L., Virgili, T., Pasini, M. (2020). BODIPY-Based Molecules, a Platform for Photonic and Solar Cells. *Molecules*, 26(1), 153. (DOI: 10.3390/molecules26010153).
- [18] Balsukuri, N., Manav, N., Lone, M. Y., Mori, S., Das, A., Sen, P., Gupta, I. (2020). Donor-Acceptor Architectures of Tetraphenylethene Linked Aza-BODIPYs: Synthesis, Crystal

- Structure, Energy Transfer and Computational Studies. *Dyes and Pigments*, 176, 108249. (DOI: 10.1016/j.dyepig.2020.108249).
- [19] Poddar M., Misra R. (2020). Recent advances of BODIPY based derivatives for optoelectronic applications. *Coord. Chem. Rev.*, 421, 213462. (DOI: 10.1016/j.ccr.2020.213462).
- [20] Patil Y., Misra R. (2019). Metal Functionalized Diketopyrrolopyrroles: A Promising Class of Materials for Optoelectronic Applications. *Chem. Rec.*, 19, 1–9. (DOI: 10.1002/tcr.201900061).
- [21] Khan T. K., Sheokand P., Agarwal N. (2014). Synthesis and Studies of Aza-BODIPY-Based π -Conjugates for Organic Electronic Applications. *EurJOC.*, 2014(7), 1416-1422. (DOI: 10.1002/ejoc.201301300).
- [22] Pinjari D. A., Alsaleh A. Z., Patil Y., Misra R., D'Souza F. (2020). Interfacing High-Energy Charge-Transfer States to a Near-IR Sensitizer for Efficient Electron Transfer upon Near-IR Irradiation. *Angew. Chem. Int. Ed.*, 59(52), 23697-23705. (DOI: 10.1002/anie.202013036).
- [23] Gut A., Lapok L., Jamroz D., Gorski A., Solarski J., Nowakowska M. (2017). Photophysics and redox properties of aza-BODIPY dyes with electron-withdrawing groups. *New J. Chem.*, 41, 12110-12122. (DOI: 10.1039/C7NJ02757E).

Chapter 5

Triphenylamine functionalized NIR absorbing α -aza-dipyrromethenes and aza-BODIPYs

5.1. Introduction

Near-infrared (NIR) absorbing dyes have been widely used in biomedical applications because of its deep NIR light penetration into most biological tissues compared to visible light.^[1] Push-pull chromophores with visible and NIR absorption have been studied for variety of technological applications including multi-photon absorption and organic photovoltaics.^[2] Our group is involved in the design and synthesis of donor-acceptor (D-A) architectures with NIR absorption for solution processed bulk heterojunction organic solar cells (BHJ-OSCs).^[3] Aza-BODIPY (Aza-boron-dipyrromethene) is a class of heteroatom-containing BODIPY dye exhibits strong electron acceptor character with NIR absorption, low optical gap and low lying LUMO levels.^[4,5,6] Its derivatives have been used for various applications including solar cells, photosensitizers, bioimaging and chemosensors.^[7,8,9] The first synthesis of aza-BODIPY was reported by Davies and Rogers in 1943, however its continent synthesis was further developed in early 2000's. Aza-BODIPY dyes received great interest due to its visible to NIR absorption and high thermal stability.^[10,11]

Tetracyanoethylene (TCNE) is a strong electron acceptor and its incorporation in molecular system provides charge-transfer character and electron-accepting potential.^[12] The convenient way of incorporating TCBD to ethyne bridged molecule is the [2 + 2] cycloaddition-retroelectrocyclization reaction, which is generally a fast, high-yielding catalyst-free reaction.^[13]

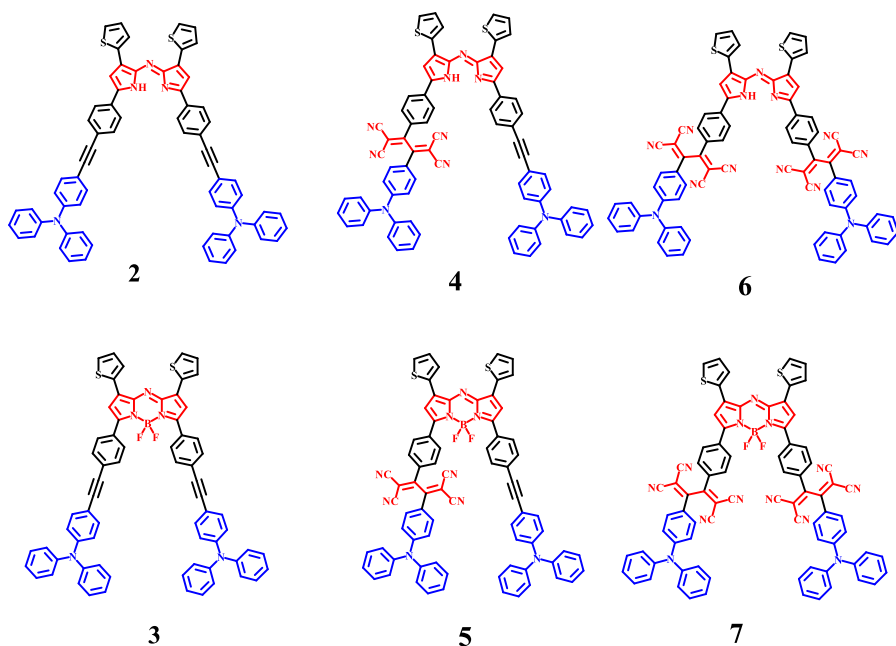


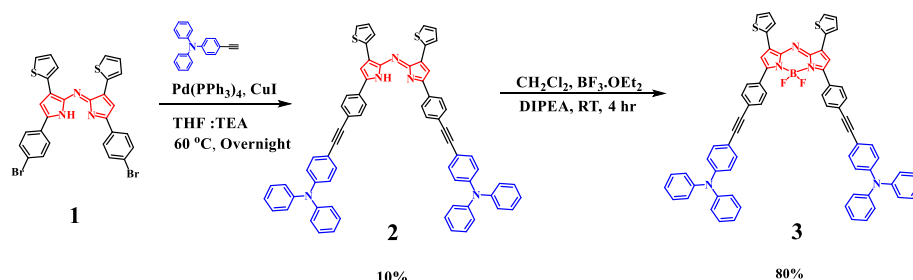
Figure 5.1. Chemical structures of aza-dipyrromethene and aza-BODIPY dyes **2–7**.

Herein we designed and synthesized triphenylamine based ethyne bridged aza-pyrromethene and aza-BODIPY dyes and further incorporated tetracyanobutadiene (TCBD) units. The incorporation of electron withdrawing TCBD in triphenylamine functionalized aza-dipyrromethenes and aza-BODIPYs will provide the high electron affinity to molecular systems. Our main objective to synthesize these small molecules was to see the effect of electron withdrawing TCBD unit on optical and electrochemical properties of triphenylamine based aza-dipyrromethenes and aza-BODIPYs.

5.2. Results and Discussion

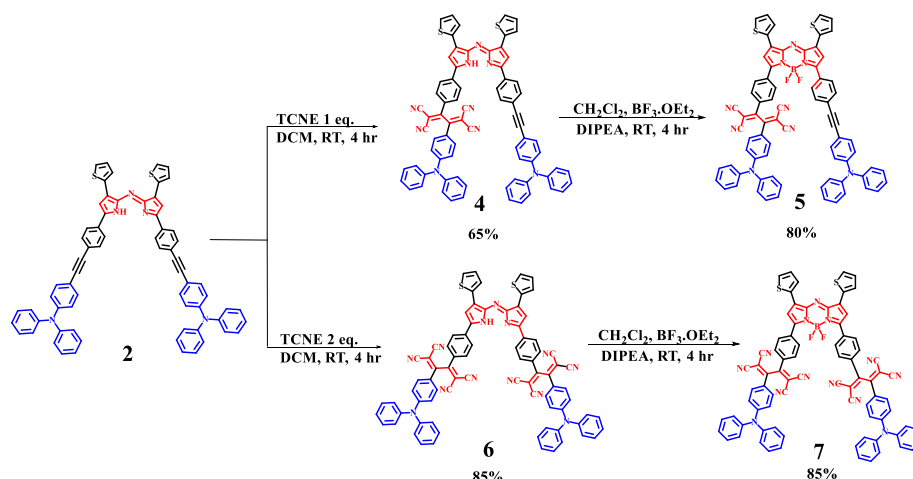
The precursor di-bromo-aza-dipyrromethene **1** was synthesized as per reported procedure.^[14] The triphenylamine based aza-dipyrromethene **2** was synthesized by the Sonogashira cross-coupling reaction of di-bromo aza-dipyrromethene **1** (1.0 eq.) with 4-ethynyl-*N,N*-diphenylaniline (2.2 eq.) in a THF/TEA mixture (v/v,1:1) at 60 °C for overnight under argon atmosphere in 10% yield. Further the triphenylamine based aza-dipyrromethene **2** was reacted with boron

trifluoride in presence of diisopropylamine at room temperature and obtained BF₂ chelated aza-BODIPY **3** in 80% yield (Scheme 5.1.).



Scheme 5.1. Synthesis of triphenylamine substituted aza-dipyrromethene **2** and aza-BODIPY **3**.

The [2 + 2] cycloaddition-retroelectrocyclization reactions of triphenylamine based aza-dipyrromethene **2** with one and two equivalents of TCNE in dichloromethane at room temperature for 4 hours resulted in mono-TCBD bridged aza-dipyrromethene **4** and di-TCBD bridged aza-dipyrromethene **6** in 65% and 85% yield respectively (Scheme 5.2.). The BF₂ chelated triphenylamine based aza-BODIPYs **5** and **7** were obtained by the complexation reaction of aza-dipyrromethenes **4** and **6** with boron trifluoride etherate (BF₃.OEt₂), diisopropylethylamine in dichloromethane solvent for 4 hours in 80% and 85% yield respectively (Scheme 5.2.).



Scheme 5.2. Synthetic route for TCBD bridged aza-dipyrromethenes and aza-BODIPY dyes **4–7**.

The triphenylamine substituted aza-dipyrromethene and aza-BODIPY dyes **2–7** were purified by column chromatography using neutral activated aluminium oxide. The dyes **2–7** are readily soluble in common organic solvents such as chloroform, toluene, dichloromethane, and were well characterized by ^1H NMR, ^{13}C NMR and HRMS techniques.

5.3. Photophysical Properties

The electronic absorption spectra of triphenylamine functionalized aza-dipyrromethenes and aza-BODIPYs **2–7** were recorded in dichloromethane solvent at room temperature (Figure 5.2.) and data are listed in Table 5.1. The absorption spectra of the dyes **2–7** exhibit broad absorption bands covering visible to NIR region from 400 nm to 880 nm. The absorption spectra show two bands, one in shorter wavelength region ~ 500 nm and another at longer wavelength region ~ 700 nm corresponds to the $\pi \rightarrow \pi^*$ transition and intramolecular charge transfer (ICT) from donor (triphenylamine) to acceptor (TCBD and aza-BODIPY) respectively.

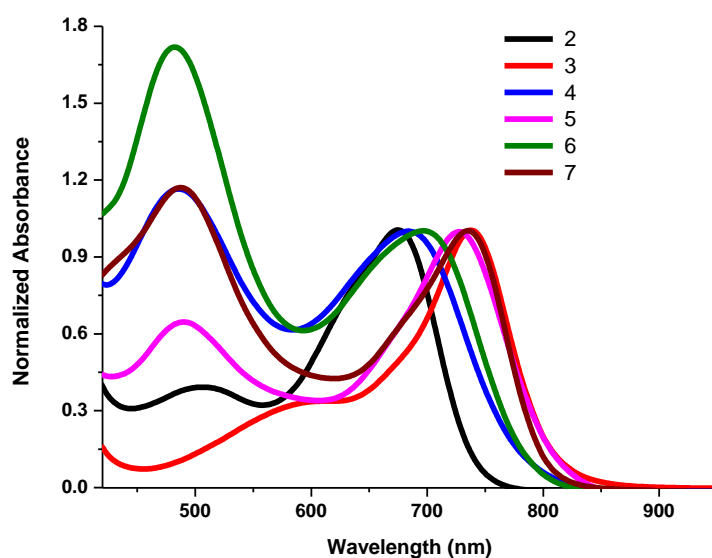


Figure 5.2. Normalized electronic absorption spectra of the aza-dipyrromethenes and aza-BODIPYs **2–7** in dichloromethane (1×10^{-5} M).

The aza-dipyrromethenes **2**, **4** and **6** show absorption maxima at 675 nm, 685 nm and 695 nm in longer wavelength region respectively and the complexation of BF₂ exhibits red shift in the absorption. The complexation of BF₂ to aza-dipyrromethenes **2**, **4** and **6** exhibited red shift of 63 nm, 44 nm and 40 nm and observed absorption bands at 738 nm (for **3**), 728 nm (for **5**) and 735 nm (for **7**) respectively. The incorporation of one and two TCNE units in triphenylamine based aza-dipyrromethene **2** showed red shift of 10 nm and 20 nm respectively, whereas the incorporation of one and two TCND units in triphenylamine based aza-BODIPY **3** exhibit blue shift of 10 nm in **5** and 3 nm in **7** respectively. The di-TCBD bridged dyes **6** and **7** showed red shifted absorption compared to its mono-TCBD bridged analogues **4** and **5** respectively.

Table 5.1. Photophysical properties of triphenylamine functionalized aza-dipyrromethenes and aza-BODIPYs **2–7**.

Dyes	λ_{abs} (nm) ^a	$\epsilon/10^4$ (M ⁻¹ .cm ⁻¹) ^a	E_g^b (eV)
2	675	4.6	1.91
	506		
3	738	8.2	1.67
	586		
4	685	5.8	1.75
	484		
5	728	2.3	1.63
	490		
6	695	3.3	1.75
	482		
7	735	3.8	1.58
	488		

^aAbsorbance measured in dichloromethane at 1×10^{-5} M concentration, ϵ : molar extinction coefficient, ^bTheoretical HOMO–LUMO gap values calculated from DFT calculation.

The strong band in visible region for TCBD bridged dyes **4–7** was observed which was assigned as $\pi \rightarrow \pi^*$ transitions of TCBD units. The complexation of BF_2 and incorporation of electron withdrawing TCNE units in aza-dipyrromethenes exhibited red shift in the absorption whereas incorporation of TCBD units to aza-BODIPY shows blue shift in the absorption bands.

5.4. Electrochemical properties

The electrochemical properties of the triphenylamine substituted aza-dipyrromethenes and aza-BODIPYs **2–7** were investigated by the cyclic voltammetric (CV) analysis in dichloromethane solution at room temperature using tetrabutylammonium hexafluorophosphate (Bu_4NPF_6) as a supporting electrolyte. The CV plots of aza-dipyrromethenes and aza-BODIPYs **2–7** are shown in Figure 5.3. and the data are listed in Table 5.2.

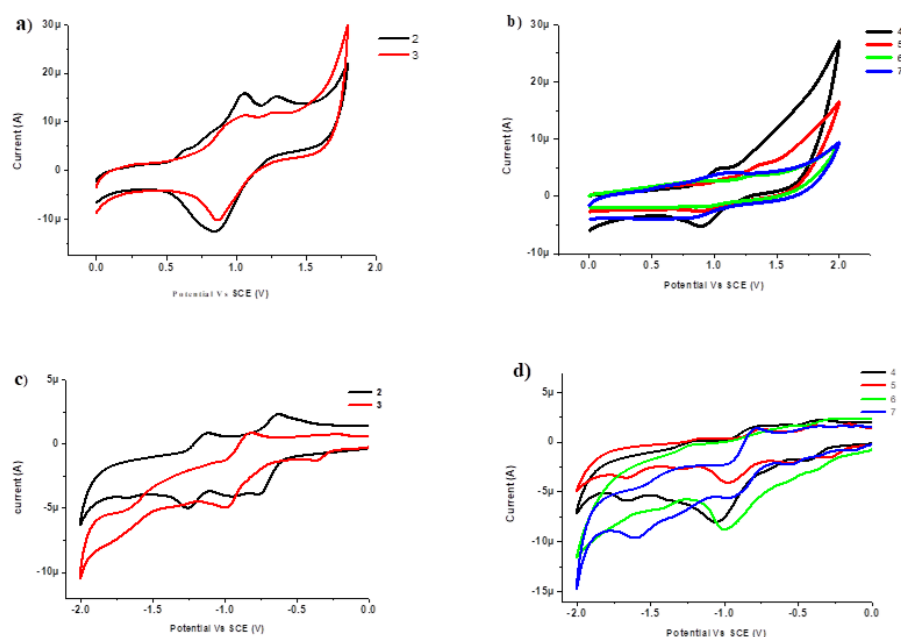


Figure 5.3. CVs plots of aza-dipyrromethenes and aza-BODIPYs **2–7**.

Generally aza-dipyrromethene and aza-BODIPY dyes exhibit one oxidation and two reduction potentials.^[15] The CV of triphenylamine substituted aza-dipyrromethene **2** and aza-BODIPY **3** show two oxidation potentials at 0.97, 1.23 and 0.96, 1.22 V due to the

triphenylamine and aza-dipyrromethene/aza-BODIPY unit respectively. The two reduction potentials were observed for aza-dipyrromethene **2** and aza-BODIPY **3** at -0.69, -1.19 and -0.31, -0.90 V due to aza-dipyrromethene and aza-BODIPY unit respectively. The TCBD bridged dyes **4–7** show two oxidation potential and four reduction potentials, the two oxidation potentials were related to triphenylamine and aza-dipyrromethene/aza-BODIPY unit and the four reduction potential for aza-dipyrromethene/aza-BODIPY and TCBD core. First and second reduction potentials in dyes **4–7** were related to the formation of mono- and di-anion at TCBD unit. The complexation of BF₂ to aza-dipyrromethenes **2**, **4** and **6** lowers the first and second reduction potentials in aza-BODIPYs **3**, **5** and **7** respectively.

Table 5.2. Electrochemical properties of aza-dipyrromethenes and aza-BODIPYs **2–7**.

Dyes	E^2	E^1	E^1	E^2	E^3	E^4
	Oxid ^a	Oxid ^a	Red ^a	Red ^a	Red ^a	Red ^a
2	1.23	0.97	-0.69	-1.19	-	-
3	1.22	0.96	-0.31	-0.90	-	-
4	1.28	0.97	-0.39	-0.64	-0.93	-1.44
5	1.32	0.98	-0.22	-0.46	-0.87	-1.37
6	1.30	0.90	-0.32	-0.57	-0.84	-1.38
7	0.99	0.48	-0.10	-0.49	-0.84	-1.45

^aThe electrochemical analysis was performed in a 0.1 M solution of Bu₄NPF₆ in dichloromethane at 100 mVs⁻¹ scan rate, versus SCE at 25 °C.

The aza-BODIPYs **3**, **5** and **7** were easier to reduce and slightly harder to oxidize than the respective aza-dipyrromethene dyes **2**, **4** and **6**. The introduction of TCBD in triphenylamine based aza-dipyrromethene dyes (**2**, **4** and **6**) exhibit two additional reduction waves at low reduction potential and hardens the reduction of aza-dipyrromethene/aza-BODIPY unit (in aza-BODIPYs **3**, **5** and **7**).

5.5. Theoretical Calculations

In order to understand the geometry and the electronic structure of triphenylamine functionalized aza-dipyrromethenes and aza-BODIPYs **2–7**, density functional theory (DFT) calculation was carried out using the Gaussian 09W program. The DFT calculation was performed at the B3LYP/6-31G (d, p) level for C, H, N, S, B and F and geometry optimization was carried out in the gas phase.

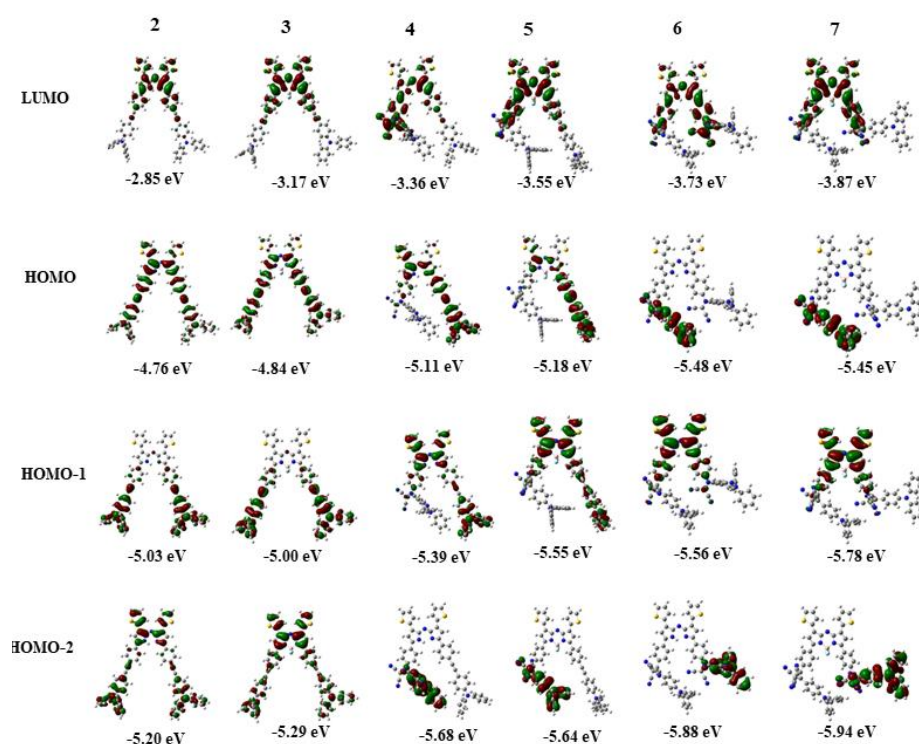


Figure 5.4. Frontier molecular orbitals of aza-dipyrromethenes and aza-BODIPYs **2–7** at the B3LYP/6-31G(d, p) level.

Figure 5.4. depicts the frontier molecular orbitals (FMOs) of the aza-dipyrromethenes and aza-BODIPYs **2–7**. The theoretically calculated highest occupied molecular orbitals (HOMOs) and lowest unoccupied molecular orbitals (LUMOs) are shown in Figure 5.4. The HOMO on dyes **2–7** are located on triphenylamine donor and LUMOs are located on aza-dipyrromethene/aza-BODIPY and TCBD unit showing its acceptor nature. The triphenylamine substituted aza-dipyrromethene **2** and aza-BODIPY **3** exhibit planar geometry whereas their TCBD

derivatives **4–7** show distorted geometry. The theoretically calculated HOMO energy levels of triphenylamine substituted aza-dipyrromethenes and aza-BODIPYs **4–7** are -5.11, -5.18, -5.48 and -5.45 eV, and the corresponding LUMO levels are -3.36, -3.55, -3.73 and -3.87 eV respectively (Figure 5.4.) which indicates that the complexation of BF₂ and incorporation of electron withdrawing TCBD unit stabilizes the HOMO and LUMO energy levels.

Table 5.3. Calculated major electronic transitions for aza-dipyrromethenes and aza-BODIPYs **2–7** in the gas phase.

Dyes	Wavelength (nm)	Composition	f^a
2	713	HOMO-LUMO (0.70)	0.76
	625	HOMO-1→LUMO (0.70)	0.43
3	851	HOMO→LUMO (0.70)	0.41
	657	HOMO-1→LUMO (0.67)	0.40
4	754	HOMO-3→LUMO (0.11)	0.38
		HOMO-1→LUMO (0.69)	
	625	HOMO-3→LUMO (0.62)	
		HOMO-1→LUMO+1 (0.29)	
5	811	HOMO→LUMO (0.70)	0.33
	678	HOMO-1→LUMO (0.69)	0.29
	660	HOMO→LUMO+1(0.69)	0.27
6	825	HOMO→LUMO (0.70)	0.58
	747	HOMO-1→LUMO (0.71)	0.41
	615	HOMO-2→LUMO (0.69)	0.43
7	701	HOMO-1→LUMO (0.45)	0.27
		HOMO-2→LUMO (0.52)	0.19
	690	HOMO-1→LUMO (0.44)	
		HOMO-2→LUMO (0.41)	

The TD-DFT calculation was performed to understand the electronic transitions in triphenylamine functionalized aza-dipyrromethenes and

aza-BODIPYs **2–7**. The electronic transitions in triphenylamine functionalized aza-dipyrromethenes and aza-BODIPYs **2–7** from TD-DFT calculation with composition and oscillator strength are shown in Table 5.3. The results of TD-DFT calculations indicate that the dyes **2–7** show two main electronic transitions in vis-NIR region occurs from HOMO to LUMO and HOMO-1 to LUMO. The charge transfer transitions from triphenylamine to aza-dipyrromethene/aza-BODIPY and TCBD unit were observed for longer wavelength region. The strong transition in visible wavelength range for di-TCBD bridged dyes **6** and **7** were observed which is assigned as $\pi \rightarrow \pi^*$ transitions due to TCBD units, which is consistent to experimental absorption spectra.

5.6. Experimental section

General methods

The chemicals were used as received unless otherwise indicated. All the moisture sensitive reactions were performed under argon atmosphere using the standard Schlenk method. ^1H NMR (400 MHz) and ^{13}C NMR (100 MHz) spectra were recorded by using CD_2Cl_2 as the solvents. The ^1H NMR chemical shifts are reported in parts per million (ppm) relative to the solvent residual peak (CD_2Cl_2 , 5.32 ppm). The multiplicities are given as: s (singlet), d (doublet), m (multiplet), and the coupling constants, J , are given in Hz. The ^{13}C NMR chemical shifts are reported with relative to the solvent residual peak (CD_2Cl_2 , 54.0 ppm). HRMS was recorded on a mass spectrometer (ESI-TOF). The UV-visible absorption spectra were recorded on UV-visible Spectrophotometer in dichloromethane. The CVs were recorded on an electrochemical analyzer using glassy carbon as working electrode, Pt wire as the counter electrode, and saturated SCE as the reference electrode.

Experimental Procedure

Synthesis of aza-dipyrromethene 2

In 100 ml round bottom flask, di-bromo aza-dipyrromethene **1** (0.200 mg, 0.3 mmol), 4-ethynyl-*N,N*-diphenylaniline (0.191 g, 0.7 mmol) were dissolved in a THF/TEA mixture (v/v,1:1) and the solution was degassed with argon for 10 minutes. To this reaction mixture Pd(PPh₃)₄ (0.020 g), CuI (0.007 g) were added. After stirring overnight at 60 °C, the solvent was removed under vacuum and the product was purified by column chromatography using neutral activated aluminium oxide (1: 1 dichloromethane: Hexane) as an eluent to yield (10%) aza-dipyrromethene **2**. **¹H NMR** (400 MHz, CD₂Cl₂, δ in ppm): 7.92-7.80 (8H, m), 7.67 (5H, m), 7.48-7.41 (6H, m), 7.31 (7H, s), 7.13 (15H, d, J = 8 Hz), 7.02 (4H, m); **¹³C NMR** (100 MHz, CD₂Cl₂, δ in ppm): 176.7, 147.6, 133.2, 132.6, 130.0, 128.6, 128.3, 127.1, 125.8, 124.4, 122.3; **HRMS** (ESI) m/z calcd for C₆₈H₄₅N₅S₂: 996.3385 [M+H]⁺, found 996.3189 [M+H]⁺.

Synthesis of aza-BODIPY 3:

In 100 ml round bottom flask, aza-dipyrromethene **2** (0.200 g, 0.2 mmol) was dissolved in dichloromethane (30 mL) and diisopropylethylamine (0.35 mL, 2.0 mmol) was added dropwise. The solution was stirred at room temperature for 15 minutes and then BF₃.Et₂O (0.53 mL, 3.0 mmol) was added and the solution was stirred at room temperature for 4 hours. Water was added to the reaction mixture and the organic layer was separated and dried over sodium sulphate. The solvent was evaporated under vacuum and the crude product was purified by column chromatography using neutral activated aluminium oxide (1:2 dichloromethane: hexane) as an eluent to yield 80% of aza-BODIPY **3**. **¹H NMR** (400 MHz, CD₂Cl₂, δ in ppm): 8.06-7.97 (4H, m), 7.63-7.61 (4H, m), 7.42-7.40 (4H, d, J = 8 Hz), 7.30-7.24 (10H, m), 7.14-6.99 (22H, m); **¹³C NMR** (100 MHz, CD₂Cl₂, δ in ppm): 149.2, 140.7, 136.7, 134.8, 133.5, 132.8, 132.0, 131.6, 130.5, 127.4, 126.0, 123.9, 119.1, 117.4, 90.8; **HRMS** (ESI) m/z

calcd for $C_{68}H_{44}BF_2N_5S_2$: 1044.3183 $[M + H]^+$, found 1044.3183 $[M + H]^+$.

Synthesis of aza-dipyrromethene **4**

In 100 ml round bottom flask, aza-dipyrromethene **2** (0.200 g, 0.20 mmol) and TCNE (0.025 g, 0.20 mmol) were dissolved in dichloromethane (30 ml). The reaction mixture was stirred at room temperature for 4 hours. The solvent was removed under vacuum and the product was purified by column chromatography using neutral activated aluminium oxide with hexane: dichloromethane (2:1) as an eluent to yield 65% of aza-dipyrromethene **4**. 1H NMR (400 MHz, CD_2Cl_2 , δ in ppm): 7.77 (4H, s), 7.73-7.69 (4H, t, $J = 8$ Hz), 7.62 (1H, s), 7.56-7.54 (2H, d, $J = 8$ Hz), 7.40-7.29 (13H, m), 7.23-7.21 (6H, m), 7.14-6.09 (7H, m), 7.04-6.95 (7H, m), 6.91 (1H, s); ^{13}C NMR (100 MHz, CD_2Cl_2 , δ in ppm): 167.3, 164.2, 164.0, 160.2, 156.2, 154.5, 149.1, 147.6, 145.7, 145.1, 141.1, 137.4, 137.2, 136.1, 135.7, 133.9, 133.3, 132.6, 132.5, 131.8, 131.5, 130.9, 130.6, 130.1, 129.6, 128.9, 128.5, 128.3, 128.1, 128.0, 127.6, 127.3, 126.7, 125.9, 125.8, 124.8, 124.5, 124.4, 122.4, 122.2, 122.0, 118.5, 117.4, 115.9, 115.7, 114.4, 113.7, 113.1, 112.4, 94.2, 89.3, 86.4, 78.9, 78.2, 77.9, 77.6, 61.0; HRMS (ESI) m/z calcd for $C_{74}H_{45}N_9S_2$: 1124.3554 $[M + H]^+$, found 1124.3312 $[M + H]^+$.

Synthesis of aza-BODIPY **5**:

In 100 ml round bottom flask, aza-dipyrromethene **4** (200 mg, 0.2 mmol) was dissolved in dichloromethane (30 mL) and diisopropylethylamine (0.35 mL, 2.0 mmol) was added dropwise. The solution was stirred at room temperature for 15 minutes and then $BF_3 \cdot Et_2O$ (0.37 mL, 3.0 mmol) was added. Then solution was stirred at room temperature for 4 hours. Water was added to the reaction mixture and the organic layer was separated and dried over sodium sulphate. The solvent was evaporated under vacuum and the crude product was purified by column chromatography using neutral activated aluminium oxide with dichloromethane: hexane (4:1) as an eluent to yield 80% of

aza-BODIPY **5**. **¹H NMR** (400 MHz, CD₂Cl₂, δ in ppm): 8.20-8.17 (2H, m), 8.06-8.00 (3H, m), 7.92-7.84 (4H, m), 7.73-7.71 (2H, d, J = 8 Hz), 7.68-7.61 (4H, m), 7.45-7.38 (6H, m), 7.33-7.24 (12H, m), 7.14-7.09 (5H, m), 7.03-6.94 (6H, m); **¹³C NMR** (100 MHz, CD₂Cl₂, δ in ppm): 167.4, 163.5, 161.5, 154.3, 148.9, 147.3, 147.0, 145.1, 144.8, 140.4, 137.5, 134.8, 134.4, 133.1, 132.9, 132.7, 132.3, 132.2, 132.1, 131.7, 131.4, 131.3, 131.2, 131.1, 130.6, 130.4, 130.3, 130.1, 129.9, 129.8, 128.9, 128.8, 128.7, 127.6, 127.4, 127.1, 127.0, 126.7, 125.6, 124.2, 121.9, 121.2, 118.3, 118.0, 117.0, 115.3, 114.0, 113.3, 112.3, 111.8, 94.4, 88.9, 87.6, 78.1; **HRMS** (ESI) m/z calcd for C₇₄H₄₄BF₂N₉S₂: 1172.3289 [M + H]⁺, found 1172.3307 [M + H]⁺.

Synthesis of aza-BODIPY **6**

In 100 ml round bottom flask, aza-dipyrromethene **2** (0.200 g, 0.10 mmol) and TCNE (0.049 g, 0.20 mmol) were dissolved in dichloromethane (30 ml). The reaction mixture was stirred at room temperature for 4 hours. The solvent was removed under vacuum and the product was purified by column chromatography using neutral activated aluminium oxide with dichloromethane as an eluent to yield 85% aza-dipyrromethene **6**. **¹H NMR** (400 MHz, CD₂Cl₂, δ in ppm): 7.74-7.73 (8H, d, J = 4Hz), 7.63-7.61 (4H, d, J = 8Hz), 7.55 (2H, s), 7.44-7.40 (8H, m), 7.30-7.26 (15H, m), 7.00-7.97 (4H, d, J = 12Hz), 6.88 (2H, s), 6.74 (2H, s); **¹³C NMR** (100 MHz, CD₂Cl₂, δ in ppm): 167.5, 164.0, 154.7, 154.3, 151.0, 145.1, 137.9, 137.0, 135.6, 133.7, 133.0, 132.6, 130.7, 129.2, 129.0, 127.7, 127.6, 127.4, 121.9, 118.5, 115.0, 114.4, 113.9, 113.0, 112.2, 87.4, 78.7; **HRMS** (ESI) m/z calcd for C₈₀H₄₅N₁₃S₂: 1252.3491 [M + H]⁺, found 1252.3435 [M + H]⁺.

Synthesis of aza-BODIPY **7**

In 100 ml round bottom flask, aza-dipyrromethene **6** (200 mg, 0.15 mmol) was dissolved in dichloromethane (30 mL) and diisopropylethylamine (0.3 mL, 1.5 mmol) was added dropwise. The solution was stirred at room temperature for 15 minutes and then BF₃.Et₂O (0.4 mL, 2.4 mmol) was added. The solution was stirred at

room temperature for 4 hours. Water was added to the reaction mixture and the organic layer was separated and dried over sodium sulphate. The solvent was evaporated under vacuum and the crude product was purified by column chromatography using neutral activated aluminium oxide with dichloromethane as an eluent to yield 85% of aza-BODIPY **7**. **¹H NMR** (400 MHz, CD₂Cl₂, δ in ppm): 8.21-8.19 (2H, d, J = 8Hz), 7.99 (1H, s), 7.87-7.85 (2H, d, J = 8Hz), 7.71-7.69 (4H, d, J = 8Hz), 7.43-7.40 (6H, m), 7.34-7.24 (16H, m), 7.07-7.05 (8H, m), 6.94-6.92 (5H, d, J = 8Hz); **¹³C NMR** (100 MHz, CD₂Cl₂, δ in ppm): 167.7, 163.6, 162.6, 154.7, 148.4, 148.0, 147.7, 145.1, 138.8, 134.7, 133.7, 132.6, 132.5, 131.5, 131.0, 130.7, 130.2, 129.9, 129.7, 129.3, 129.1, 129.0, 127.7, 127.4, 126.2, 125.5, 125.3, 125.0, 124.7, 123.8, 123.3, 121.4, 118.5, 118.0, 115.0, 114.2, 113.6, 112.5, 112.0, 107.4, 78.4, 55.6; **HRMS** (ESI) m/z calcd for C₈₀H₄₄BF₂N₁₃S₂: 1322.3426 [M + Na]⁺, found 1322.3250 [M + Na]⁺.

5.7. Conclusion

We have synthesized triphenylamine substituted aza-dipyrromethene and aza-BODIPY dyes **2–7** by the Pd-catalyzed Sonogashira cross-coupling reaction and [2 + 2] cycloaddition retroelectrocyclization reaction. The BF₂ containing aza-BODIPYs **3**, **5** and **7** show red shifted absorption as compared to aza-dipyrromethenes **2**, **4** and **6**. The DFT and TD-DFT results reveal that electron density transfers from triphenylamine (donor) to aza-BODIPY and TCBD (acceptor) core. The DFT calculations show that the triphenylamine substituted aza-BODIPYs **3**, **5** and **7** exhibit low HOMO–LUMO gap values as compared to aza-dipyrromethenes **2**, **4** and **6**.

5.8. References

- [1] Chen, Y., Xue, L., Zhu, Q., Feng, Y., Wu, M. (2021). Recent Advances in Second Near-Infrared Region (NIR-II) Fluorophores and Biomedical Applications. *Front. Chem.*, 9. (DOI: 10.3389/fchem.2021.750404)

- [2] Dalton, L. R., Sullivan, P. A., Bale, D. H. (2010). Electric Field Poled Organic Electro-Optic Materials: State of the Art and Future Prospects. *Chem. Rev.*, 110(1), 25–55. (DOI: 10.1021/cr9000429).
- [3] Blanchard-Desce, M., Alain, V., Bedworth, P. V., Marder, S. R., Fort, A., Runser, C., Barzoukas, M., Lebus, S., Wortmann, R. (1997). Large Quadratic Hyperpolarizabilities with Donor–Acceptor Polyenes Exhibiting Optimum Bond Length Alternation: Correlation Between Structure and Hyperpolarizability. *Chem. – Eur. J.*, 3(7), 1091–1104. (DOI: 10.1002/chem.19970030717).
- [4] Patil, Y., Misra, R., Singhal, R., D. Sharma, G. (2017). Ferrocene-Diketopyrrolopyrrole Based Non-Fullerene Acceptors for Bulk Heterojunction Polymer Solar Cells. *J. Mater. Chem. A*, 5(26), 13625–13633. (DOI: 10.1039/C7TA03322B).
- [5] Patil, Y., Misra, R., L. Keshtov, M., D. Sharma, G. (2017). Small Molecule Carbazole-Based Diketopyrrolopyrroles with Tetracyanobutadiene Acceptor Unit as a Non-Fullerene Acceptor for Bulk Heterojunction Organic Solar Cells. *J. Mater. Chem. A*, 5(7), 3311–3319. (DOI: 10.1039/C6TA09607G).
- [6] Patil, Y., Misra, R., Keshtov, M. L., Sharma, G. D. (2016). 1,1,4,4-Tetracyanobuta-1,3-Diene Substituted Diketopyrrolopyrroles: An Acceptor for Solution Processable Organic Bulk Heterojunction Solar Cells. *J. Phys. Chem. C*, 120(12), 6324–6335. (DOI: 10.1021/acs.jpcc.5b12307).
- [7] Shimizu, S. (2019). Aza-BODIPY Synthesis towards Vis/NIR Functional Chromophores Based on a Schiff Base Forming Reaction Protocol Using Lactams and Heteroaromatic Amines. *Chem. Commun.*, 55(60), 8722–8743. (DOI: 10.1039/C9CC03365C).

- [8] Loudet, A., Burgess, K. (2007). BODIPY Dyes and Their Derivatives: Syntheses and Spectroscopic Properties. *Chem. Rev.*, 107(11), 4891–4932. (DOI: 10.1021/cr078381n).
- [9] Lu, H., Mack, J., Yang, Y., Shen, Z. (2014). Structural Modification Strategies for the Rational Design of Red/NIR Region BODIPYs. *Chem. Soc. Rev.*, 43(13), 4778–4823. (DOI: 10.1039/C4CS00030G).
- [10] Klifout, H., Stewart, A., Elkhalfa, M., He, H. (2017). BODIPYs for Dye-Sensitized Solar Cells. *ACS Appl. Mater. Interfaces*, 9(46), 39873–39889. (DOI: 10.1021/acsami.7b07688).
- [11] Chen, J. J., Conron, S. M., Erwin, P., Dimitriou, M., McAlahney, K., Thompson, M. E. (2015). High-Efficiency BODIPY-Based Organic Photovoltaics. *ACS Appl. Mater. Interfaces*, 7(1), 662–669. (DOI: 10.1021/am506874k).
- [12] Ulrich, G., Ziessel, R., Harriman, A. (2008). The Chemistry of Fluorescent Bodipy Dyes: Versatility Unsurpassed. *Angew. Chem. Int. Ed.*, 47(7), 1184–1201. (DOI: 10.1002/anie.200702070).
- [13] Boens, N., Verbelen, B., Ortiz, M. J., Jiao, L., Dehaen, W. (2019). Synthesis of BODIPY Dyes through Postfunctionalization of the Boron Dipyrrromethene Core. *Coord. Chem. Rev.*, 399, 213024. (DOI: 10.1016/j.ccr.2019.213024).
- [14] Bessette, A., S. Hanan, G. (2014). Design, Synthesis and Photophysical Studies of Dipyrrromethene-Based Materials: Insights into Their Applications in Organic Photovoltaic Devices. *Chem. Soc. Rev.*, 43(10), 3342–3405. (DOI: 10.1039/C3CS60411J).
- [15] Kyeong, M., Lee, J., Lee, K., Hong, S. (2018). BODIPY-Based Conjugated Polymers for Use as Dopant-Free Hole Transporting Materials for Durable Perovskite Solar Cells: Selective Tuning of

HOMO/LUMO Levels. *ACS Appl. Mater. Interfaces*, 10(27), 23254–23262. (DOI: 10.1021/acsami.8b05956).

- [16] Srinivasa Rao, R., Yadagiri, B., D. Sharma, G., Prakash Singh, S. (2019). Butterfly Architecture of NIR Aza-BODIPY Small Molecules Decorated with Phenothiazine or Phenoxazine. *Chem. Commun.*, 55(83), 12535–12538. (DOI: 10.1039/C9CC06300E).
- [17] Boens, N., Leen, V., Dehaen, W. (2012). Fluorescent Indicators Based on BODIPY. *Chem. Soc. Rev.*, 41(3), 1130–1172. (DOI: 10.1039/C1CS15132K).
- [18] Zatsikha, Y. V., Didukh, N. O., Swedin, R. K., Yakubovskiy, V. P., Blesener, T. S., Healy, A. T., Herbert, D. E., Blank, D. A., Nemykin, V. N., Kovtun, Y. P. (2019). Preparation of Viscosity-Sensitive Isoxazoline/Isoxazolyl-Based Molecular Rotors and Directly Linked BODIPY–Fullerisoxazoline from the Stable Meso-(Nitrile Oxide)-Substituted BODIPY. *Org. Lett.*, 21(14), 5713–5718. (DOI: 10.1021/acs.orglett.9b02082).
- [19] Zhao, J., Xu, K., Yang, W., Wang, Z., Zhong, F. (2015). The Triplet Excited State of Bodipy: Formation, Modulation and Application. *Chem. Soc. Rev.*, 44(24), 8904–8939. (DOI: 10.1039/C5CS00364D).
- [20] Turksoy, A., Yildiz, D., Akkaya, E. U. (2019). Photosensitization and Controlled Photosensitization with BODIPY Dyes. *Coord. Chem. Rev.*, 379, 47–64. (DOI: 10.1016/j.ccr.2017.09.029).
- [21] Ramos-Torres, Á., Avellanal-Zaballa, E., Prieto-Castañeda, A., García-Garrido, F., Bañuelos, J., Agarrabeitia, A. R., Ortiz, M. J. (2019). FormylBODIPYs by PCC-Promoted Selective Oxidation of α -MethylBODIPYs. Synthetic Versatility and Applications. *Org. Lett.*, 21(12), 4563–4566. (DOI: 10.1021/acs.orglett.9b01465).

- [22] Kowada, T., Maeda, H., Kikuchi, K. (2015). BODIPY-Based Probes for the Fluorescence Imaging of Biomolecules in Living Cells. *Chem. Soc. Rev.*, 44(14), 4953–4972. (DOI: 10.1039/C5CS00030K).
- [23] Patalag, L. J., Ulrichs, J. A., Jones, P. G., Werz, D. B. (2017). Decorated BODIPY Fluorophores and Thiol-Reactive Fluorescence Probes by an Aldol Addition. *Org. Lett.*, 19(8), 2090–2093. (DOI: 10.1021/acs.orglett.7b00693).
- [24] Wu, D., C. Daly, H., Grossi, M., Conroy, E., Li, B., M. Gallagher, W., Elmes, R., F. O'Shea, D. (2019). RGD Conjugated Cell Uptake off to on Responsive NIR-AZA Fluorophores: Applications toward Intraoperative Fluorescence Guided Surgery. *Chem. Sci.*, 10(29), 6944–6956. (DOI: 10.1039/C9SC02197C).
- [25] Kolemen, S., Akkaya, E. U. (2018). Reaction-Based BODIPY Probes for Selective Bio-Imaging. *Coord. Chem. Rev.*, 354, 121–134. (DOI: 10.1016/j.ccr.2017.06.021).
- [26] Killoran, J., Allen, L., F. Gallagher, J., M. Gallagher, W., F. O'Shea, D. (2002). Synthesis of BF₂ Chelates of Tetraarylazadipyrromethenes and Evidence for Their Photodynamic Therapeutic Behaviour. *Chem. Commun.*, 0(17), 1862–1863. (DOI: 10.1039/B204317C).
- [27] Ge, Y., F. O'Shea, D. (2016). Azadipyrromethenes: From Traditional Dye Chemistry to Leading Edge Applications. *Chem. Soc. Rev.*, 45(14), 3846–3864. (DOI: 10.1039/C6CS00200E).
- [28] Kamkaew, A., Hui Lim, S., Boon Lee, H., Voon Kiew, L., Yong Chung, L., Burgess, K. (2013). BODIPY Dyes in Photodynamic Therapy. *Chem. Soc. Rev.*, 42(1), 77–88. (DOI: 10.1039/C2CS35216H).

- [29] Stefko, M., Tzirakis, M. D., Breiten, B., Ebert, M.-O., Dumele, O., Schweizer, W. B., Gisselbrecht, J.-P., Boudon, C., Beels, M. T., Biaggio, I., Diederich, F. (2013). Donor–Acceptor (D–A)-Substituted Polyyne Chromophores: Modulation of Their Optoelectronic Properties by Varying the Length of the Acetylene Spacer. *Eur. J. Chem.*, 19(38), 12693–12704. (DOI: 10.1002/chem.201301642).
- [30] Kivala, M., Boudon, C., Gisselbrecht, J.-P., Seiler, P., Gross, M., Diederich, F. (2007). A Novel Reaction of 7,7,8,8-Tetracyanoquinodimethane (TCNQ): Charge-Transfer Chromophores by [2 + 2] Cycloaddition with Alkynes. *Chem. Commun.*, 0(45), 4731–4733. (DOI: 10.1039/B713683H).
- [31] Michinobu, T., C. May, J., H. Lim, J., Boudon, C., Gisselbrecht, J.-P., Seiler, P., Gross, M., Biaggio, I., Diederich, F. (2005). A New Class of Organic Donor–Acceptor Molecules with Large Third-Order Optical Nonlinearities. *Chem. Commun.*, 0(6), 737–739. (DOI: 10.1039/B417393G).
- [32] Kivala, M., Diederich, F. (2009). Acetylene-Derived Strong Organic Acceptors for Planar and Nonplanar Push–Pull Chromophores. *Acc. Chem. Res.*, 42(2), 235–248. (DOI: 10.1021/ar8001238).
- [33] Michinobu, T., Boudon, C., Gisselbrecht, J.-P., Seiler, P., Frank, B., Moonen, N. N. P., Gross, M., Diederich, F. (2006). Donor-Substituted 1,1,4,4-Tetracyanobutadienes (TCBDs): New Chromophores with Efficient Intramolecular Charge-Transfer Interactions by Atom-Economic Synthesis. *Eur. J. Chem.*, 12(7), 1889–1905. (DOI: 10.1002/chem.200501113).
- [34] Liu, S., Shi, Z., Xu, W., Yang, H., Xi, N., Liu, X., Zhao, Q., Huang, W. (2014). A Class of Wavelength-Tunable near-Infrared Aza-BODIPY Dyes and Their Application for Sensing Mercury

- Ion. *Dyes and Pigments*, 103, 145–153. (DOI: 10.1016/j.dyepig.2013.12.004).
- [35] Gut, A., Lapok, L., Jamróz, D., Gorski, A., Solarski, J., Nowakowska, M. (2017). Photophysics and Redox Properties of Aza-BODIPY Dyes with Electron-Withdrawing Groups. *New J. Chem.*, 41(20), 12110–12122. (DOI: 10.1039/C7NJ02757E).

Chapter 6

Near-infrared Absorbing Different Donor Functionalized β -Aza-BODIPY Derivatives

6.1. Introduction

Near-infrared (NIR) absorbing dyes are extensively used in bioimaging and environmental applications due to their ability to use NIR light, which offers excellent optical transparency, low auto-fluorescence, minimal damage, and deep penetration into samples.^[1–8] NIR-absorbing organic chromophores are becoming more widely used in a variety of applications, such as organic photovoltaics, organic light-emitting diodes, telecommunications, and photothermal therapy.^[9–19]

Aza-Boron-dipyrromethene (aza-BODIPY) dyes are BODIPY derivatives that feature a nitrogen atom replacing the *meso*-carbon atom, which connects the two pyrrole rings.^[20–22] Aza-BODIPY dyes possess favorable spectroscopic properties, including high molar absorption coefficients, intense NIR region absorption and excellent photostability.^[23–26] Aza-BODIPYs have been used for various applications, such as solar cells, photosensitizers, chemosensors and bioimaging.^[27,28] Our group is involved in the design and synthesis of donor–acceptor (D–A) architectures with NIR absorption for solution processed bulk heterojunction organic solar cells (BHJ-OSCs).^[29–32]

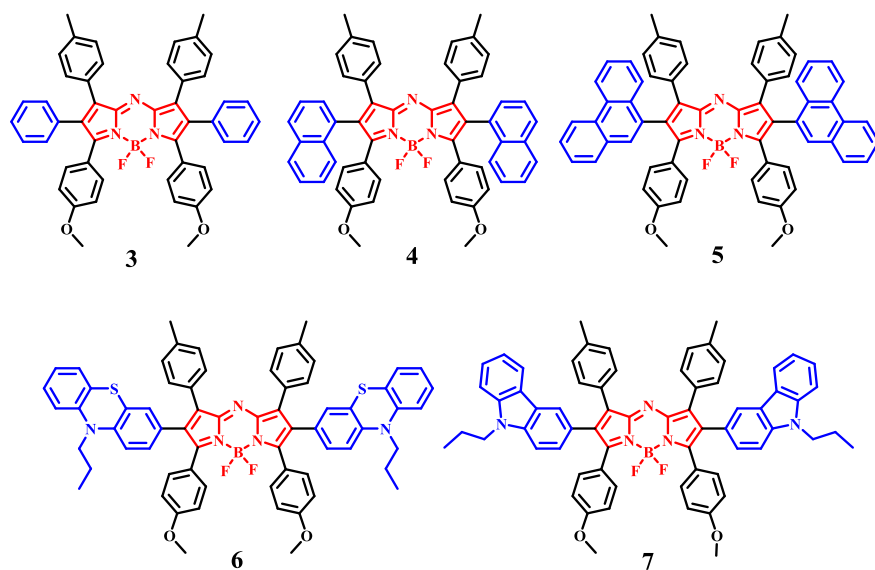


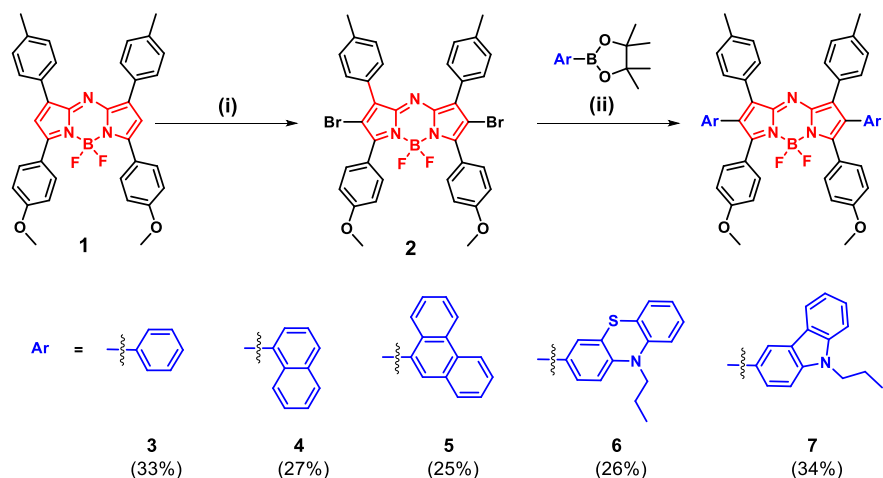
Figure 6.1. Chemical structures of synthesized aza-BODIPY dyes **3–7**.

Herein, we report the design and synthesis of a series of novel aza-BODIPY dyes **3–7**, which are functionalized with various donor groups including phenyl, naphthalene, phenanthrene, phenothiazine, and carbazole. These donor groups were chosen to tune the photophysical, electrochemical, and computational studies of the dyes. To explore the geometry and electronic structures of the synthesized aza-BODIPY dyes **3–7**, calculations using density functional theory (DFT) were conducted. The main aim of this research was to investigate how various donor groups affect the photophysical, electrochemical, and computational studies of aza-BODIPY cores in NIR-absorbing molecules.

6.2. Results and Discussion

The synthesis of 2,6-diarylated aza-BODIPY dyes **3–7** is shown in Scheme 6.1. The aza-BODIPYs **3–7** were synthesized *via* the Suzuki cross-coupling reaction of 2,6-dibromo aza-BODIPY **2** with respective aryl boronate esters (phenyl, naphthalene, phenanthrene, phenothiazine, and carbazole) in a mixture of tetrahydrofuran, toluene, and water (1:1:1) [Scheme 6.1]. The reaction flask was degassed with argon gas for 15 minutes before adding $\text{Pd(PPh}_3)_4$ as a catalyst and

Na_2CO_3 as the base, and then reaction mixture was heated overnight at 80 °C.



Scheme 6.1. Synthesis of aza-BODIPY derivatives **3–7**. Reagents and conditions: (i) Br_2 , Benzene, RT, 2 hrs; (ii) Na_2CO_3 , $\text{Pd}(\text{PPh}_3)_4$, toluene/THF/water, 80 °C, 24 hrs.

The precursors for BF_2 -chelated aza-BODIPY **1** and 2,6-dibromo aza-BODIPY **2** were synthesized using a reported procedure^[33,34] by reacting 4-methylbenzaldehyde with 4-methoxyacetophenone followed by complexation with $\text{BF}_3 \cdot \text{OEt}_2$ and bromination with bromine. The 2,6-diarylated aza-BODIPY dyes **3–7** were purified with the help of silica gel column chromatography, using hexane:dichloromethane solvents. The aza-BODIPY dyes **3–7** are readily soluble in common organic solvents, including dichloromethane, chloroform, acetonitrile, and tetrahydrofuran. The aza-BODIPY dyes **3–7** were characterized using ^1H NMR, ^{13}C NMR, and HRMS techniques. The aza-BODIPY derivatives **3–5** were prepared according to the method previously reported in our group's MSc thesis.^[35]

6.3. Photophysical Properties

The electronic absorption spectra (Figure 6.2.) of 2,6-diarylated aza-BODIPY dyes **3–7** were recorded in dichloromethane, and the resulting data are listed in Table 6.1.

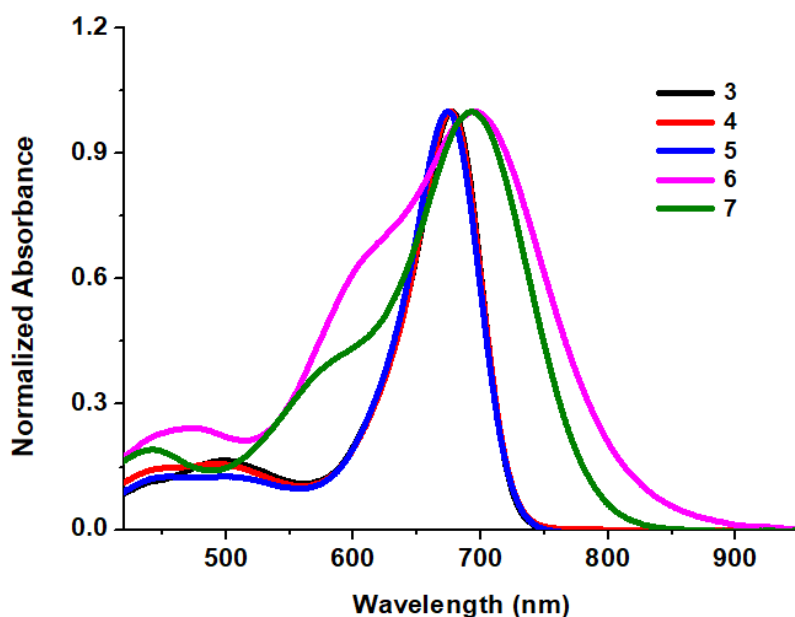


Figure 6.2. Normalized electronic absorption spectra of aza-BODIPY dyes **3–7** in dichloromethane ($1 \times 10^{-5} \text{M}$).

The absorption spectra of aza-BODIPY dyes **3–7** exhibit two intense bands. The lower absorption band (between 400–600 nm) corresponds to the $\pi \rightarrow \pi^*$ transitions of aza-BODIPY moiety, whereas the higher absorption band (between 674–695 nm) is related to the intramolecular charge transfer from various donors to aza-BODIPY acceptor.^[36] In dichloromethane, the absorption maxima were observed at 677 nm, 676 nm, 674 nm, 695 nm, and 692 nm for aza-BODIPY dyes **3–7**, respectively. These dyes showed molar extinction coefficients of $62,382 \text{ M}^{-1}\text{cm}^{-1}$ for **3**, $75,623 \text{ M}^{-1}\text{cm}^{-1}$ for **4**, $51,192 \text{ M}^{-1}\text{cm}^{-1}$ for **5**, $37,263 \text{ M}^{-1}\text{cm}^{-1}$ for **6**, and $56,112 \text{ M}^{-1}\text{cm}^{-1}$ for **7** (Table 6.1.).

Table 6.1. The photophysical and computational properties of aza-BODIPY dyes **3–7**.

Dyes	λ_{abs} (nm) ^a	ϵ (M ⁻¹ .cm ⁻¹) ^a	E_g^b (eV)
3	677	62,382	2.13
	498		
4	676	75,623	2.16
	497		
5	674	51,192	2.15
	502		
6	695	37,263	1.99
	473		
7	692	56,112	2.07
	442		

^aAbsorbance measured in dichloromethane at a concentration of 1×10^{-5} M, ϵ ; molar extinction coefficient, ^bTheoretical values of the HOMO-LUMO gap calculated from the DFT calculation.

Aza-BODIPY dyes **6** and **7** exhibit a red-shifted absorption compared to aza-BODIPY dyes **3**, **4**, and **5**, due to the presence of a strong donor unit. In particular phenothiazine substituted aza-BODIPY **6** shows a red-shifted absorption compared to the carbazole-substituted aza-BODIPY dye **7**. The strong electron-donating nature of the phenothiazine and carbazole units in aza-BODIPYs **6** and **7** causes a red-shift in the absorption compared to aza-BODIPY dyes **3–5**.

6.4. Electrochemical properties

The oxidation and reduction potentials of the 2,6-diarylated aza-BODIPY dyes **3–7** were determined using cyclic voltammetry, 0.1 M solution of tetrabutylammonium hexafluorophosphate (Bu₄NPF₆) in dichloromethane was used as a supporting electrolyte, with glassy carbon as a working electrode, Pt wire as a counter electrode, and an

Ag/AgCl reference electrode. Figure 6.3. shows the cyclic voltammograms of the aza-BODIPY dyes **3–7**.

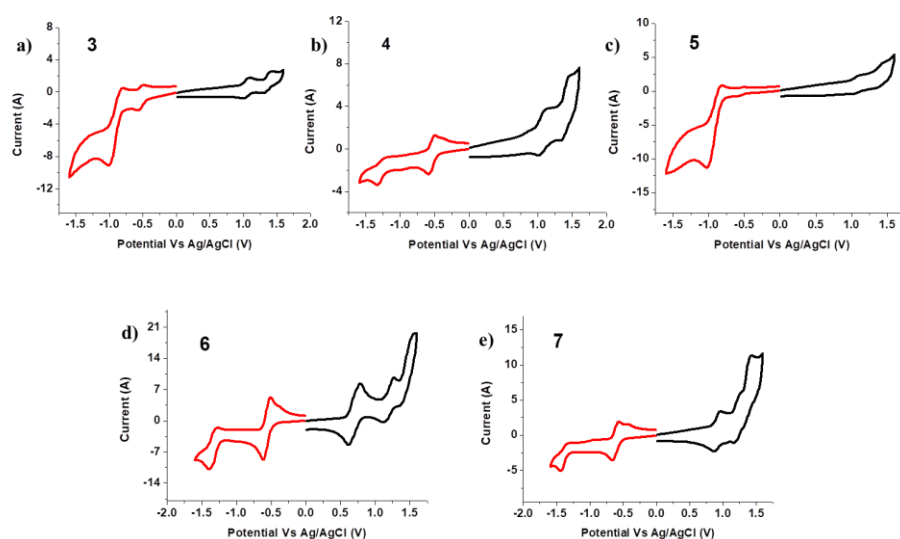


Figure 6.3. Cyclic voltammogram plots of: (a) aza-BODIPY **3**, (b) aza-BODIPY **4**, (c) aza-BODIPY **5**, (d) aza-BODIPY **6**, and (e) aza-BODIPY **7**.

In aza-BODIPY dyes **3–7**, two oxidation and two reduction potentials were observed due to the aza-BODIPY moiety. The first and second oxidation potentials were observed at +0.97 V, 1.34 V for aza-BODIPY **3**; at +0.99 V, 1.36 V for **4**; at +0.99 V, 1.37 V for **5**; at +1.19 V, 1.46 V for **6**, and at +0.91 V, 1.23 V for **7**, corresponding to aza-BODIPY unit. The oxidation potentials of aza-BODIPY dyes **3–5** and **7** were anodically shifted compared to aza-BODIPY dye **6**, which made them difficult to oxidize. An additional oxidation potential was observed at +0.68 V for aza-BODIPY dye **6** due to phenothiazine unit.

Table 6.2. Electrochemical data of aza-BODIPY dyes **3–7**.

Dyes	E^1 (V)	E^2 (V)	E^3 (V)	E^1 (V)	E^2 (V)
	Oxid ^a	Oxid ^a	Oxid ^a	Red ^a	Red ^a
3	0.97	1.34	-	-0.48	-0.93
4	0.99	1.36	-	-0.47	-1.21
5	0.99	1.37	-	-0.50	-0.91
6	0.68	1.19	1.46	-0.51	-1.29
7	0.91	1.23	-	-0.66	-1.32

^aThe electrochemical analysis was carried out using a 0.1 M solution of Bu₄NPF₆ in dichloromethane at a scan rate of 100 mVs⁻¹ versus Ag/AgCl at 25 °C.

The first reduction potentials of aza-BODIPY dyes **3–7** were found to be -0.48 V, -0.47 V, -0.50 V, -0.51 V, and -0.66 V respectively, due to aza-BODIPY unit. In comparison to aza-BODIPY dye **7**, the first and second reduction potentials of aza-BODIPY dyes **3–6** showed an anodic shift, making them easier to reduce. For aza-BODIPY dyes **3–7**, the second reduction potential was observed at -0.93 V, -1.21 V, -0.91 V, -1.29 V, and -1.32 V respectively, due to aza-BODIPY unit.

6.5. Theoretical Calculations

The ground state electronic structures and geometries of the 2,6-diarylated aza-BODIPY dyes **3–7** were studied using DFT calculations at the B3LYP/6-31G(d, p) level. The distributions of the frontier molecular orbitals (FMOs) of aza-BODIPY dyes **3–7** are shown in Figure 6.4.

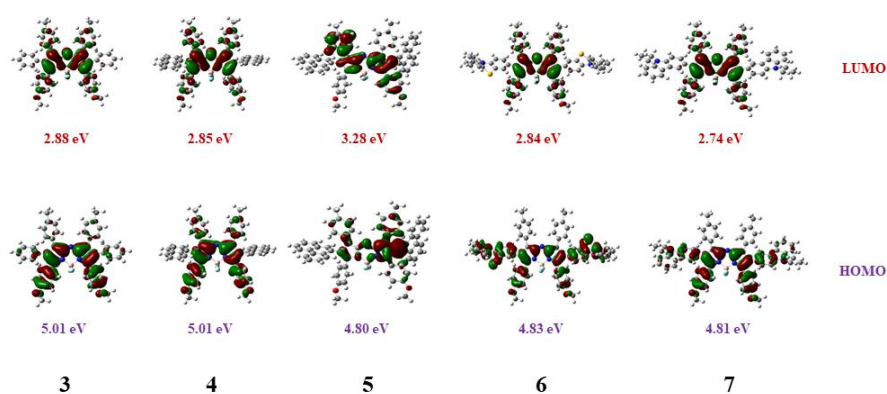


Figure 6.4. The FMOs of aza-BODIPY dyes **3–7** at the B3LYP/6-31G(d, p) level.

The optimized structures of aza-BODIPY dyes **3–7** have distorted geometry. The theoretically calculated highest occupied molecular orbitals (HOMOs) and lowest unoccupied molecular orbitals (LUMOs) are shown in Figure 6.4. The HOMOs are mainly located on the acceptor (aza-BODIPY) unit and are also weakly localized on the donor moiety, whereas the LUMOs are mainly localized on the acceptor (aza-BODIPY) moiety. According to the computational calculations of aza-BODIPYs **3–7**, the HOMO energy levels are -5.01 eV, -5.01 eV, -5.02 eV, -4.83 eV, -4.81 eV and the corresponding LUMO energy levels are -2.88 eV, -2.85 eV, -2.87 eV, -2.84 eV, and -2.74 eV respectively.

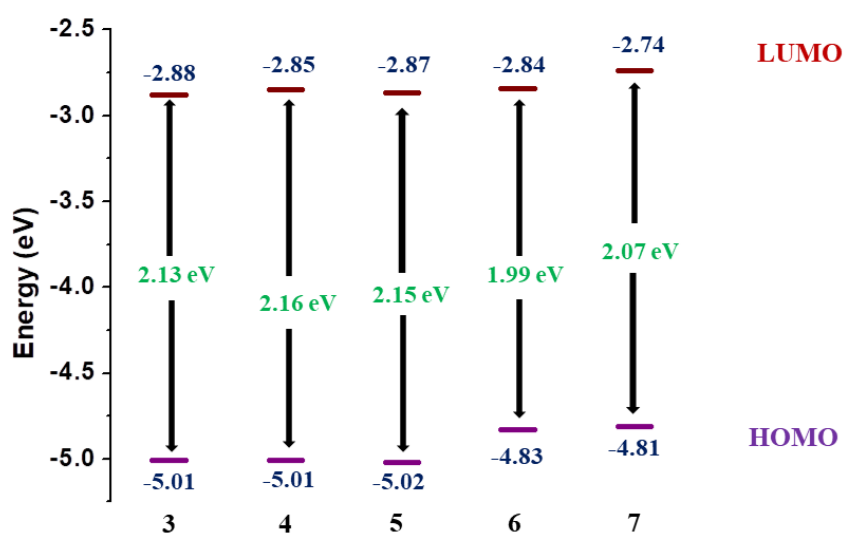


Figure 6.5. Energy level diagram and FMOs of aza-BODIPY dyes **3–7** as estimated by DFT calculations.

Figure 6.5. shows the energy level diagram containing the HOMO-LUMO gap of the orbitals for aza-BODIPY dyes **3–7**. The theoretical HOMO-LUMO gap values for these dyes are 2.13, 2.16, 2.15, 1.99, and 2.07 eV, respectively. The HOMO-LUMO gap in aza-BODIPY dyes **3–7** follows the order aza-BODIPY **4** > aza-BODIPY **5** > aza-BODIPY **3** > aza-BODIPY **7** > aza-BODIPY **6**.

6.6. Experimental section

General methods

The chemicals were used as received, unless otherwise indicated. All moisture-sensitive reactions were performed under an argon atmosphere using the standard Schlenk method. ^1H NMR (500 MHz) and ^{13}C NMR (100 MHz/125 MHz) spectra were recorded using CDCl_3 as the solvent. The ^1H NMR chemical shifts are reported in parts per million (ppm) relative to the solvent residual peak (CDCl_3 , 7.26 ppm). The multiplicities are given as s (singlet), d (doublet), and m (multiplet), and the coupling constants, J , are given in Hz. The ^{13}C NMR chemical shifts are reported relative to the solvent residual peak (CDCl_3 , 77.0 ppm). HRMS was recorded on a mass spectrometer (ESI-TOF). The UV-visible absorption spectra were recorded on a UV-visible spectrophotometer in dichloromethane. Cyclic voltammograms (CVs) were recorded on an electrochemical analyzer using glassy carbon as the working electrode, Pt wire as the counter electrode, and Ag/AgCl as the reference electrode.

General method for the synthesis of aza-BODIPY dyes **3–7**:

A mixture of 2,6-dibromo aza-BODIPY **2** (0.100 g, 0.14 mmol), phenylboronic ester (0.055 g, 0.28 mmol), and Na_2CO_3 (0.224 g, 1.68 mmol) was taken in a 100 mL round-bottom flask fitted with a reflux condenser and stirred under N_2 for 5 minutes in a 1:1:1 mixture of water/THF/toluene (20 mL). A catalytic amount of $\text{Pd}(\text{PPh}_3)_4$ (0.016 g, 0.014 mmol) was added and the reaction mixture was refluxed at 80 °C 24 hrs. After completion of the reaction, as monitored by TLC

analysis, the reaction mixture was allowed to cool down to room temperature. Water (50 mL) was added and extracted the reaction mixture with dichloromethane. The organic layer was separated and washed with water and brine, dried over anhydrous Na₂SO₄. The solvent was evaporated, and the crude product was purified on a silica gel column chromatography (40:60, dichloromethane/hexane) to afford diarylated aza-BODIPY dyes **3–7**.

Aza-BODIPY 3:

Yield: 33%; **¹H NMR** (500 MHz, CDCl₃, δ in ppm): 8.08–7.98 (3H, m), 7.46–7.37 (6H, m), 7.28 (1H, s), 7.23–7.18 (6H, m), 7.11–7.10 (1H, d, $J = 7.9$ Hz), 7.06–7.96 (6H, m), 6.80–6.75 (3H, m), 3.88–3.77 (6H, m), 2.44–2.35 (6H, m). **¹³C NMR** (125 MHz, CDCl₃, δ in ppm): 162.1, 160.7, 160.6, 159.4, 146.2, 143.8, 139.8, 138.4, 138.2, 133.6, 133.5, 132.4, 131.7, 131.0, 131.0, 130.7, 129.5, 129.4, 129.2, 129.1, 129.0, 128.5, 128.3, 128.2, 127.1, 127.0, 124.0, 123.4, 123.1, 118.1, 114.3, 113.2, 55.4, 55.1, 21.5, 21.5; **HRMS** (ESI) m/z : [M+H]⁺ calcd for C₄₈H₃₉BF₂N₃O₂: 738.3106; found 738.3106.

Aza-BODIPY 4:

Yield: 27%; **¹H NMR** (500 MHz, CDCl₃, δ in ppm): 8.08–8.05 (2H, t, $J = 7.5$ Hz), 7.82–7.73 (4H, m), 7.41–7.32 (11H, m), 7.25–7.22 (5H, m), 7.07–6.98 (2H, m), 6.94–6.88 (3H, m), 6.61–6.57 (3H, m) 3.89–3.66 (6H, m), 2.45–2.124 (6H, m). **¹³C NMR** (100 MHz, CDCl₃, δ in ppm): 162.1, 160.6, 160.4, 159.3, 158.8, 150.1, 145.3, 142.4, 139.8, 138.5, 138.3, 133.6, 132.4, 131.7, 130.4, 130.3, 129.6, 129.4, 129.3, 129.1, 128.5, 128.3, 128.3, 128.2, 128.1, 126.3, 126.2, 126.0, 125.8, 125.8, 125.5, 124.0, 123.6, 123.3, 118.2, 115.5, 114.3, 114.0, 113.1, 113.1, 55.4, 55.0, 21.5, 21.4; **HRMS** (ESI) m/z : [M + H]⁺ calcd for C₅₆H₄₃BF₂N₃O₂: 838.3488; found 838.3420.

Aza-BODIPY 5:

Yield: 25%; **¹H NMR** (500 MHz, CDCl₃, δ in ppm): 8.69 (4H, s), 8.09 (2H, s), 7.90–7.88 (2H, m), 7.75–7.42 (18H, m), 7.09–6.99 (2H, m),

6.92–6.87 (3H, m), 6.56–6.54 (3H, m), 3.89–3.61 (6H, m), 2.44–2.21 (6H, m). **¹³C NMR** (100 MHz, CDCl₃, δ in ppm): 160.6, 160.4, 159.0, 145.4, 142.6, 139.8, 138.6, 138.3, 131.6, 131.5, 131.4, 130.6, 130.5, 130.4, 130.4, 130.3, 130.1, 129.6, 129.4, 129.3, 129.2, 128.9, 128.6, 128.4, 126.9, 126.8, 126.7, 126.7, 126.6, 126.6, 126.5, 124.0, 123.3, 123.3, 122.9, 122.5, 114.3, 114.0, 113.2, 113.2, 55.4, 55.0, 22.6, 21.3; **HRMS** (ESI) m/z : [M+H]⁺ calcd for C₆₄H₄₇BF₂N₃O₂: 938.3734; found 938.3763.

Aza-BODIPY 6:

Yield: 26%; **¹H NMR** (500 MHz, CDCl₃, δ in ppm): 7.43-7.39 (8H, t, $J = 8.6$ Hz), 7.15-7.11 (2H, m), 7.08-7.04 (6H, m), 6.90-6.87 (2H, t, $J = 7.3$ Hz), 6.82-6.78 (6H, m), 6.71-6.69 (4H, m), 6.63-6.61 (2H, m), 3.78 (6H, s), 3.75-3.72 (4H, m), 2.36 (6H, s), 1.83-1.79 (4H, m), 1.01-0.98 (6H, m). **¹³C NMR** (125 MHz, CDCl₃, δ in ppm): 160.8, 158.1, 145.2, 144.8, 144.1, 140.3, 138.3, 132.3, 131.7, 130.9, 129.7, 129.0, 128.9, 128.6, 127.4, 127.3, 127.2, 124.3, 124.1, 123.0, 122.3, 115.2, 114.9, 113.4, 55.2, 49.3, 22.3, 21.5, 20.0, 11.3; **HRMS** (ESI) m/z : [M+H]⁺ calcd for C₆₆H₅₇BF₂N₅O₂S₂: 1064.4020; found 1064.4029.

Aza-BODIPY 7:

Yield: 34%; **¹H NMR** (500 MHz, CDCl₃, δ in ppm): 7.90-7.89 (2H, *d*, $J = 7.6$ Hz), 7.72 (2H, *s*), 7.48 - 7.38 (12H, *m*), 7.24-7.23 (2H, *d*, $J = 8.5$ Hz), 7.18-7.15 (2H, *t*, $J = 7.2$ Hz), 7.09-7.07 (2H, *d*, $J = 8.5$ Hz), 7.00-6.99 (4H, *d*, $J = 8.1$ Hz), 6.71-6.70 (4H, *d*, $J = 8.9$ Hz), 4.25-4.22 (4H, *t*, $J = 7.2$ Hz), 3.72 (6H, *s*), 2.31 (6H, *s*), 1.94 - 1.89 (4H, *m*), 1.02-0.99 (6H, *t*, $J = 7.4$ Hz) **¹³C NMR** (100 MHz, CDCl₃, δ in ppm): 160.5, 158.3, 145.3, 140.7, 140.3, 139.7, 138.0, 133.8, 132.5, 131.0, 129.4, 128.6, 128.5, 125.6, 124.0, 123.5, 122.9, 122.8, 122.5, 120.5, 118.8, 113.2, 108.8, 108.6, 55.1, 44.8, 22.4, 21.4, 11.9; **HRMS** (ESI) m/z : [M+H]⁺ calcd for C₆₆H₅₇BF₂N₅O₂: 1000.4579; found 1000.4651.

6.7. Conclusion

In conclusion, we report the design and synthesis of NIR absorbing 2,6-diarylated BF₂-chelated aza-BODIPY dyes with different donor aromatic substituents. A red shift in the absorption maxima of aza-BODIPY dyes **6** and **7** was observed compared to aza-BODIPY dyes **3–5**, which can be attributed to the presence of π -extended and strong electron-donating groups at the 2,6 positions of the aza-BODIPY core. The electrochemical investigations showed the presence of two oxidation and two reduction potentials. Computational calculations demonstrated a lower HOMO-LUMO gap for phenanthrene, carbazole and phenothiazine functionalized aza-BODIPYs (**5**, **6** and **7**), compared to other aza-BODIPY derivatives (**3** and **4**). These findings provide valuable insights for the design and development of new dyes with improved photophysical properties and potential applications in optoelectronics.

6.8. References

- (1) Cui, J., Sheng, W., Wu, Q., Yu, C., Hao, E., Bobadova-Parvanova, P., ... & Jiao, L. (2017). Synthesis, Structure, and Properties of Near-Infrared [b] Phenanthrene-Fused BF₂ Azadipyrrromethenes. *Chemistry—An Asian Journal*, 12(18), 2486-2493. (DOI: 10.1002/asia.201700876).
- (2) Yuan, L., Lin, W., Zheng, K., He, L., & Huang, W. (2013). Far-red to near infrared analyte-responsive fluorescent probes based on organic fluorophore platforms for fluorescence imaging. *Chemical Society Reviews*, 42(2), 622-661. (DOI: 10.1039/C2CS35313J).
- (3) D Nolting, D., C Gore, J., & Pham, W. (2011). Near-infrared dyes: probe development and applications in optical molecular imaging. *Current organic synthesis*, 8(4), 521-534. (DOI: 10.2174/157017911796117223).
- (4) Jiang, X. D., Guan, J., Zhao, J., Le Guennic, B., Jacquemin, D., Zhang, Z., ... & Xiao, L. (2017). Synthesis, structure and

- photophysical properties of NIR aza-BODIPYs with F/N3/NH₂ groups at 1, 7-positions. *Dyes and Pigments*, 136, 619-626. (DOI: 10.1016/j.dyepig.2016.09.019).
- (5) Khopkar, S., & Shankarling, G. (2019). Synthesis, photophysical properties and applications of NIR absorbing unsymmetrical squaraines: A review. *Dyes and Pigments*, 170, 107645. (DOI: 10.1016/j.dyepig.2019.107645).
 - (6) Zhong, S., Chen, H., Yi, J., Yang, T., Gan, Z., Su, X., ... & Ying, L. (2022). Design, synthesis and properties of a new near-infrared small molecule acceptor for organic photodetector. *Organic Electronics*, 109, 106610. (DOI: 10.1016/j.orgel.2022.106610).
 - (7) Chen, Y., Xue, L., Zhu, Q., Feng, Y., & Wu, M. (2021). Recent advances in second near-infrared region (NIR-II) fluorophores and biomedical applications. *Frontiers in Chemistry*, 9, 750404. (DOI: 10.3389/fchem.2021.750404)
 - (8) Zhu, S., Yung, B. C., Chandra, S., Niu, G., Antaris, A. L., & Chen, X. (2018). Near-infrared-II (NIR-II) bioimaging via off-peak NIR-I fluorescence emission. *Theranostics*, 8(15), 4141. (DOI: 10.7150/thno.27995).
 - (9) Feng, R., Sato, N., Yasuda, T., Furuta, H., & Shimizu, S. (2020). Rational design of pyrrolopyrrole-aza-BODIPY-based acceptor–donor–acceptor triads for organic photovoltaics application. *Chemical Communications*, 56(20), 2975-2978. (DOI: 10.1039/D0CC00398K).
 - (10) Pucelik, B., Sułek, A., & Dąbrowski, J. M. (2020). Bacteriochlorins and their metal complexes as NIR-absorbing photosensitizers: Properties, mechanisms, and applications. *Coordination Chemistry Reviews*, 416, 213340. (DOI: 10.1016/j.ccr.2020.213340).

- (11) Tadle, A. C., El Roz, K. A., Soh, C. H., Sylvinson Muthiah Ravinson, D., Djurovich, P. I., Forrest, S. R., & Thompson, M. E. (2021). Tuning the photophysical and electrochemical properties of aza-boron-dipyridylmethenes for fluorescent blue OLEDs. *Advanced Functional Materials*, 31(27), 2101175. (DOI: 10.1002/adfm.202101175).
- (12) Cheacharoen, R., Rolston, N., Harwood, D., Bush, K. A., Dauskardt, R. H., & McGehee, M. D. (2018). Design and understanding of encapsulated perovskite solar cells to withstand temperature cycling. *Energy & Environmental Science*, 11(1), 144-150. (DOI: 10.1039/C7EE02564E).
- (13) Beć, K. B., Grabska, J., & Huck, C. W. (2021). Principles and applications of miniaturized near-infrared (NIR) spectrometers. *Chemistry—A European Journal*, 27(5), 1514-1532. (DOI: 10.1002/chem.202002838).
- (14) Liu, X., Zhang, J., Li, K., Sun, X., Wu, Z., Ren, A., & Feng, J. (2013). New insights into two-photon absorption properties of functionalized aza-BODIPY dyes at telecommunication wavelengths: a theoretical study. *Physical Chemistry Chemical Physics*, 15(13), 4666-4676. DOI: 10.1039/C3CP44435J).
- (15) Beć, K. B., Grabska, J., & Huck, C. W. (2020). Near-infrared spectroscopy in bio-applications. *Molecules*, 25(12), 2948. (DOI: 10.3390/molecules25122948).
- (16) Shi, Z., Han, X., Hu, W., Bai, H., Peng, B., Ji, L., ... & Huang, W. (2020). Bioapplications of small molecule Aza-BODIPY: from rational structural design to in vivo investigations. *Chemical Society Reviews*, 49(21), 7533-7567. (DOI: 10.1039/D0CS00234H).
- (17) Ma, Z. Y., Pan, X. F., Xu, Z. L., Yu, Z. L., Qin, B., Yin, Y. C., ... & Yu, S. H. (2022). Nanosheet-coated synthetic wood with enhanced flame-retardancy by vacuum-assisted sonocoating

- technique. *Nano Research*, 15(10), 9440-9446. (DOI: 10.1007/s12274-022-4407-2).
- (18) Otero, C. M., Simal, G. B., Scocozza, M. F., Rubert, A., Grillo, C. A., Hannibal, L., ... & Vericat, C. (2022). Optimized biocompatible gold nanotriangles with NIR absorption for photothermal applications. *ACS Applied Nano Materials*, 5(1), 341-350. (DOI: 10.1021/acsanm.1c03148).
- (19) Chen, D., Zhong, Z., Ma, Q., Shao, J., Huang, W., & Dong, X. (2020). Aza-BODIPY-based nanomedicines in cancer phototheranostics. *ACS applied materials & interfaces*, 12(24), 26914-26925. (DOI: 10.1021/acsaami.0c05021).
- (20) Bandi, V., El-Khouly, M. E., Ohkubo, K., Nesterov, V. N., Zandler, M. E., Fukuzumi, S., & D'Souza, F. (2014). Bisdonor–azaBODIPY–fullerene supramolecules: syntheses, characterization, and light-induced electron-transfer studies. *The Journal of Physical Chemistry C*, 118(5), 2321-2332. (DOI: 10.1021/jp4112469).
- (21) Loudet, A., Bandichhor, R., Wu, L., & Burgess, K. (2008). Functionalized BF₂ chelated azadipyrrromethene dyes. *Tetrahedron*, 64(17), 3642-3654. (DOI: 10.1016/j.tet.2008.01.117).
- (22) Zhao, W., & Carreira, E. M. (2006). Conformationally restricted aza-BODIPY: highly fluorescent, stable near-infrared absorbing dyes. *Chemistry–A European Journal*, 12(27), 7254-7263. (DOI: 10.1002/chem.200600527).
- (23) Zhao, J., Wang, H., Zhang, D., Shen, Y., Zhang, S., Ren, J., ... & Wang, G. (2022). Synthesis of aza-BODIPYs with barrier-free rotation of the–t Bu group at 3-site and enhancement of photothermal therapy by triggering cancer cell apoptosis. *Journal of Materials Chemistry B*, 10(41), 8443-8449. (DOI: 10.1039/D2TB01513G).

- (24) Chen, X., Yu, B., Wang, J., Luo, Z., Meng, H., Xie, B., ... & Zhao, Q. (2023). A near-infrared organic photodetector based on an aza-BODIPY dye for a laser microphone system. *Journal of Materials Chemistry C*, 11(6), 2267-2272. (DOI: 10.1039/D2TC04274F).
- (25) Wang, Y., Zhang, D., Xiong, K., Shang, R., & Jiang, X. D. (2022). Near-infrared absorbing (> 700 nm) aza-BODIPYs by freezing the rotation of the aryl groups. *Chinese Chemical Letters*, 33(1), 115-122. (DOI: 10.1016/j.cclet.2021.06.083).
- (26) McDonnell, S. O., & O'Shea, D. F. (2006). Near-infrared sensing properties of dimethylamino-substituted BF₂-azadipyrromethenes. *Organic letters*, 8(16), 3493-3496. (DOI: 10.1021/ol061171x).
- (27) Balsukuri, N., Manav, N., Lone, M. Y., Mori, S., Das, A., Sen, P., & Gupta, I. (2020). Donor-acceptor architectures of tetraphenylethene linked aza-BODIPYs: Synthesis, crystal structure, energy transfer and computational studies. *Dyes and Pigments*, 176, 108249. (DOI: 10.1016/j.dyepig.2020.108249).
- (28) Wang, L., Ding, H., Xiong, Z., Ran, X., Tang, H., & Cao, D. (2022). Design, synthesis and applications of NIR-emissive scaffolds of diketopyrrolopyrrole-aza-BODIPY hybrids. *Chemical Communications*, 58(40), 5996-5999. (DOI: 10.1039/D2CC00774F).
- (29) Sekaran, B., & Misra, R. (2022). β -Pyrrole functionalized porphyrins: Synthesis, electronic properties, and applications in sensing and DSSC. *Coordination Chemistry Reviews*, 453, 214312. (DOI: 10.1016/j.ccr.2021.214312).
- (30) Misra, R., Maragani, R., Arora, D., Sharma, A., & Sharma, G. D. (2016). Positional isomers of pyridine linked triphenylamine-based donor-acceptor organic dyes for efficient dye-sensitized

solar cells. *Dyes and Pigments*, 126, 38-45. (DOI: 10.1016/j.dyepig.2015.11.008).

- (31) Patil, Y., & Misra, R. (2019). Rational molecular design towards NIR absorption: efficient diketopyrrolopyrrole derivatives for organic solar cells and photothermal therapy. *Journal of Materials Chemistry C*, 7(42), 13020-13031. (DOI: 10.1039/C9TC03640G).
- (32) Patil, Y., & Misra, R. (2018). Diketopyrrolopyrrole-Based and Tetracyano-Bridged Small Molecules for Bulk Heterojunction Organic Solar Cells. *Chemistry–An Asian Journal*, 13(3), 220-229. (DOI: 10.1002/asia.201701493).
- (33) Yılmaz, H., Sevinç, G., & Hayvalı, M. (2021). 3, 3, 5 and 2, 6 Expanded Aza-BODIPYs Via Palladium-Catalyzed Suzuki-Miyaura Cross-Coupling Reactions: Synthesis and Photophysical Properties. *Journal of Fluorescence*, 31(1), 151-164. (DOI: 10.1007/s10895-020-02646-4).
- (34) Adarsh, N., Avirah, R. R., & Ramaiah, D. (2010). Tuning photosensitized singlet oxygen generation efficiency of novel aza-BODIPY dyes. *Organic letters*, 12(24), 5720-5723. (DOI: 10.1021/ol102562k).
- (35) Link: <http://dspace.iiti.ac.in:8080/jspui/handle/123456789/10213>
- (36) Pinjari, D., Alsaleh, A. Z., Patil, Y., Misra, R., & D'Souza, F. (2020). Interfacing High-Energy Charge-Transfer States to a Near-IR Sensitizer for Efficient Electron Transfer upon Near-IR Irradiation. *Angewandte Chemie International Edition*, 59(52), 23697-23705. (DOI: 10.1002/anie.202013036).

Chapter 7

Exploring the effect of electron withdrawing functionalities (formyl, nitrile, and fullerene) on di- and tetra-methoxy substituted β -aza-BODIPYs

7.1. Introduction

Aza-boron-dipyrromethene (aza-BODIPY) is a structural analogue of BODIPY, where the carbon atom at the *meso*-position of the BODIPY is replaced by the nitrogen,^[1–6] which leads to the significant bathochromic shift (~100 nm) in the absorbance.^[7–9] Aza-BODIPY derivatives have been recognized as promising candidates with near-infrared (NIR) absorbing ability used in various applications such as photovoltaics, bioimaging, and photodynamic therapy.^[10–18]

Fullerene (C₆₀) stands out as a widely used electron acceptor in bulk heterojunction organic solar cells and perovskite solar cells due to its high efficiency.^[19–24] Its significant features such as small reorganization energy, good thermal stability, and tunable LUMO energy level are beneficial in various optoelectronic applications.^[25–30] Our research group is involved in the development of π -conjugated chromophores based on BODIPY, aza-BODIPY, diketopyrrolopyrrole, isoindigo, porphyrin for various optoelectronic applications.^[31–36] We have recently reported triphenylamine functionalized aza-BODIPYs by incorporating electron withdrawing tetracyanobutadiene bridge.^[37] The literature reveals that the fullerene has been attached to BODIPY at various positions, including alpha, beta, *meso*, and even at the boron site of the BODIPY.^[8,38–43] However, the fullerene connected to aza-BODIPY is predominantly observed at alpha and boron site.^[44–46]

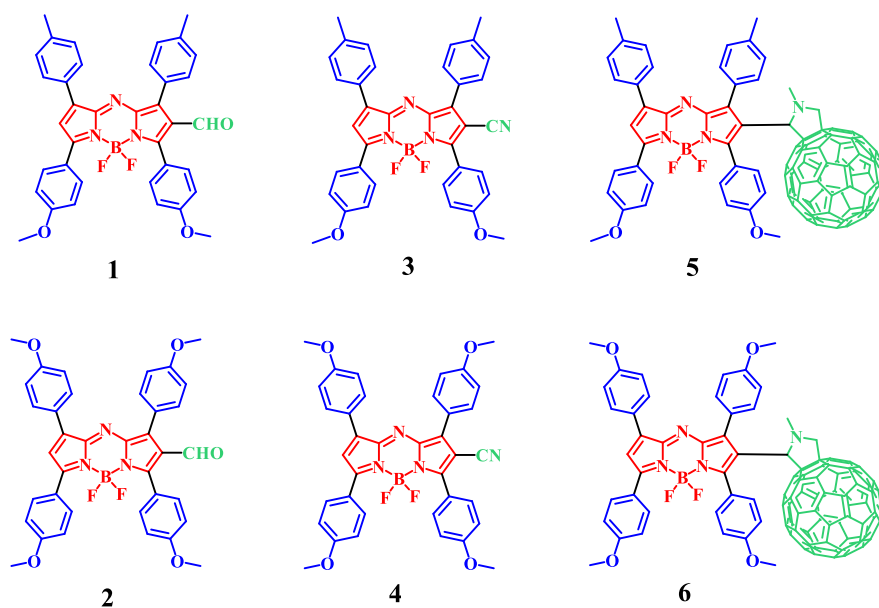


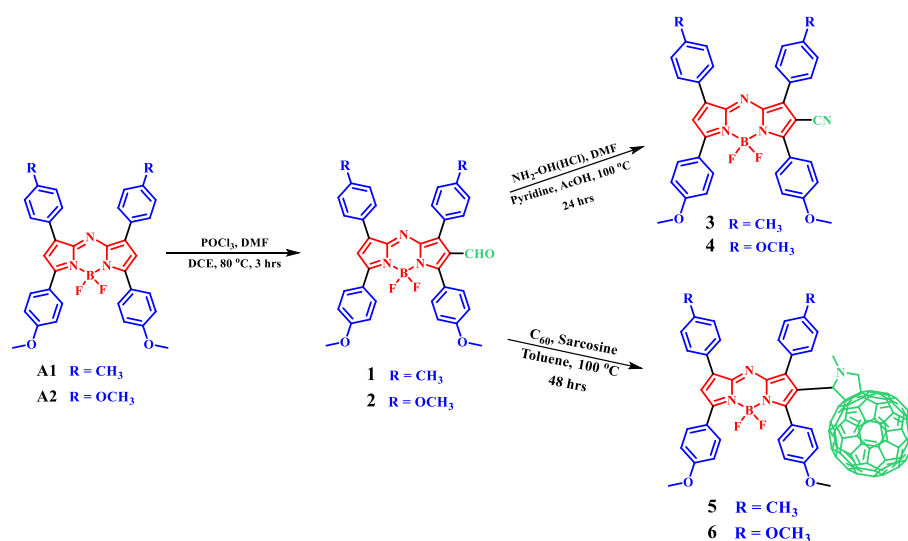
Figure 7.1. Chemical structures of formyl, nitrile, and fullerene functionalized di- and tetra-methoxy substituted aza-BODIPYs **1–6**.

In this article, we describe the design and synthesis of formyl, nitrile, and fullerene substituted di- and tetra-methoxy based aza-BODIPY dyes (**1–6**). The photophysical and electrochemical properties of aza-BODIPY dyes were thoroughly investigated, and their computational studies were carried out. The objective of this work was to study and compare the impact of substitution of electron withdrawing moieties formyl, nitrile, and fullerene on the optical and electrochemical properties of aza-BODIPY dyes **1–6**.

7.2. Results and Discussion

The synthesis of formyl, nitrile and fullerene containing di- and tetra-methoxy substituted aza-BODIPY dyes **1–6** are shown in Scheme 7.1. The synthesis of formyl substituted di-methoxy based aza-BODIPY **1** and tetra-methoxy based aza-BODIPY **2** was carried out using a well-established formylation procedure (Scheme 7.1).^[47,48] The formylation of aza-BODIPY **A1** and **A2** was carried out with POCl₃ in dichloroethane solvent at 80 °C for 3 hours to obtain aza-BODIPYs **1** and **2**. The reaction intermediates di and tetra-methoxy based aza-BODIPYs **A1** and **A2** were synthesized by following literature

procedures.^[49]



Scheme 7.1. Synthesis of formyl, nitrile, and fullerene substituted di- and tetra-methoxy based aza-BODIPY dyes **1–6**.

The nitrile substituted aza-BODIPYs **3** and **4** were synthesized by the reaction of formyl substituted aza-BODIPYs **1** and **2** with a mixture of hydroxylamine hydrochloride, glacial acetic acid, pyridine and dimethylformamide (DMF) solvents at 100 °C for 24 hours. The fullerene based aza-BODIPYs **5** and **6** were synthesized using Prato reaction by reacting formyl substituted aza-BODIPYs **1** and **2** with C₆₀ in the presence of sarcosine in dry toluene. The reaction was carried out at 100 °C for 48 hours and the aza-BODIPY **5** and aza-BODIPY **6** was obtained in 30% and 25% yield respectively. The purification of aza-BODIPY dyes **1–6** was achieved by silica gel column chromatography. The aza-BODIPYs **1–6** were fully characterized by ¹H, ¹³C NMR and HRMS techniques and are soluble in common organic solvents such as dichloromethane, chloroform, acetone, toluene and tetrahydrofuran.

7.3. Photophysical Properties

The electronic absorption spectra of the formyl, nitrile and fullerene substituted di- and tetra-methoxy based aza-BODIPY dyes **1–6** were

recorded in dichloromethane solvent (Figure 7.2.) and the data are listed in Table 7.1.

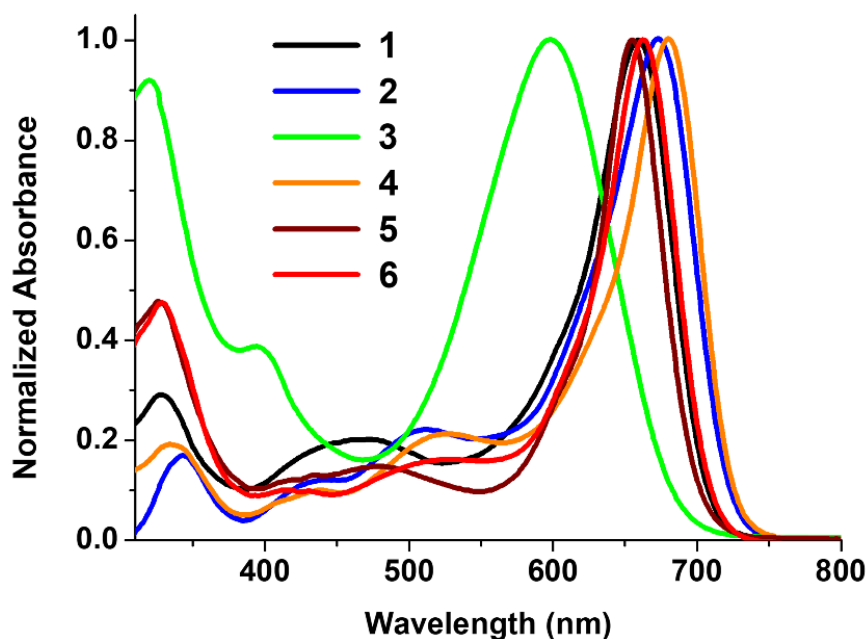


Figure 7.2. Normalized electronic absorption spectra of aza-BODIPYs **1–6** in dichloromethane solvent ($1 \times 10^{-5} \text{M}$).

The di and tetra-methoxy substituted aza-BODIPYs, namely **1–6**, display absorption spectra in the ultraviolet to visible region ranging from 250–750 nm. Aza-BODIPY dyes **1**, **3**, and **5** exhibit absorption maxima at 659 nm, 598 nm, and 655 nm, respectively, whereas their tetra-methoxy aza-BODIPY analogues **2**, **4**, and **6** show absorption maxima at comparatively longer wavelength region at 673 nm, 680 nm, and 663 nm, respectively. This red shift in the tetra-methoxy substituted aza-BODIPYs was related to the presence of additional two electron donating methoxy moieties. The precursor aza-BODIPYs **A1** and **A2** exhibited absorption maxima at 686 nm and 690 nm respectively.^[40] This indicates the substitution of electron withdrawing moieties to **A1** and **A2** leads to the blue shift in the absorption (Table 7.1.). The molar absorption coefficients (ϵ) observed for these aza-BODIPY derivatives are $65,000 \text{ M}^{-1}\text{cm}^{-1}$ for aza-BODIPY **1**, $42,000 \text{ M}^{-1}\text{cm}^{-1}$ for aza-BODIPY **2**, $43,000 \text{ M}^{-1}\text{cm}^{-1}$ for aza-BODIPY **3**,

66,000 M⁻¹cm⁻¹ for aza-BODIPY **4**, 46,000 M⁻¹cm⁻¹ for aza-BODIPY **5**, and 48,000 M⁻¹cm⁻¹ for aza-BODIPY **6**.

Table 7.1. The photophysical and computational properties of aza-BODIPY dyes **1–6**.

Dyes	λ_{abs} (nm) ^a	$\epsilon \times 10^4$ (M ⁻¹ .cm ⁻¹) ^a	λ_{abs} (nm) ^b
1	659	6.5	649
2	673	4.2	663
3	598	4.3	658
4	680	6.6	679
5	655	4.6	646
6	663	4.8	670

^aAbsorbance measured in dichloromethane at a concentration of 1×10^{-5} M, ϵ ; molar extinction coefficient. ^bAbsorbance calculated from TD-DFT calculation.

The blue shift of around 82 nm was observed in case of nitrile substituted di-methoxy substituted aza-BODIPY **3** compared to its tetra-methoxy substituted aza-BODIPY analogue **4**, due to strong electron pulling towards the nitrile group. This behaviour has also been supported by electrochemical and computational investigations i.e. lower first reduction potential and presence of low lying HOMO (-5.25) in di-methoxy based nitrile substituted aza-BODIPY **3** compared to other aza-BODIPY derivatives (Table 7.2. and Figure 7.7.). The intense absorption band in the ultraviolet region 250–400 nm in fullerene substituted aza-BODIPYs **5** and **6** corresponds to the absorption of fullerene. The absorption values calculated from time dependent density theory (TD-DFT) calculation are in good agreement with experimental absorption values (See Table 7.1.).

7.4. Electrochemical properties

The electrochemical properties of the formyl, nitrile and fullerene substituted di- and tetra-methoxy based aza-BODIPYs **1–6** were

studied by cyclic voltammetry (CV). The measurements were performed in dichloromethane solvent using 0.1 M solution of tetrabutylammonium tetrafluoroborate (nBu_4NBF_4) as the supporting electrolyte, Ag/AgCl was used as a reference electrode, glassy carbon was used as a working electrode and Pt wire was used as a counter electrode. The CV plots of aza-BODIPYs **1–6** are shown in Figure 7.3., 7.4. and the corresponding data are listed in Table 7.2.

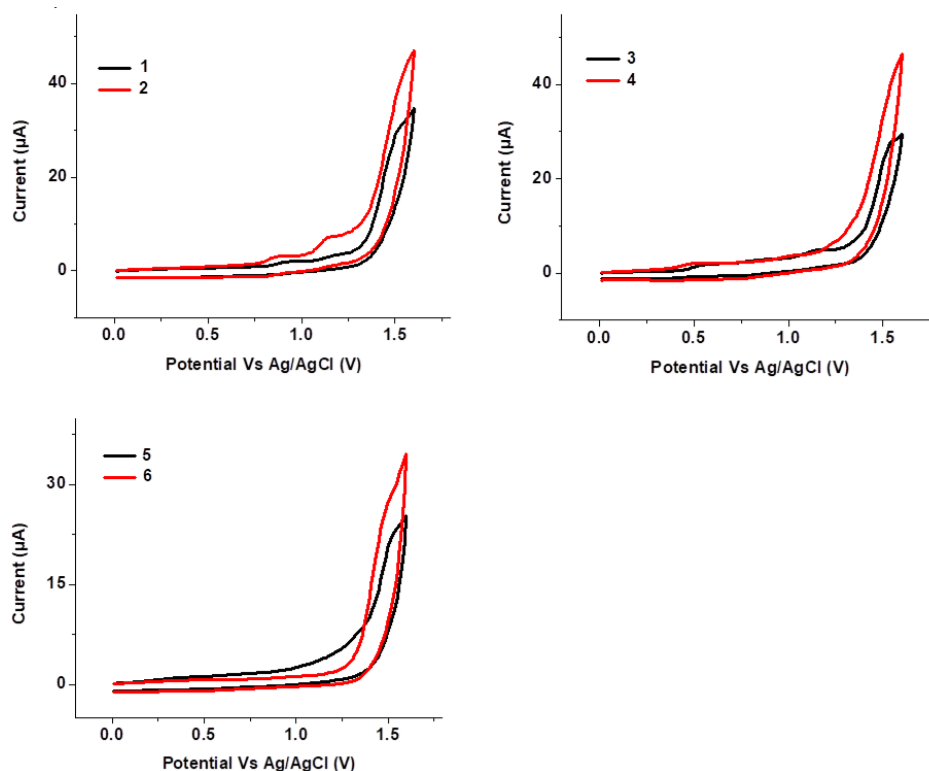


Figure 7.3. CV plots of di- and tetra-methoxy based aza-BODIPYs **1–6**.

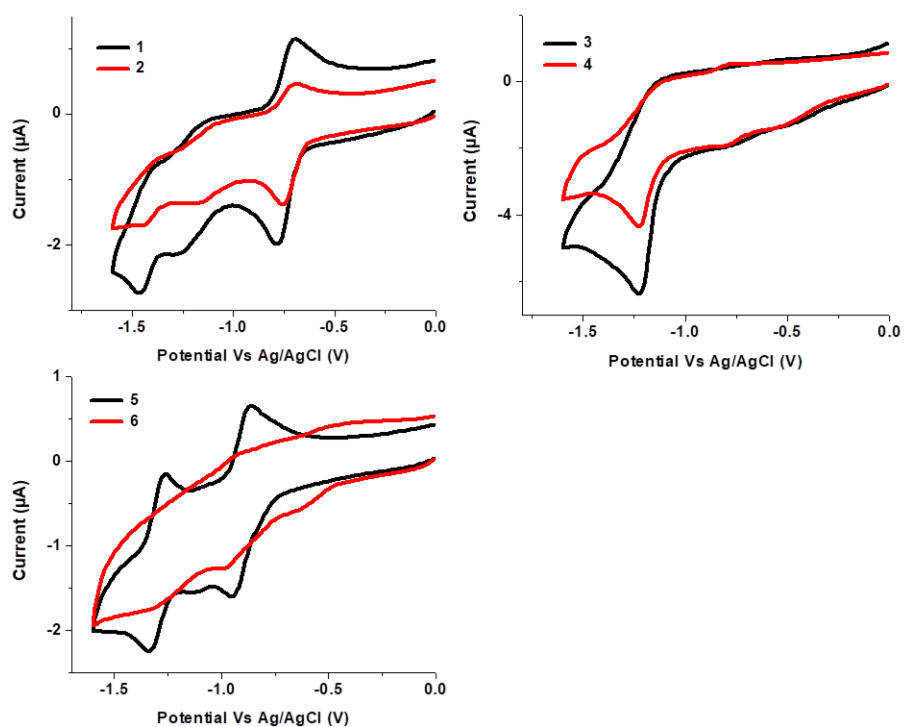


Figure 7.4. CV plots of di- and tetra-methoxy based aza-BODIPYs **1–6**.

The formyl, nitrile, and fullerene substituted di- and tetra-methoxy based aza-BODIPYs **1–6** show two oxidation and three reduction potentials. Aza-BODIPY itself shows two oxidations and two reductions. The additional low voltage reduction potential is related to corresponding electron withdrawing (formyl, nitrile, and fullerene) moiety. Formyl and nitrile based aza-BODIPYs **1–4** exhibited oxidation potentials at 0.90 V, 1.52 V; 0.86 V, 1.51 V; 0.52 V, 1.53 V, and at 0.48 V, 1.52 V respectively. In case of fullerene substituted aza-BODIPYs **5** and **6**, the oxidation potentials were observed at 0.52 V, 1.53 V, and 0.44 V, 1.49 V respectively. The oxidation potentials of tetra-methoxy substituted aza-BODIPYs **2**, **4**, and **6** exhibited cathodic shift compared to di-methoxy analogues **1**, **3**, and **5**, making them easier to oxidize due to the presence of two additional electron donating methoxy groups.

Table 7.2. Electrochemical properties of di- and tetra-methoxy based aza-BODIPYs **1–6**.

Dyes	E^1 Oxid^a	E^2 Oxid^a	E^1 Red^a	E^2 Red^a	E^3 Red^a
1	0.90	1.52	-0.79	-1.26	-1.46
2	0.86	1.51	-0.76	-1.17	-1.44
3	0.52	1.53	-0.47	-0.80	-1.22
4	0.48	1.52	-0.53	-0.81	-1.23
5	0.52	1.53	-0.95	-1.13	-1.34
6	0.44	1.49	-0.63	-0.99	-1.30

^aThe electrochemical analysis was performed in a 0.1 M solution of nBu₄NPF₆ in dichloromethane at 100 mVs⁻¹ scan rate, versus Ag/AgCl at 25 °C.

The substitution of electron withdrawing formyl, nitrile and fullerene to di- and tetra-methoxy based aza-BODIPYs resulted in additional low voltage reduction in each aza-BODIPY. The first reduction potentials in aza-BODIPYs **1–6** are at -0.79 V, -0.76 V, -0.47, -0.53 V, -0.95 V, and -0.63 V, respectively is related to the corresponding substitution of electron withdrawing (formyl, nitrile and fullerene) moiety. The nitrile substituted di-methoxy based aza-BODIPYs **3** displayed an anodic shift in their reduction potentials compared to remaining aza-BODIPY dyes which makes them more easily reducible. This indicates enhanced pulling of electrons from aza-BODIPY core which has also been seen from the blue shift of absorption in aza-BODIPYs **3** compared to other aza-BODIPYs.

The presence of two additional electron donating methoxy groups in tetra-methoxy based formyl and fullerene substituted aza-BODIPYs makes easier oxidation and reduction of aza-BODIPY core. On the other hand, in case of tetra-methoxy based nitrile substituted aza-BODIPY (**4**), despite of having two additional electron donating

methoxy groups, the oxidation and reduction processes are difficult compared to di-methoxy based aza-BODIPY **3**.

7.5. Theoretical properties

The ground state geometries and electronic structure of formyl, nitrile and fullerene containing di- and tetra-methoxy based aza-BODIPYs (**1–6**) were investigated using density functional theory (DFT) in the gas phase. Gaussian 09 program was used to run the theoretical calculations at the B3LYP/6-31G (d, p) level. The frontier molecular orbitals (FMOs) obtained from the DFT calculation for aza-BODIPYs **1–6** is illustrated in Figure 7.5. and 7.6. The highest occupied molecular orbitals (HOMOs) and lowest occupied molecular orbitals (LUMOs) of formyl, and nitrile substituted di- and tetra-methoxy substituted aza-BODIPYs **1–4** are localized on the aza-BODIPY core (Figure 7.5.) indicates $\pi \rightarrow \pi^*$ transition.

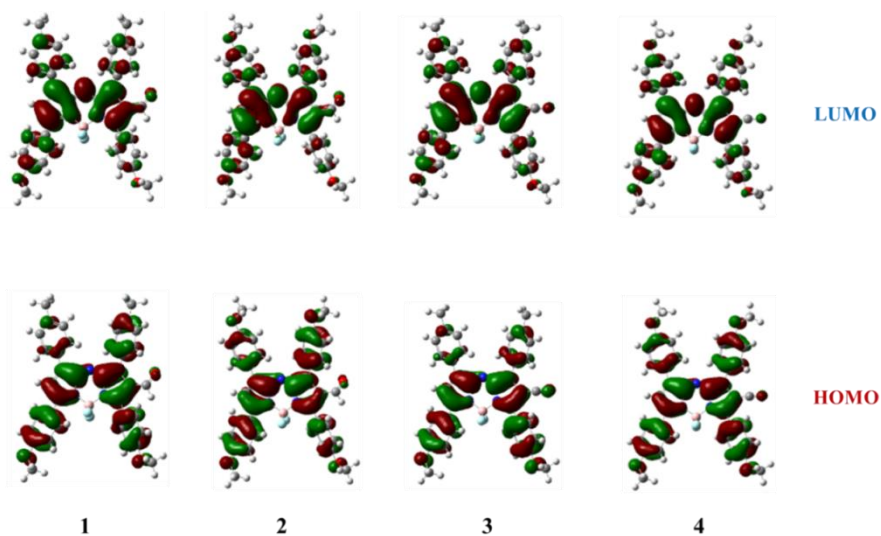


Figure 7.5. Frontier molecular orbitals of di- and tetra-methoxy aza-BODIPYs **1–4**.

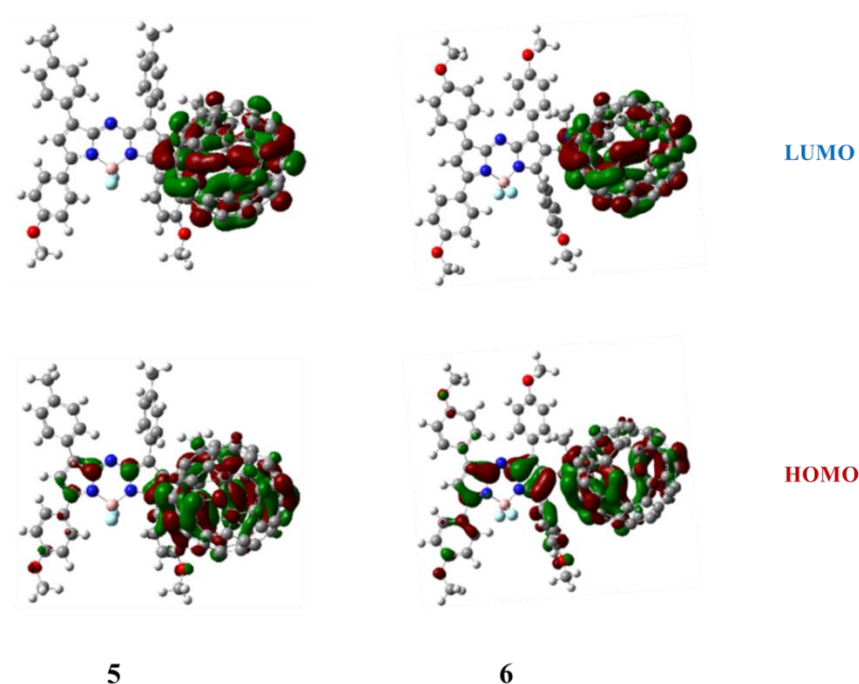


Figure 7.6. Frontier molecular orbitals of fullerene substituted di- and tetra-methoxy aza-BODIPYs **5** and **6**.

On the other hand, in fullerene substituted di- and tetra-methoxy based aza-BODIPYs **5** and **6**, HOMOs are mainly located on fullerene moiety and some part on aza-BODIPY core whereas the LUMOs are completely located on fullerene moiety indicating the strong acceptor nature of the fullerene moiety. The theoretically calculated HOMO levels of aza-BODIPYs **1–6** are at -5.23, -5.09, -5.25, -5.13, -5.08 and -5.07 eV and the corresponding LUMO levels are -3.13, -3.03, -3.19, -3.10, -3.25 and -3.25 eV, respectively. Energy level diagram for aza-BODIPYs **1–6** are depicted in Figure 7.7. and the HOMO-LUMO gap follows the order **1** > **2** = **3** > **4** > **5** > **6**. Notably, the fullerene substituted di- and tetra-methoxy based aza-BODIPY dyes **5** and **6** exhibit a lower HOMO-LUMO energy gap compared to formyl and nitrile substituted aza-BODIPY dyes **1–4**.

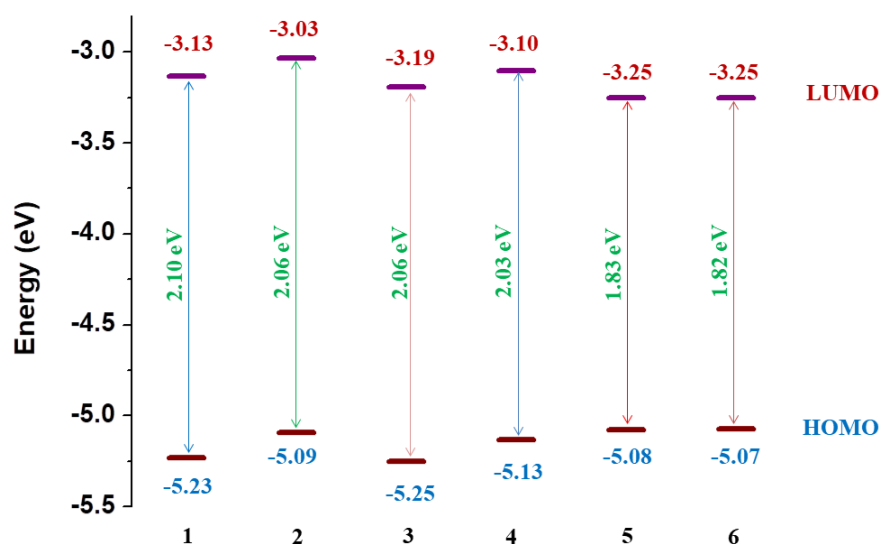


Figure 7.7. The HOMO–LUMO energy level diagram of di- and tetra-methoxy substituted aza-BODIPYs **1–6**.

The TD-DFT calculations were performed on formyl, nitrile and fullerene containing di and tetra-methoxy based aza-BODIPYs (**1–6**) at the B3LYP/6-31G (d, p) level to achieve correlation with the absorption studies. The major electronic transitions in **1–6** obtained from TD-DFT calculation with their composition and oscillator strength are shown in Table 7.3. In the case of formyl substituted aza-BODIPY derivatives **1** and **2**, the major electronic transitions were observed in visible region, which occurs from the HOMO to LUMO at 649 nm and 663 nm respectively. Other lower wavelength transitions HOMO-2→LUMO were also observed at 513 nm and 525 nm respectively. In case of nitrile substituted aza-BODIPY derivatives **3** and **4**, the two major transitions were found in the visible region, one from HOMO to LUMO+1 in 655–680 nm and another from HOMO-2 to LUMO+1 in 500–545 nm. The fullerene substituted aza-BODIPY derivatives **5** and **6** show major transitions in the visible region from HOMO to LUMO+1 in 645–670 region (Figure 7.8.). The transitions from HOMO-1 to LUMO+3 in **5** and from HOMO to LUMO+3 in **6** were also seen in TD-DFT calculations.

Table 7.3. Calculated major electronic transition for aza-BODIPY dyes **1–6** in the gas phase.

Dyes	Wavelength (nm)	Composition	f^a
1	649	HOMO→LUMO (0.70)	0.61
		HOMO-1→LUMO (0.13)	
	513	HOMO-2→LUMO (0.69)	0.34
2	663	HOMO→LUMO (0.55)	0.52
		HOMO→LUMO+1 (0.41)	
	525	HOMO-2→LUMO (0.39)	0.28
		HOMO-1→LUMO (0.31)	
		HOMO-1→LUMO+1 (0.35)	
3	658	HOMO→LUMO+1 (0.70)	0.62
	504	HOMO-2→LUMO+1 (0.50)	0.23
4	679	HOMO→LUMO+1 (0.70)	0.57
	541	HOMO-2→LUMO+1 (0.60)	0.25
5	646	HOMO→LUMO+1 (0.37)	0.51
		HOMO→LUMO+3 (0.31)	
6	670	HOMO→LUMO+1 (0.40)	0.32
		HOMO-1→LUMO+2 (0.36)	
	652	HOMO→LUMO+3 (0.42)	0.34
		HOMO→LUMO+1 (0.34)	

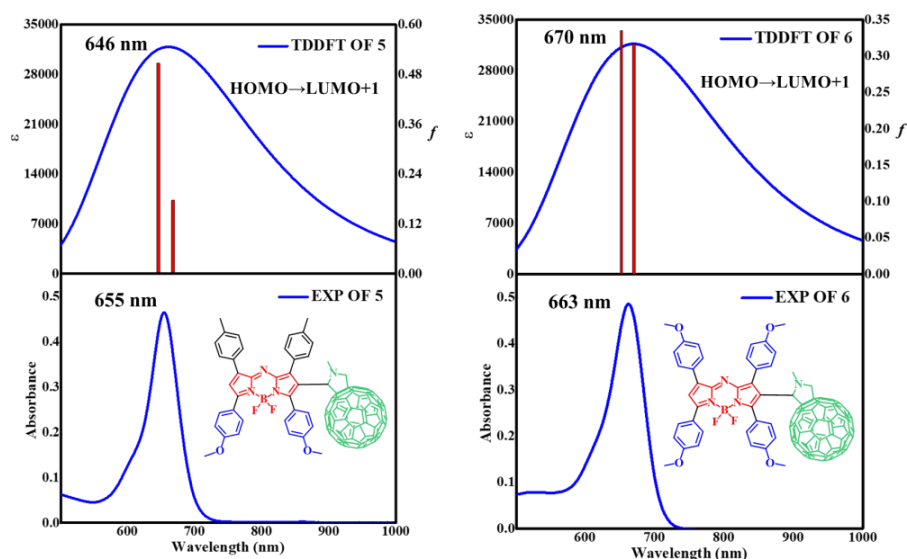


Figure 7.8. Theoretical (top) and experimental (bottom) absorption spectra of fullerene substituted di and tetra-methoxy based azabodipy dyes **5** and **6**.

7.6. Experimental section

General methods

The chemicals were used as received unless otherwise indicated. All the moisture sensitive reactions were performed under argon atmosphere using the standard Schlenk method. ^1H NMR (500 MHz) and ^{13}C NMR (125 MHz) spectra were recorded by using CDCl_3 as the solvent. The ^1H NMR chemical shifts are reported in parts per million (ppm) relative to the solvent residual peak (CDCl_3 , 7.26 ppm). The multiplicities are given as: s (singlet), d (doublet), m (multiplet), and the coupling constants, J , are given in Hz. The ^{13}C NMR chemical shifts are reported with relative to the solvent residual peak (CDCl_3 , 77.0 ppm). HRMS was recorded on a mass spectrometer (ESI-TOF). The UV-visible absorption spectra were recorded on UV-visible Spectrophotometer in DCM. Cyclic voltammograms (CVs) were recorded on an electrochemical analyzer using glassy carbon as working electrode, Pt wire as the counter electrode, and Ag/AgCl as the reference electrode.

Aza-BODIPY 1:

A mixture of DMF (3 mL) and POCl₃ (3 mL) was stirred in an ice bath for 5 min under argon. After being warmed to room temperature, it was stirred for an additional 30 min. To this reaction mixture was added aza-BODIPY **A1** (0.200 g, 0.34 mmol) in dichloroethane (6 mL); the mixture was raised to 70 °C for overnight. The mixture was then cooled to room temperature and slowly poured in to saturated aqueous NaHCO₃ (200 mL) under ice cold conditions. After being warmed to room temperature, the mixture was stirred for 1h. The organic layers were combined, dried over anhydrous Na₂SO₄, and evaporated in vacuum. The crude product was further purified using column chromatography (DCM/hexane) to gives aza-BODIPY **1** with yield 70%. ¹H NMR (500 MHz, CDCl₃, δ in ppm): 9.77 (1H, s), 8.15-8.13 (2H, d, *J*=9 Hz), 8.01-7.99 (2H, d, *J*=8 Hz), 7.77-7.76 (2H, d, *J*=8 Hz), 7.71-7.69 (2H, m, *J*=9 Hz), 7.32-7.31 (2H, m, *J*=8 Hz), 7.24-7.22 (3H, m), 7.03-7.00 (4H, t, *J*=8 Hz), 3.89 (6H, s), 2.48 (3H, s), 2.43 (3H, s); ¹³C NMR (125 MHz, CDCl₃, δ in ppm): 186.6, 165.0, 163.7, 161.1, 158.0, 148.9, 146.8, 141.6, 141.5, 141.2, 139.8, 133.0, 132.3, 131.9, 129.6, 129.4, 128.5, 128.4, 128.2, 125.0, 122.5, 122.2, 120.6, 114.7, 113.4, 55.6, 55.3, 21.7, 21.6; HRMS (ESI) *m/z* [M+nH] calcd for C₃₇H₃₁BF₂N₃O₃: 614.2427, found: 624.2428.

Aza-BODIPY 2:

Aza-BODIPY **2** was synthesized by following a reported literature procedure.⁴⁸

Aza-BODIPY 3:

A mixture of aza-BODIPY **1** (0.200 g, 0.33 mmol), H₂NOH·HCl (0.068 g, 0.99 mmol), pyridine (0.5 mL), HOAc (1.0 mL), and DMF (5 mL) was stirred and refluxed at 100 °C for 24 hrs. After cooling to room temperature, the mixture was poured into 150 mL H₂O and

stirred for 20 min. The solid was collected by filtration and purified by chromatography (DCM/hexane) (3 : 2 v/v) as an eluent to yield 0.070 g (35%) aza-BODIPY **3**. **¹H NMR** (500 MHz, CDCl₃, δ in ppm): 8.29 (1H, s), 7.98-7.96 (2H, d, J =8.1 Hz), 7.92-7.90 (2H, d, J =8.7 Hz), 7.82-7.80 (2H, d, J =8.7 Hz), 7.60-7.59 (2H, m, J =7.9 Hz), 7.29-7.28 (1H, d, J =7.9 Hz), 7.22 (1H, s), 7.14-7.13 (2H, d, J =7.9 Hz), 7.07-7.01 (4H, m), 3.92-3.90 (6H, m), 2.47 (3H, s), 2.39 (3H, s); **¹³C NMR** (125 MHz, CDCl₃, δ in ppm): 163.0, 162.1, 161.7, 160.6, 154.6, 147.6, 146.0, 145.3, 141.1, 138.7, 138.4, 137.5, 131.3, 130.4, 130.3, 130.0, 129.0, 128.8, 128.5, 125.3, 125.0, 116.9, 114.6, 114.2, 55.5, 53.4, 21.5, 21.4; **HRMS** (ESI) m/z [$M+nCH_3CN^+$] calcd for C₃₉H₃₂BF₂N₅O₂ m/z : 651.2618, found 651.2077.

Aza-BODIPY **4**:

A mixture of aza-BODIPY **2** (0.200 g, 0.31 mmol), H₂NOH·HCl (0.065 g, 93 mmol), pyridine (0.5 mL), HOAc (1.0 mL), and DMF (5 mL) was stirred and refluxed at 100 °C for 24 hrs. After cooling to room temperature, the mixture was poured into 150 mL H₂O and stirred for 20 min. The solid was collected by filtration and purified by chromatography (DCM/hexane) (3 : 2 v/v) as an eluent to yield 0.060 g (30%) aza-BODIPY **4**. **¹H NMR** (500 MHz, CDCl₃, δ in ppm): 8.00-7.99 (4H, m), 7.76-7.74 (2H, d, J = 8.7 Hz,), 7.65-7.64 (2H, d, J = 8.5 Hz), 7.02- 6.91(9H, m), 3.91-3.87 (12H, m); **¹³C NMR** (125 MHz, CDCl₃, δ in ppm): 163.3, 162.7, 161.3, 160.8, 160.5, 159.1, 156.9, 144.9, 133.0, 131.0, 130.6, 128.4, 128.3, 127.5, 124.6, 123.1, 115.3, 114.5, 114.4, 114.2, 114.0, 113.7, 113.5, 113.3, 94.5, 55.4, 55.3; **HRMS** (ESI) m/z [$M+nCH_3CN^+$] calcd for C₃₉H₃₂BF₂N₅O₄ : 683.2517, found 683.2415.

Aza-BODIPY **5**:

To a solution of aza-BODIPY **1** (0.200 g, 0.33 mmol) and C₆₀ (0.470 g, 0.66 mmol) in dry toluene (100 ml), sarcosine (0.233 g, 2.64 mmol) were added. The solution mixture was refluxed at 100 °C for 48 hrs and then solvent was removed under vacuum. The residue was purified

by column chromatography (silica) with DCM/toluene (4 : 1) as an eluent to yield 0.132 g (30%) aza-BODIPY **5**. **¹H NMR** (500 MHz, CDCl₃, δ in ppm): 8.04-8.02 (2H, d, J =8.7 Hz), 7.94-7.93 (2H, d, J =7.5 Hz), 7.86-7.85 (2H, d, J =7.9 Hz), 7.22-7.7.13 (6H, m), 7.06 (1H, s), 6.96-6.86 (4H, m), 4.87 (2H, s), 3.92-3.85 (7H, m), 2.99 (3H, m), 2.43 (3H, s), 2.37 (3H, s); **¹³C NMR** (125 MHz, CDCl₃, δ in ppm): 162.8, 161.6, 161.0, 160.8, 160.3, 156.2, 154.4, 154.1, 147.3, 146.2, 146.1, 145.8, 145.7, 145.4, 145.3, 145.2, 145.0, 144.7, 144.6, 144.5, 144.3, 144.2, 143.7, 143.0, 142.9, 142.6, 142, 5, 142.3, 142.1, 142.0, 141.8, 141.6, 141.2, 140.7, 140.4, 140.1, 139.2, 138.6, 138.1, 138.0, 137.0, 136.6, 136.4, 136.0, 135.0, 132.6, 132.2, 131.8, 129.8, 129.4, 129.2, 128.9, 128.4, 123.4, 123.2, 114.5, 89.3, 87.3, 81.3, 69.2, 55.5, 55.3, 40.1, 21.5; **HRMS** (ESI) m/z [$M+nNa^+$] calcd for C₉₉H₃₅BF₂N₄O₂Na⁺: 1383.2728, found: 1383.2738.

Aza-BODIPY 6:

To a solution of aza-BODIPY **1** (0.200 g, 0.31 mmol) and C₆₀ (0.446 g, 0.62 mmol) in dry toluene (100 ml), sarcosine (0.221 g, 2.48 mmol) were added. The solution mixture was refluxed at 100 °C for 48 hrs and then solvent was removed under vacuum. The residue was purified by column chromatography (silica) with DCM/toluene (4 : 1) as an eluent to yield 0.109 g (25%) aza-BODIPY **6**. **¹H NMR** (500 MHz, CDCl₃, δ in ppm): 8.04-7.96 (7H, m), 6.99-6.94 (6H, m), 6.87-6.85 (4H, d, J =8.9 Hz), 4.87 (2H, s), 3.91-3.87 (7H, m), 3.85-3.84 (6H, m), 3.0 (3H, s); **¹³C NMR** (125 MHz, CDCl₃, δ in ppm): 162.7, 161.3, 160.3, 156.3, 156.2, 155.4, 154.6, 154.5, 154.0, 153.2, 151.8, 151.7, 151.2, 150.2, 149.8, 149.6, 147.7, 147.5, 146.1, 145.9, 145.7, 145.5, 145.2, 143.1, 142.3, 142.0, 141.6, 136.4, 134.2, 132.1, 131.0, 127.6, 123.5, 114.4, 114.2, 113.4, 101.2, 94.7, 91.1, 74.0, 69.8, 69.2, 55.7, 55.3, 50.7, 45.8, 40.1, 22.7; **HRMS** (ESI) m/z [$M+nH$] calcd for C₉₉H₃₆BF₂N₄O₄: 1393.2807, found: 1393.2830.

7.7. Conclusion

In conclusion, we designed and synthesized a series of formyl, nitrile, and fullerene substituted di- and tetra-methoxy based aza-BODIPY dyes (**1–6**). The optical investigation of these aza-BODIPYs highlighted a notable red shift in the absorption for tetra-methoxy based aza-BODIPY dyes (**2**, **4**, and **6**) compared to their di-methoxy counterparts (**1**, **3**, and **5**), owing to the strong electron donating ability of the methoxy substituent over the methyl substituent. The electrochemical study suggests that the substitution of electron-withdrawing moieties (formyl, nitrile, and fullerene) led to multiple reduction potentials. The DFT calculations on aza-BODIPYs **1–6** showed low HOMO–LUMO gap values ranging from 1.82–2.10 eV. Tunable absorption covering the ultraviolet to visible region, combined with multi-redox properties and low HOMO-LUMO gap values, make these aza-BODIPYs as a promising candidate for optoelectronic applications.

7.8. References

- [1] Gupta, I., Kesavan, P. E. (2019). Carbazole Substituted BODIPYs. *Frontiers in Chemistry*, 7. (DOI: 10.3389/fchem.2019.00841).
- [2] Wang, J., Yu, C., Hao, E., Jiao, L. (2022). Conformationally Restricted and Ring-Fused Aza-BODIPYs as Promising near Infrared Absorbing and Emitting Dyes. *Coordination Chemistry Reviews*, 470, 214709. (DOI: 10.1016/j.ccr.2022.214709).
- [3] David, S., Chang, H.-J., Lopes, C., Brännlund, C., Le Guennic, B., Berginc, G., van Stryland, E., Bondar, M. V., Hagan, D. J., Jacquemin, D., Andraud, C., Maury, O. (2021). Benzothiadiazole Substituted Aza-BODIPY Dyes: Two-Photon Absorption Enhancement for Improved Optical Limiting Performances in the SWIR Range. *Chemistry - A European Journal*, 27(10), 3517–3525. (DOI: 10.1002/chem.202004899).

- [4] Guennic, B. L., Maury, O., Jacquemin, D. (2012). Aza-Boron-Dipyrromethene Dyes : TD-DFT Benchmarks, Spectral Analysis and Design of Original near-IR Structures. *Physical Chemistry Chemical Physics*, 14(1), 157–164. (DOI: 10.1039/C1CP22396H).
- [5] Merkushev, D., Vodyanova, O., Telegin, F., Melnikov, P., Yashtulov, N., Marfin, Y. (2022). Design of Promising Aza-BODIPYs for Bioimaging and Sensing. *Designs*, 6, 21. (DOI: 10.3390/designs6020021).
- [6] Dolati, H., Haufe, L. C., Denker, L., Lorbach, A., Grotjahn, R., Hörner, G., Frank, R. (2020). Two π -Electrons Make the Difference: From BODIPY to BODIIM Switchable Fluorescent Dyes. *Chemistry – A European Journal*, 26(6), 1422–1428. (DOI: 10.1002/chem.201905344).
- [7] Çinar, M. E. (2022). Dimeric Aza-BODIPY and Dichloro-Aza-BODIPY: A DFT Study. *Gazi University Journal of Science*, 35(2), 388–402. (DOI: 10.35378/gujs.846075).
- [8] I. Shamova, L., V. Zatsikha, Y., N. Nemykin, V. (2021). Synthesis Pathways for the Preparation of the BODIPY Analogues: Aza-BODIPYs, BOPHYs and Some Other Pyrrole-Based Acyclic Chromophores. *Dalton Transactions*, 50(5), 1569–1593. (DOI: 10.1039/D0DT03964K).
- [9] Rana, P., Singh, N., Majumdar, P., Prakash Singh, S. (2022). Evolution of BODIPY/Aza-BODIPY Dyes for Organic Photoredox/Energy Transfer Catalysis. *Coordination Chemistry Reviews*, 470, 214698. (DOI: 10.1016/j.ccr.2022.214698).
- [10] Chinna Ayya Swamy, P., Sivaraman, G., Priyanka, R. N., Raja, S. O., Ponnuvel, K., Shanmugpriya, J., Gulyani, A. (2020). Near Infrared (NIR) Absorbing Dyes as Promising Photosensitizer for Photo Dynamic Therapy. *Coordination Chemistry Reviews*, 411, 213233. (DOI: 10.1016/j.ccr.2020.213233).

- [11] Shi, Z., Han, X., Hu, W., Bai, H., Peng, B., Ji, L., Fan, Q., Li, L., Huang, W. (2020). Bioapplications of Small Molecule Aza-BODIPY: From Rational Structural Design to in Vivo Investigations. *Chem. Soc. Rev.*, 49(21), 7533–7567. (DOI: 10.1039/D0CS00234H).
- [12] Wang, L., Ding, H., Xiong, Z., Ran, X., Tang, H., Cao, D. (2022). Design, Synthesis and Applications of NIR-Emissive Scaffolds of Diketopyrrolopyrrole-Aza-BODIPY Hybrids. *Chem. Commun.*, 58(40), 5996–5999. (DOI: 10.1039/D2CC00774F).
- [13] Sadikogullari, B. C., Koramaz, I., Sütay, B., Karagoz, B., Özdemir, A. D. (2023). Application of Aza-BODIPY as a Nitroaromatic Sensor. *ACS Omega*, 8(28), 25254–25261. (DOI: 10.1021/acsomega.3c02349).
- [14] Zhang, W., Ahmed, A., Cong, H., Wang, S., Shen, Y., Yu, B. (2021). Application of Multifunctional BODIPY in Photodynamic Therapy. *Dyes and Pigments*, 185, 108937. (DOI: 10.1016/j.dyepig.2020.108937).
- [15] Zhao, M., Zeng, Q., Li, X., Xing, D., Zhang, T. (2022). Aza-BODIPY-Based Phototheranostic Nanoagent for Tissue Oxygen Auto-Adaptive Photodynamic/Photothermal Complementary Therapy. *Nano Res.*, 15(1), 716–727. (DOI: 10.1007/s12274-021-3552-3).
- [16] Kubo, Y., Shimada, T., Maeda, K., Hashimoto, Y. (2019). Thieno[1,3,2]Oxazaborinine-Containing Aza-BODIPYs with near Infrared Absorption Bands: Synthesis, Photophysical Properties, and Device Applications. *New J. Chem.*, 44(1), 29–37. (DOI: 10.1039/C9NJ04612G).
- [17] Bhat, G., [Link to external site, this link will open in a new window](#), Kielar, M., [Link to external site, this link will open in a new window](#), Rao, H., [Link to external site, this link will open in a new window](#), Gholami, M. D., [Link to external site, this](#)

link will open in a new window, Mathers, I., Larin, A. C. R., Link to external site, this link will open in a new window, Flanagan, T., Link to external site, this link will open in a new window, Erdenebileg, E., Bruno, A., Pannu, A. S., Link to external site, this link will open in a new window, Fairfull-Smith, K. E., Link to external site, this link will open in a new window, Izake, E. L., Link to external site, this link will open in a new window, Sah, P., Link to external site, this link will open in a new window, Lam, Y. M., Link to external site, this link will open in a new window, Pandey, A. K., Link to external site, this link will open in a new window, Sonar, P., Link to external site, this link will open in a new window. Versatile azabodipy-based Low-bandgap Conjugated Small Molecule for Light Harvesting and Near-infrared Photodetection. *Infomat*, 4 (12). (DOI: 10.1002/inf2.12345).

- [18] Chinna Ayya Swamy, P., Sivaraman, G., Priyanka, R. N., Raja, S. O., Ponnuvel, K., Shanmugpriya, J., Gulyani, A. (2020). Near Infrared (NIR) Absorbing Dyes as Promising Photosensitizer for Photo Dynamic Therapy. *Coordination Chemistry Reviews*, 411, 213233. (DOI: 10.1016/j.ccr.2020.213233).
- [19] Dai, S.-M., Deng, L.-L., Zhang, M.-L., Chen, W.-Y., Zhu, P., Wang, X., Li, C., Tan, Z., Xie, S.-Y., Huang, R.-B., Zheng, L.-S. (2017). Two Cyclohexanofullerenes Used as Electron Transport Materials in Perovskite Solar Cells. *Inorganica Chimica Acta*, 468, 146–151. (DOI: 10.1016/j.ica.2017.05.056).
- [20] Mumyatov, A. V., Troshin, P. A. (2023). A Review on Fullerene Derivatives with Reduced Electron Affinity as Acceptor Materials for Organic Solar Cells. *Energies*, 16(4), 1924. (DOI: 10.3390/en16041924).
- [21] Li, S., Zhan, L., Sun, C., Zhu, H., Zhou, G., Yang, W., Shi, M., Li, C.-Z., Hou, J., Li, Y., Chen, H. (2019). Highly Efficient Fullerene-Free Organic Solar Cells Operate at Near Zero Highest

Occupied Molecular Orbital Offsets. *J. Am. Chem. Soc.*, 141(7), 3073–3082. (DOI: 10.1021/jacs.8b12126).

- [22] Benatto, L., Marchiori, C. F. N., Talka, T., Aramini, M., Yamamoto, N. A. D., Huotari, S., Roman, L. S., Koehler, M. (2020). Comparing C60 and C70 as Acceptor in Organic Solar Cells: Influence of the Electronic Structure and Aggregation Size on the Photovoltaic Characteristics. *Thin Solid Films*, 697, 137827. (DOI: 10.1016/j.tsf.2020.137827).
- [23] Paukov, M., Kramberger, C., Begichev, I., Kharlamova, M., Burdanova, M. (2023). Functionalized Fullerenes and Their Applications in Electrochemistry, Solar Cells, and Nanoelectronics. *Materials*, 16(3), 1276. (DOI: 10.3390/ma16031276).
- [24] Lopez, S. A., Sanchez-Lengeling, B., de Goes Soares, J., Aspuru-Guzik, A. (2017). Design Principles and Top Non-Fullerene Acceptor Candidates for Organic Photovoltaics. *Joule*, 1(4), 857–870. (DOI: 10.1016/j.joule.2017.10.006).
- [25] Zahran, R., Hawash, Z. (2022). Fullerene-Based Inverted Perovskite Solar Cell: A Key to Achieve Promising, Stable, and Efficient Photovoltaics. *Advanced Materials Interfaces*, 9(35), 2201438. (DOI: 10.1002/admi.202201438).
- [26] Huang, Y.-Y., Sharma, S. K., Yin, R., Agrawal, T., Chiang, L. Y., Hamblin, M. R. (2014). Functionalized Fullerenes in Photodynamic Therapy. *Journal of Biomedical Nanotechnology*, 10(9), 1918–1936. (DOI: 10.1166/jbn.2014.1963).
- [27] Ganesamoorthy, R., Sathiyam, G., Sakthivel, P. (2017). Review: Fullerene Based Acceptors for Efficient Bulk Heterojunction Organic Solar Cell Applications. *Solar Energy Materials and Solar Cells*, 161, 102–148. (DOI: 10.1016/j.solmat.2016.11.024).
- [28] Shafiq, I., Khalid, M., Asghar, M. A., Baby, R., Braga, A. A. C., Alshehri, S. M., Ahmed, S. (2023). Influence of Azacycle Donor

- Moieties on the Photovoltaic Properties of Benzo[c][1,2,5]Thiadiazole Based Organic Systems: A DFT Study. *Sci Rep*, 13(1), 14630. (DOI: 10.1038/s41598-023-41679-0).
- [29] Ai, M., Chen, M., Yang, S. (2023). Recent Advances in Functionalized Fullerenes in Perovskite Solar Cells. *Chinese Journal of Chemistry*, 41(18), 2337–2353. (DOI: 10.1002/cjoc.202300105).
- [30] Chen, J., Chen, Y., Feng, L.-W., Gu, C., Li, G., Su, N., Wang, G., Swick, S. M., Huang, W., Guo, X., Facchetti, A., Marks, T. J. (2020). Hole (Donor) and Electron (Acceptor) Transporting Organic Semiconductors for Bulk-Heterojunction Solar Cells. *EnergyChem*, 2(5), 100042. (DOI: 10.1016/j.enchem.2020.100042).
- [31] Alsaleh, A. Z., Pinjari, D., Misra, R., D’Souza, F. (2023). Far-Red Excitation Induced Electron Transfer in Bis Donor-AzaBODIPY Push-Pull Systems, Role of Nitrogenous Donors in Promoting Charge Separation. *Chemistry – A European Journal*, 29(53), e202301659. (DOI: 10.1002/chem.202301659).
- [32] Sekaran, B., Misra, R. (2022). β -Pyrrole Functionalized Porphyrins: Synthesis, Electronic Properties, and Applications in Sensing and DSSC. *Coordination Chemistry Reviews*, 453, 214312. (DOI: 10.1016/j.ccr.2021.214312).
- [33] Poddar, M., Misra, R. (2020). Recent Advances of BODIPY Based Derivatives for Optoelectronic Applications. *Coordination Chemistry Reviews*, 421, 213462. (DOI: 10.1016/j.ccr.2020.213462).
- [34] Rout, Y., Chauhan, V., Misra, R. (2020). Synthesis and Characterization of Isoindigo-Based Push–Pull Chromophores. *J. Org. Chem.*, 85(7), 4611–4618. (DOI: 10.1021/acs.joc.9b03267).

- [35] Patil, Y., Misra, R. (2019). Rational Molecular Design towards NIR Absorption: Efficient Diketopyrrolopyrrole Derivatives for Organic Solar Cells and Photothermal Therapy. *Journal of Materials Chemistry C*, 7(42), 13020–13031. (DOI: 10.1039/C9TC03640G).
- [36] Patil, Y., Misra, R. (2020). Metal Functionalized Diketopyrrolopyrroles: A Promising Class of Materials for Optoelectronic Applications. *The Chemical Record*, 20(6), 596–603. (DOI: 10.1002/tcr.201900061).
- (37) Pinjari, D., Alsaleh, A. Z., Patil, Y., Misra, R., D'Souza, F. (2020). Interfacing High-Energy Charge-Transfer States to a Near-IR Sensitizer for Efficient Electron Transfer upon Near-IR Irradiation. *Angew Chem Int Ed.*, 59(52), 23697–23705. (DOI: 10.1002/anie.202013036).
- [38] Rocha-Ortiz, J. S., Montalvo-Acosta, J. J., He, Y., Insuasty, A., Hirsch, A., Brabec, C. J., Ortiz, A. (2023). Structure and Linkage Assessment of T-Shaped Pyrrolidine[60]Fullerene- and Isoxazoline[60]Fullerene-BODIPY-Triarylamine Hybrids. *Dyes and Pigments*, 217, 111445. (DOI: 10.1016/j.dyepig.2023.111445).
- [39] Madrid-Úsuga, D., Ortiz, A., Reina, J. H. (2022). Photophysical Properties of BODIPY Derivatives for the Implementation of Organic Solar Cells: A Computational Approach. *ACS Omega*, 7(5), 3963–3977. (DOI: 10.1021/acsomega.1c04598).
- [40] Ünlü, H., Okutan, E. (2017). Preparation of BODIPY- Fullerene and Monostyryl BODIPY-Fullerene Dyads as Heavy Atom Free Singlet Oxygen Generators. *Dyes and Pigments*, 142, 340–349. (DOI: 10.1016/j.dyepig.2017.03.055).
- [41] Calderon Cerquera, K., Parra, A., Madrid-Úsuga, D., Cabrera-Espinoza, A., Melo-Luna, C. A., Reina, J. H., Insuasty, B., Ortiz, A. (2021). Synthesis, Characterization and Photophysics of

- Novel BODIPY Linked to Dumbbell Systems Based on Fullerene[60]Pyrrolidine and Fullerene[60]Isoxazoline. *Dyes and Pigments*, 184, 108752. (DOI: 10.1016/j.dyepig.2020.108752).
- [42] Heredia, D. A., Durantini, A. M., Durantini, J. E., Durantini, E. N. (2022). Fullerene C60 Derivatives as Antimicrobial Photodynamic Agents. *Journal of Photochemistry and Photobiology C: Photochemistry Reviews*, 51, 100471. (DOI: 10.1016/j.jphotochemrev.2021.100471).
- [43] El-Khouly, M. E., Fukuzumi, S., D'Souza, F. (2014). Photosynthetic Antenna–Reaction Center Mimicry by Using Boron Dipyrromethene Sensitizers. *ChemPhysChem*, 15(1), 30–47. (DOI: 10.1002/cphc.201300715).
- [44] Bandi, V., B. Gobeze, H., N. Nesterov, V., A. Karr, P., D'Souza, F. (2014). Phenothiazine–azaBODIPY–Fullerene Supramolecules: Syntheses, Structural Characterization, and Photochemical Studies. *Physical Chemistry Chemical Physics*, 16(46), 25537–25547. (DOI: 10.1039/C4CP03400G).
- [45] Bandi, V., D'Souza, F. P., Gobeze, H. B., D'Souza, F. (2015). Multistep Energy and Electron Transfer in a “V-Configured” Supramolecular BODIPY–azaBODIPY–Fullerene Triad: Mimicry of Photosynthetic Antenna Reaction-Center Events. *Chemistry – A European Journal*, 21(6), 2669–2679. (DOI: 10.1002/chem.201405663).
- [46] Bandi, V., El-Khouly, M. E., Ohkubo, K., Nesterov, V. N., Zandler, M. E., Fukuzumi, S., D'Souza, F. (2014). Bisdonor–azaBODIPY–Fullerene Supramolecules: Syntheses, Characterization, and Light-Induced Electron-Transfer Studies. *J. Phys. Chem. C*, 118(5), 2321–2332. (DOI: 10.1021/jp4112469).

- [47] Jiao, L., Yu, C., Li, J., Wang, Z., Wu, M., Hao, E. (2009). β -Formyl-BODIPYs from the Vilsmeier–Haack Reaction. *J. Org. Chem.*, 74(19), 7525–7528. (DOI: 10.1021/jo901407h).
- [48] Wang, J., Wu, Y., Sheng, W., Yu, C., Wei, Y., Hao, E., Jiao, L. (2017). Synthesis, Structure, and Properties of β -Vinyl Ketone/Ester Functionalized AzaBODIPYs from FormylazaBODIPYs. *ACS Omega*, 2(6), 2568–2576. (DOI: 10.1021/acsomega.7b00393).
- [49] R. Zarccone, S., J. Yarbrough, H., J. Neal, M., C. Kelly, J., L. Kaczynski, K., J. Bloomfield, A., M. Bowers, G., D. Montgomery, T., T. Chase, D. (2022). Synthesis and Photophysical Properties of Nitrated Aza-BODIPYs. *New Journal of Chemistry*, 46(9), 4483–4496. (DOI: 10.1039/D1NJ05976A).

Chapter 8

Conclusions and scope for future work

8.1. Conclusions

Near-infrared (NIR) absorbing organic chromophores have been extensively used in variety of applications such as organic electronics, organic solar cells (OSCs), organic light emitting diodes (OLEDs), photothermal therapy, and bioimaging.^[1-4] Aza-boron-difluoride dipyrromethenes (Aza-BODIPYs) are a class of NIR absorbing organic dyes derived from BODIPY by the replacement of *meso*-carbon with a nitrogen atom.^[5-7] In aza-BODIPY, the presence of a nitrogen atom in *meso*-position with a lone pair of electrons perturbs the energy levels, which leads to the lowering of the band gap compared to parent BODIPY.^[8, 9] It is one of the widely used acceptor unit for the synthesis of small molecules for various applications including organic photovoltaics, photodynamic therapy, boron neutron capture therapy, fluorescence sensor, photo-redox catalysis, and photoacoustic probes.^[10, 11]

In this regard we designed and synthesized various donors and acceptors functionalized aza-BODIPY dyes. We have investigated their photophysical, thermal and electrochemical properties. The systematic variation of donor or acceptor functionalization on aza-BODIPY core at different positions and their impact on optical and electrochemical properties were investigated.

In chapter 3, we have reported the design and synthesis of different donor functionalized tetra-aryl substituted aza-BODIPY dyes **2–5**, **7**, and **9**. Further we studied their photophysical and electrochemical properties and compared with reported aza-BODIPYs **1**, **6**, **8**, and **10**. The electronic absorption spectra of the aza-BODIPYs **1–10** exhibited a broad absorption covering visible to near-infrared region. The diphenothiazine and di-thioanisole based aza-BODIPY **5** as well as tetra-thiophene based aza-BODIPY **10**, exhibited red-shifted absorption

maximum as compared to tetra-aryl aza-BODIPY dyes. The cyclic voltammetry investigation show multiple oxidation and reduction potentials in aza-BODIPYs **1–10** related to corresponding donor and acceptor (aza-BODIPY) moieties. The intramolecular charge transfer (ICT) from different aryl donors to aza-BODIPY acceptor leads to the decrease in HOMO-LUMO gap. The results obtained in this work demonstrated that simple electron donating substitution on aza-BODIPY core can induce huge bathochromic shift in their absorption and hence this will be a useful strategy to develop NIR dyes. A broad absorption in the vis-NIR range, multiple redox peaks, and low HOMO-LUMO gap values in these aza-BODIPY derivatives indicate the suitability as a potential candidate for organic photovoltaics and bioimaging.

In Chapter 4, a series of donor-functionalized aza-BODIPY dyes (**2–6**) were successfully synthesized *via* the Pd-catalyzed Sonogashira cross-coupling reaction. In optical properties, the *N, N*-dimethylaniline-substituted aza-BODIPY dye **4** showed a red-shifted absorption compared to the other aza-BODIPY dyes (**2**, **3**, **5**, and **6**). Electrochemical studies exhibited multiple oxidation and reduction waves associated with the donor and acceptor groups. Computational calculations showed that the aza-BODIPY dyes (**2–6**) have low HOMO-LUMO gap values. These aza-BODIPY derivatives exhibit promising features such as their absorption in the visible-to-near-infrared (vis-NIR) range, multiple redox peaks, and low HOMO-LUMO gap values, which suggest their potential use in organic photovoltaics and bioimaging.

In chapter 5, we have reported the design and synthesis of triphenylamine substituted aza-dipyrrromethene and aza-BODIPY dyes **2–7** by the Pd-catalyzed Sonogashira cross-coupling reaction and [2 + 2] cycloaddition retroelectrocyclization reaction. The BF₂ containing aza-BODIPYs **3**, **5** and **7** show red shifted absorption as compared to aza-dipyrrromethenes **2**, **4** and **6**. The DFT and TD-DFT results reveal that electron density transfers from triphenylamine (donor) to aza-

BODIPY and TCBD (acceptor) core. The DFT calculations show that the triphenylamine substituted aza-BODIPYs **3**, **5** and **7** exhibit low HOMO–LUMO gap values as compared to aza-dipyrromethenes **2**, **4** and **6**.

In chapter 6, we have reported the design and synthesis of NIR absorbing 2,6-diarylated BF₂-chelated aza-BODIPY dyes **3–7** with different donor aromatic substituents. A red shift in the absorption maxima of aza-BODIPY dyes **6** and **7** was observed compared to aza-BODIPY dyes **3–5**, which can be attributed to the presence of π -extended and strong electron-donating groups at the 2,6 positions of the aza-BODIPY core. The electrochemical investigations showed the presence of two oxidation and two reduction potentials. Computational calculations demonstrated a lower HOMO-LUMO gap for carbazole and phenothiazine functionalized aza-BODIPYs (**6** and **7**), compared to other aza-BODIPY derivatives (**3**, **4** and **5**). These findings provide valuable insights for the design and development of new dyes with improved photophysical properties and potential applications in optoelectronics.

In Chapter 7, we have reported the design and synthesis of a series of formyl, nitrile, and fullerene substituted di- and tetra-methoxy based aza-BODIPY dyes (**1–6**). The optical investigation of these aza-BODIPYs highlighted a notable red shift in the absorption for tetra-methoxy based aza-BODIPY dyes (**2**, **4**, and **6**) compared to their di-methoxy counterparts (**1**, **3**, and **5**), owing to the strong electron donating ability of the methoxy substituent over the methyl substituent. The electrochemical study suggests that the substitution of electron-withdrawing moieties (formyl, nitrile, and fullerene) led to multiple reduction potentials. The DFT calculations on aza-BODIPYs **1–6** showed low HOMO–LUMO gap values ranging from 1.82–2.10 eV. Tunable absorption covering the ultraviolet to visible region, combined with multi-redox properties and low HOMO-LUMO gap values, make these aza-BODIPYs as a promising candidate for optoelectronic applications.

8.2. Scope for future work

The thesis highlights smart methodology for design of aza-BODIPY based donor and acceptor small molecules. The optical, electrochemical properties and HOMO–LUMO gap of the aza-BODIPY based donor-acceptor molecules have been tuned by varying terminal donor or acceptor units at various positions. The functionalization of aza-BODIPY with terminal donor unit and incorporation of cyano-bridged acceptors (TCBD and DCNQ) in the ethyne bridged aza-BODIPY resulted in broader absorption spectrum in visible and near infrared region. The strong absorption in near infrared region along with low HOMO-LUMO gap of aza-BODIPY based small molecules make them promising candidates for optoelectronic applications.

The rising demand for developing sustainable energy sources indicates the urgent need of high-performing NIR absorbing dyes. Further research development is necessary to optimize the synthesis, optical features, and exploration of their potential performance in NIR absorbing aza-BODIPY dyes. We believe the continuous improvement in the performance of these dyes indicates that aza-BODIPY will play a vital role in the development of highly efficient next-generation materials. This study will be very useful to make efficient materials in the fields of molecular chemistry, material science, and molecular biology.

8.3. References

- [1] Khan, M. U., Hussain, R., Yasir Mehboob, M., Khalid, M., Shafiq, Z., Aslam, M., ... & Janjua, M. R. S. A. (2020). In silico modeling of new “Y-Series”-based near-infrared sensitive non-fullerene acceptors for efficient organic solar cells. *ACS omega*, 5(37), 24125-24137. (DOI: 10.1021/acsomega.0c03796).
- [2] Bellier, Q., Pégaz, S., Aronica, C., Guennic, B. L., Andraud, C., & Maury, O. (2011). Near-infrared nitrofluorene substituted aza-

- boron-dipyrromethenes dyes. *Organic Letters*, 13(1), 22-25. (DOI: 10.1021/ol102701v).
- [3] Zhao, Y., Luo, Y., Wu, S., Wang, C., Ahmidayi, N., L  v  que, G., ... & Xu, T. (2023). Enhanced near-infrared photoresponse for efficient organic solar cells using hybrid plasmonic nanostructures. *Physica E: Low-dimensional Systems and Nanostructures*, 146, 115534. (DOI: 10.1016/j.physe.2022.115534).
- [4] Liu, K., Ouyang, B., Guo, X., Guo, Y., & Liu, Y. (2022). Advances in flexible organic field-effect transistors and their applications for flexible electronics. *npj Flexible Electronics*, 6(1), 1. (DOI: 10.1038/s41528-022-00133-3).
- [5] Jiang, X. D., Fu, Y., Zhang, T., & Zhao, W. (2012). Synthesis and properties of NIR aza-BODIPYs with aryl and alkynyl substituents on the boron center. *Tetrahedron Letters*, 53(42), 5703-5706. (DOI: 10.1016/j.tetlet.2012.08.056).
- [6] Zhang, L., Zhao, L., Wang, K., & Jiang, J. (2016). Chiral benzo-fused Aza-BODIPYs with optical activity extending into the NIR range. *Dyes and Pigments*, 134, 427-433. (DOI: 10.1016/j.dyepig.2016.07.039).
- [7] Gut, A., Cie  ka, J., Makuszewski, J., Majewska, I., Brela, M., &   lapok,   . (2022). Near-Infrared fluorescent unsymmetrical aza-BODIPYs: Synthesis, photophysics and TD-DFT calculations. *Spectrochimica Acta Part A: Molecular and Biomolecular Spectroscopy*, 271, 120898. (DOI: 10.1016/j.saa.2022.120898).
- [8] Gawale, Y., & Sekar, N. (2018). Investigating the excited state optical properties and origin of large stokes shift in Benz [c, d] indole N-Heteroarene BF₂ dyes with ab initio tools. *Journal of Photochemistry and Photobiology B: Biology*, 178, 472-480. (DOI: 10.1016/j.jphotobiol.2017.12.006).

- [9] Schafer, C., Mony, J., Olsson, T., & Borjesson, K. (2022). Effect of the Aza-N-Bridge and Push–Pull Moieties: A Comparative Study between BODIPYs and Aza-BODIPYs. *The Journal of Organic Chemistry*, 87(5), 2569-2579. (DOI: 10.1021/acs.joc.1c02525).
- [10] David, S., Chang, H. J., Lopes, C., Brännlund, C., Le Guennic, B., Berginc, G., ... & Maury, O. (2021). Benzothiadiazole-Substituted Aza-BODIPY Dyes: Two-Photon Absorption Enhancement for Improved Optical Limiting Performances in the Short-Wave IR Range. *Chemistry–A European Journal*, 27(10), 3517-3525. (DOI: 10.1002/chem.202004899).
- [11] Ipek, O. S., Topal, S., & Ozturk, T. (2021). Synthesis, characterization and sensing properties of donor-acceptor systems based Dithieno [3, 2-b; 2', 3'-d] thiophene and boron. *Dyes and Pigments*, 192, 109458. (DOI: 10.1016/j.dyepig.2021.109458).